AD_____

Award Number: DAMD17-00-1-0415

TITLE: Functional Analysis of the ErbB4 Receptor Tyrosine Kinase

PRINCIPAL INVESTIGATOR: David J. Riese, II, Ph.D.

CONTRACTING ORGANIZATION: Purdue Research Foundation
West Lafayette, IN 47907-1063

REPORT DATE: July 2004

TYPE OF REPORT: Annual Summary

PREPARED FOR: U.S. Army Medical Research and Materiel Command
Fort Detrick, Maryland 21702-5012

DISTRIBUTION STATEMENT: Approved for Public Release;
Distribution Unlimited

The views, opinions and/or findings contained in this report are
those of the author(s) and should not be construed as an official
Department of the Army position, policy or decision unless so
designated by other documentation.

20050105 022

REPORT DOCUMENTATION PAGE

Form Approved
OMB No. 074-0188

1. AGENCY USE ONLY (Leave blank)	2. REPORT DATE July 2004	3. REPORT TYPE AND DATES COVERED Annual Summary (1 Jul 2000 – 30 Jun 2004)

4. TITLE AND SUBTITLE
Functional Analysis of the ErbB4 Receptor Tyrosine Kinase

5. FUNDING NUMBERS
DAMD17-00-1-0415

6. AUTHOR(S)
David J. Riese, II, Ph.D.

7. PERFORMING ORGANIZATION NAME(S) AND ADDRESS(ES)
Purdue Research Foundation
West Lafayette, IN 47907-1063

E-Mail: driese@purdue.edu

8. PERFORMING ORGANIZATION REPORT NUMBER

9. SPONSORING / MONITORING AGENCY NAME(S) AND ADDRESS(ES)
U.S. Army Medical Research and Materiel Command
Fort Detrick, Maryland 21702-5012

10. SPONSORING / MONITORING AGENCY REPORT NUMBER

11. SUPPLEMENTARY NOTES
Original contains color plates: ALL DTIC reproductions will be in black and white

12a. DISTRIBUTION / AVAILABILITY STATEMENT
Approved for Public Release; Distribution Unlimited

12b. DISTRIBUTION CODE

13. ABSTRACT (Maximum 200 Words)

My laboratory studies the signaling network comprised of the epidermal growth factor (EGF) family of peptide hormones and the ErbB family of receptor tyrosine kinases. We are particularly interested in elucidating the roles that these hormones and receptors play in breast cancer and in developing reagents that target these hormones and receptor and may be use in diagnosing or treating breast cancer. In part due to the generous support of this career development award, we have made progress on four fronts. (1) We have identified and characterized novel small-molecule EGFR antagonists. Some of these hold promise as breast tumor imaging agents specific for tumors that overexpress EGFR. (2) We have used a set of constitutively active ErbB4 mutants to determine that ErbB4 signaling inhibits the proliferation of non-malignant and malignant human mammary cell lines. This suggests that ErbB4 may be a mammary-specific tumor suppressor. (3) We have characterized four novel EGF family hormones. (4) Moreover, we have made mutants of two EGF family hormones that have enabled us to identify residues critical for activation of ErbB4 signaling by these hormones. These data may lead to synthetic, specific ErbB4 agonists and antagonists that could be used to define the role of ErbB4 in breast cancer or could be used to prevent breast cancer.

14. SUBJECT TERMS
EGFR, ErbB2, HER2, Neu, ErbB4, EGF, Neuregulins, Heregulins

15. NUMBER OF PAGES
60

16. PRICE CODE

17. SECURITY CLASSIFICATION OF REPORT Unclassified	18. SECURITY CLASSIFICATION OF THIS PAGE Unclassified	19. SECURITY CLASSIFICATION OF ABSTRACT Unclassified	20. LIMITATION OF ABSTRACT Unlimited

Table of Contents

Introduction

My laboratory studies the signaling network comprised of the epidermal growth factor (EGF) family of peptide hormones and the ErbB family of receptor tyrosine kinases. We are particularly interested in elucidating the roles that these hormones and receptors play in breast cancer and in developing reagents that target these hormones and receptor and may be use in diagnosing or treating breast cancer. In part due to the generous support of this career development award, we have made progress on four fronts. (1) We are continuing to characterize novel small-molecule EGFR antagonists. Some of these hold promise as breast tumor imaging agents specific for tumors that overexpress EGFR. (2) We have used a set of constitutively active ErbB4 mutants to determine that ErbB4 signaling inhibits colony formation on plastic by human prostate mammary cell lines. This suggests that ErbB4 may be a mammary-specific tumor suppressor. Furthermore, we have demonstrated that constitutive ErbB4 signaling causes growth arrest of these cells and that ErbB4 kinase activity and ErbB4 Tyr1056 are critical for inhibition of colony formation on plastic. (3) We have characterized four novel EGF family hormones. (4) Moreover, we have made mutants of two EGF family hormones that have enabled us to identify residues critical for activation of ErbB4 signaling by these hormones. We have demonstrated that the Phe45 residue of the ErbB4 agonist NRG2beta regulates the potency of this agonist. Furthermore, we have demonstrated that the Gln43 and Met47 residues of NRG2beta contribute to the efficacy of NRG2beta. These data may lead to synthetic, specific ErbB4 agonists and antagonists that could be used to define the role of ErbB4 in breast cancer or could be used to prevent breast cancer.

Report Body

1. Characterize putative inhibitors of ErbB family receptor tyrosine kinases. We have screened novel quinazolines and novel analogs of lavendustin A to identify novel, specific inhibitors of ErbB family receptor tyrosine kinases. This is the first step in developing novel breast tumor imaging agents that identify the most aggressive tumors by targeting tumor cells that overexpress EGFR or ErbB2. These experiments are being performed in collaboration with the laboratory of Dr. Mark Cushman at Purdue University and the laboratory of Dr. Henry VanBrocklin at the Lawrence Berkeley National Laboratory.

The results of the screen of the lavendustin A analogs are described in a research article published in the *Journal of Medicinal Chemistry* [1]. We reported these results in a previous progress report and we included a copy of this paper in that report. To summarize, several of the lavendustin A analogs inhibit the EGFR tyrosine kinase domain; however none are as potent as analogs that are in clinical trials as antitumor agents. Furthermore, the lavendustin A analogs exhibit tubulin polymerization IC_{50} values that are approximately the same as the EGFR tyrosine kinase IC_{50} values. Moreover, the DNA synthesis IC_{50} values are approximately the same for MCF-7 (EGF-independent) and MCF-10A (EGF-dependent) cells. These data suggest that the lavendustin A analogs are not specific for the EGFR and hold little promise as tumor imaging agents specific for tumors that overexpress EGFR.

We reported the results of the screen of the quinazolines in a previous progress report. To summarize, several quinazolines are potent, specific inhibitors of the EGFR tyrosine kinase domain. We hope that some of these molecules are suitable for radiolabeling with radioactive fluorine or bromine in order to use in positron emission tomography scanning. Late in 2002 Dr. VanBrocklin and I submitted a manuscript to the *Journal of Medicinal Chemistry* that describes these results. A revised manuscript is in preparation. We have also designed a high-throughput screening strategy that will facilitate the rapid evaluation of a second generation of quinazolines analogs.

We have also screened an oligonucleotide library for high affinity aptamer ligands for EGFR, ErbB2, and ErbB4 *in vitro*. We have identified a low affinity ligand ($K_d \sim 1$ uM) for EGFR. We are currently identifying the pharmacaphore of this aptamer ligand and we will perform additional experiments to optimize this lead molecule. In the meantime, we have developed a cell-based screen for additional aptamer ligands for EGFR, ErbB2, and ErbB4.

These experiments were supported in part by NIH grants to Dr. Riese (R21CA080770 and R21CA089274). These grants have expired and are not renewable. Late in 2002 Dr. VanBrocklin and I were awarded an NIH R01 grant to support our efforts to screen additional quinazolines analogs and to isolate EGFR aptamer ligands (R01CA094253).

2. Define ErbB4 coupling to biological responses. We have generated three constitutively active mutants of the ErbB4 receptor tyrosine kinase that exhibit ligand-independent kinase activity and ligand-independent tyrosine phosphorylation. These mutants, unlike constitutively active ErbB2/HER2/Neu mutants, do NOT cause anchorage independence, increased growth rates, increased saturation densities, or a loss of contact inhibition in a fibroblast cell line. We reported these results in a previous progress report and we published these data in 2002 in a paper in *Cell Growth and Differentiation* [2].

More recently we developed an assay for growth inhibition and have used this assay to demonstrate that the constitutively active Q646C ErbB4 mutant specifically inhibits drug-resistant colony formation on plastic by the DU-145 and PC-3 human prostate tumor cell lines.

These data suggest that ErbB4 may be a prostate tumor suppressor and that reduced ErbB4 expression and signaling plays a causative role in prostate tumorigenesis. We reported these results in a previous progress report and in 2003 we published a paper in *Cancer Letters* that describes inhibition of colony formation of prostate tumor cell lines by the constitutively active Q646C ErbB4 mutant [3].

More recently we have documented that ErbB4 expression is absent in human pancreatic tumor cell lines. These data contrast published data documenting ErbB4 expression in normal pancreatic tissues. We have used the constitutively active Q646C mutant to evaluate the consequences of restoring ErbB4 expression and signaling on human pancreatic tumor cell lines. We have demonstrated that the Q646C mutant inhibits drug-resistant colony formation on plastic in the CaPan-1, HPAC, PANC-1, and MIA PaCa-2 human pancreatic tumor cell lines by 69-99% (Figure 1 and Figure 2). These results are described in a manuscript that is being reviewed for publication in *Molecular Cancer Research*.

Finally, we have also used the constitutively active Q646C ErbB4 mutant to evaluate the effect of ErbB4 signaling on mammary cell lines. We have demonstrated that this ErbB4 mutant inhibits drug-resistant colony formation by the MCF-10A human mammary epithelial cell line and the MCF-7 and SKBR3 human breast tumor cell lines (Figure 3, Figure 4, Figure 5). However, the constitutively active Q646C ErbB4 mutant does not inhibit drug-resistant colony formation by the T47D and MDA-MB-453 human breast tumor cell lines (data not shown). ErbB4 kinase activity is required for inhibition of breast cell line colony formation by the ErbB4 Q646C mutant (Figure 3, Figure 4, Figure 5). An ErbB4 Q646C mutant in which the nine putative carboxyl-terminal ErbB4 tyrosine phosphorylation sites (Tyr1022, Tyr1056, Tyr1150, Tyr1162, Tyr1188, Tyr1202, Tyr1242, Tyr1258, and Tyr1284) have been mutated to phenylalanine fails to inhibit colony formation by MCF-10A cells. However, an ErbB4 Q646C mutant lacking eight of the nine tyrosine phosphorylation sites (it retains Tyr1056) inhibits colony formation by MCF-10A cells (Figure 6). Moreover, an ErbB4 Q646C mutant lacking just a single site of tyrosine phosphorylation (Tyr1056) fails to inhibit colony formation by MCF-10A cells (Figure 6). These data suggest that phosphorylation of Tyr1056 is sufficient and necessary to couple the ErbB4 Q646C mutant to inhibition of colony formation by MCF-10A cells. The constitutively active ErbB4 Q646C mutant causes growth arrest, rather than cell death, in MCF-10A cells (Figure 7, Figure 8). Collectively, these data indicate that ErbB4 may act as a mammary tumor suppressor by causing mammary cell growth arrest and that this activity is dependent on ErbB4 kinase activity as well as phosphorylation of ErbB4 Tyr1056. A manuscript that describes these results is in preparation.

These experiments were supported by a USAMRMC BCRP Idea grant (DAMD-17-00-1-0416) to Dr. Riese. This grant expired in June 2003. These experiments are now supported by a USAMRMC PCRP New Investigator grant (DAMD-17-02-1-0130) to Dr. Riese. An application for additional grant support from the NIH will be submitted in the next twelve months.

3. Characterize biological responses to recombinant neuregulins. In last year's progress report we reported that we had developed a system to express and purify novel recombinant neuregulins, which are members of the EGF family of peptide hormones. One of the most significant findings is that NRG2β is the most potent ErbB4 agonist whereas NRG2α is a weak ErbB4 agonist [4]. These results were described in a previous progress report as well as in a paper that was published in 2002 in *Oncogene* [4]. A copy of that paper is included in this

report. These experiments were supported in part by an NIH grant to Dr. Riese (R21CA80770). However, this grant expired in March 2001 and it is not renewable.

4. Identify and characterize the ErbB4 binding domain of neuregulin2β (NRG2β). NRG2α and NRG2β are splicing isoforms of the same gene. However, as we described in a previous progress report, NRG2β is a potent ErbB4 agonist, whereas NRG2α is not [4]. We have generated mutants of NRG2α and NRG2β to identify amino acid residues that are sufficient and necessary for activation of ErbB4 signaling by NRG2 isoforms. In a previous progress report we presented data indicating that Phe45 of NRG2β is sufficient and necessary for potent stimulation of ErbB4 tyrosine phosphorylation by NRG2 isoforms. However, substitution of Phe45 for Lys45 in NRG2α is not sufficient to enable NRG2α to stimulate ErbB4 coupling to downstream signaling events, nor does substitution of Lys45 for Phe45 in NRG2β disrupt the ability of NRG2β to stimulate ErbB4 coupling to downstream signaling events. We concluded that the potency of NRG2β is regulated by Phe45, but the efficacy of NRG2β (the ability of NRG2β to stimulate ErbB4 coupling to downstream signaling events) is regulated independently of Phe45. These data were published in *Oncogene* earlier this year and a copy of that paper is included with this report.

More recently, we have demonstrated that Gln43 and Met47 of NRG2β are required for NRG2β to stimulate receptor coupling to downstream signaling events; mutating either of these residues to the corresponding residues of NRG2α (Leu43 and Pro47) disrupts the ability of the resulting NRG2β mutant to stimulate receptor coupling to downstream signaling events. However, these mutations do not disrupt the ability of these ligands to bind ErbB4 with high affinity or to potently stimulate ErbB4 tyrosine phosphorylation. Indeed, like the NRG2α K45F mutant, the NRG2β Q43L mutant antagonizes the ability of wild-type NRG2β mutant to stimulate ErbB4 coupling to downstream signaling events. This fundamental difference in the activities of NRG2α and NRG2β (independent of their affinity for ErbB4) establishes a new paradigm for the regulation of ligand-induced receptor signaling.

In sum, the results of these experiments are giving us important clues as to how binding of EGF family hormones to ErbB4 is specified and as to how activation of ErbB4 signaling by EGF family hormones is specified. These clues are the first steps in our attempts to generate specific synthetic or recombinant ErbB4 agonists and antagonists. Such molecules will be useful in probing ErbB4 function and may be useful in staging or treating breast and prostate cancers. These experiments have been supported in part by an NIH grant to Dr. Riese (R21CA80770) and an NIH sabbatical leave fellowship to Dr. Robert P. Hammer of Louisiana State University (F33CA85049). However, both of these grants have expired and neither is renewable. An application made earlier this year to NIH for additional support for this project was not selected for funding (R01CA105068). A revised application is under consideration.

Key Research Accomplishments

Task 1

- Screened novel lavendustin A analogs for inhibition of EGFR, ErbB2, and ErbB4 tyrosine kinase activity and for inhibition of EGFR coupling to cell proliferation.
- Screened novel quinazolines for inhibition of EGFR, ErbB2, and ErbB4 tyrosine kinase activity and for inhibition of EGFR coupling to cell proliferation.
- Established a high-throughput, cell-based screen for EGFR tyrosine kinase inhibitors and other EGFR antagonists.
- Identified a low-affinity aptamer ligand for EGFR. Pursued experiments to optimize this ligand.
- Established cell-based screens for aptamer ligands for EGFR, ErbB2, and ErbB4.

Task 2

- Generated a set of three constitutively active ErbB4 mutants and demonstrated that these mutants do not malignantly transform the growth of a rodent fibroblast cell line.
- Demonstrated that one of the constitutively active ErbB4 mutants inhibits colony formation by the DU-145 and PC-3 human prostate tumor cell lines.
- Demonstrated that one of the constitutively active ErbB4 mutants inhibits colony formation by several human pancreatic tumor cell lines.
- Demonstrated that the constitutively active Q646C ErbB4 mutant inhibits colony formation by some members of a panel of human mammary cell lines. Demonstrated that this inhibition of colony formation is characterized by growth arrest rather than apoptosis. Demonstrated that this inhibition of colony formation requires ErbB4 kinase activity and phosphorylation of ErbB4 Tyr1056.

Task 3

- Developed a system to express and purify recombinant neuregulins.
- Assayed recombinant neuregulins for stimulation of ErbB family receptor tyrosine phosphorylation.
- Determined that NRG2β stimulates abundant levels of ErbB4 tyrosine phosphorylation, whereas NRG3 and NRG4 stimulate more modest levels of ErbB4 tyrosine phosphorylation and NRG2α stimulates minimal ErbB4 tyrosine phosphorylation.

Task 4

- Generated putative NRG2α "gain of function" and NRG2β "loss of function" mutants.
- Assayed NRG2α and NRG2β mutants for activation of ErbB4 tyrosine phosphorylation.
- Assayed NRG2α and NRG2β mutants for stimulation of ErbB4 coupling to IL3 independence in the BaF3 mouse hematopoietic cell line.
- Developed a competitive ligand-binding assay to determine the affinity of NRG2α, NRG2β, and NRG2 mutants for ErbB4.
- Determined that NRG2β Phe45 regulates ligand potency (with respect to stimulation of ErbB4 tyrosine phosphorylation) but not efficacy. Determined that NRG2β Gln43 and Met47 cooperate to regulate ligand efficacy (with respect to stimulation of ErbB4 coupling to biological responses).

Reportable Outcomes

Publications Related to Project

Mu, F., S.L. Coffing, D.J. Riese II, R.L. Geahlen, P. Verdier-Pinard, E. Hamel, J. Johnson, and M. Cushman. "Design, synthesis, and biological evaluation of a series of Lavendustin A analogues that inhibit EGFR and Syk tyrosine kinases, as well as tubulin polymerization." *J. Med. Chem.* **44**: 441-452 (2001).

Penington, D.J., I. Bryant, and D.J. Riese II. "Constitutively Active ErbB4 and ErbB2 Mutants Exhibit Distinct Biological Activity." *Cell Growth Differentiation* **13**: 247-256 (2002).

Hobbs, S.S., S.L. Coffing, A.T.D. Le, E.M. Cameron, E.E. Williams, M. Andrew, E.N. Blommel, R.P. Hammer, H. Chang, and D.J. Riese II. "Neuregulin isoforms exhibit distinct patterns of ErbB family receptor activation." *Oncogene* **21**: 8442-8452 (2002).

Williams, E.E., L.J. Trout, R.M. Gallo, S.E. Pitfield, I. Bryant, D.J. Penington, and D.J. Riese II. "A Constitutively-Active ErbB4 Mutant Inhibits Drug-Resistant Colony Formation by the DU-145 and PC-3 Human Prostate Tumor Cell Lines." *Cancer Letters* **192**: 67-74 (2003).

Hobbs, S.S., E.M. Cameron, R.P. Hammer, A.T.D. Le, R.M. Gallo, E.N. Blommel, S.L. Coffing, H. Chang, and D.J. Riese II. "Five carboxyl-terminal residues of Neuregulin2 are critical for stimulation of signaling by the ErbB4 receptor tyrosine kinase." *Oncogene* **23**: 883-893 (2004).

Lim, J., S.S. Coffing, I. Bryant, D.J. Riese II, and H.F. VanBrocklin. "Dialkoxyquinazolines: Screening Epidermal Growth Factor Receptor Tyrosine Kinase Inhibitors for Potential Tumor Imaging Probes." Under revision for *Journal of Medicinal Chemistry*.

Gilmore, J.G. and D.J. Riese II. "secErbB4-26/549 antagonizes ligand-induced ErbB4 tyrosine phosphorylation." Under revision for *Oncology Research*.

Gettinger, K. and D.J. Riese II. "Restoration of ErbB4 signaling inhibits colony formation by human pancreatic tumor cell lines." Submitted to *Molecular Cancer Research*.

Gilmore, J.G. and D.J. Riese II. "A partial gain-of-function EGFR mutant displays broader agonist specificity." In preparation.

Pitfield, S.E., I. Bryant, D.J. Penington, and D.J. Riese II. "ErbB4 tyrosine kinase activity and phosphorylation of ErbB4 Tyr1056 are critical for coupling a constitutively-active ErbB4 mutant to inhibition of colony formation and growth arrest in human breast cell lines." In preparation.

Reportable Outcomes (Continued)

Meeting Abstracts Related to Project (Last 16 months)

Pitfield, S.E., I. Bryant, D. Penington, and D.J. Riese II. "Functional Analyses of the ErbB4 Receptor Tyrosine Kinase." Tyrosine Phosphorylation and Signal Transduction Meeting, Salk Institute, La Jolla, CA, July 2004.

Hobbs, S.S., K. Wilson, S.L. Coffing, A.T.D. Le, E.M. Cameron, E.E. Williams, M. Andrew, E.N. Blommel, R.P. Hammer, H. Chang, and D.J. Riese II. "Splicing of Neuregulin-2 Modulates Its Interaction With ErbB4." Tyrosine Phosphorylation and Signal Transduction Meeting, Salk Institute, La Jolla, CA, July 2004.

Pitfield, S.E., E.E Williams, L.J. Trout, R.M. Gallo, I. Bryant, D.J. Penington and D.J. Riese II. "A Constitutively Active ErbB4 Mutant Inhibits Drug-Resistant Colony Formation By Human Breast and Prostate Cell Lines." Nineteenth Annual Meeting On Oncogenes, Hood College, Frederick, MD, June 2003.

Funded Grant Applications Related to Project

A grant application submitted to the USAMRMC PCRP for additional funding to support our efforts to analyze ErbB4 function in prostate cancer cells was selected for funding (DAMD17-02-1-0130; Dr. David J. Riese II, PI).

A grant application submitted to NIH/NCI for additional funding to support our efforts to screen for aptamer ligands for ErbB2 was selected for funding (R21CA089274; Dr. David J. Riese II, PI).

A grant application submitted to NIH/NCI for additional funding to support our efforts to screen novel quinazolines for specific inhibition of EGFR tyrosine kinase activity and EGFR coupling to downstream responses was selected for funding (R01CA094253; Dr. Henry VanBrocklin, LBNL, PI; Dr. David J. Riese II, co-PI).

We were awarded an undergraduate research fellowship by the American Association of Colleges of Pharmacy to support our efforts to analyze ErbB4 function in prostate cancer cells (Mr. Eric Williams, PI; Dr. David J. Riese II, mentor).

We were awarded an undergraduate research fellowship by the American Society for Microbiology to support our efforts to analyze ErbB4 function in breast and prostate cancer cells (Ms. Ianthe Bryant, PI; Dr. David J. Riese II, mentor).

Graduate Degrees Earned Related to Project

Mr. Desi Penington wrote and successfully defended a master's degree thesis entitled "Construction and analysis of constitutively-active mutants of the ErbB4 receptor tyrosine kinase" that is based on the results of the studies described in Task 2. Mr. Penington was awarded an MS in August 2001.

Ms. Jennifer Gilmore is expected to have defended her PhD dissertation and earned her doctorate by the end of the 2004 calendar year. The tentative title for her dissertation is, "Characterization of a novel ErbB4 antagonist and dissection of EGF family hormone/ErbB family receptor interactions: The road to rational design of ErbB receptor antagonists."

Mr. Stuart Hobbs is expected to have defended his PhD dissertation and earned his doctorate by the end of the 2004 calendar year. The tentative title for his dissertation is, "Characterization of Neuregulin/ErbB4 interactions."

Conclusions

We have made significant progress on all four of our goals. We have screened and novel quinazolines and lavendustin A analogs to identify EGFR tyrosine kinase inhibitors that may be suitable for the development of novel tumor imaging agents. We are continuing to screen additional quinazolines analogs, making use of a high-throughput screen that we have developed. We are also optimizing a low-affinity aptamer ligand for EGFR and we are performing cell-based screens for additional aptamer ligands for EGFR, ErbB2, and ErbB4. We have generated three constitutively active ErbB4 mutants that have enabled us to demonstrate that ErbB4 is a potential prostate, pancreatic, and breast tumor suppressor. Analyses of additional ErbB4 mutants have demonstrated that coupling to tumor suppression requires ErbB4 kinase activity and phosphorylation of ErbB4 Tyr1056. We have characterized the patterns of ErbB family receptor signaling stimulated by four novel NRGs. We have identified three amino acid residues in NRG2β that regulate the potency and efficacy of this ligand.

References

1. Mu, F., S.L. Coffing, D.J. Riese II, R.L. Geahlen, P. Verdier-Pinard, E. Hamel, J. Johnson, and M. Cushman. "Design, synthesis, and biological evaluation of a series of Lavendustin A analogues that inhibit EGFR and Syk tyrosine kinases, as well as tubulin polymerization." *J. Med. Chem.* **44**: 441-452 (2001).
2. Penington, D.J., I. Bryant, and D.J. Riese II. "Constitutively active ErbB4 and ErbB2 mutants exhibit distinct biological activities." *Cell Growth Diff.* **13**: 247-256 (2002).
3. Williams, E.E., L.J. Trout, R.M. Gallo, S.E. Pitfield, I. Bryant, D.J. Penington, and D.J. Riese II. "A Constitutively-Active ErbB4 Mutant Inhibits Drug-Resistant Colony Formation by the DU-145 and PC-3 Human Prostate Tumor Cell Lines." *Cancer Letters* **192**: 67-74 (2003).
4. Hobbs, S.S., S.L. Coffing, A.T.D. Le, E.M. Cameron, E.E. Williams, M. Andrew, E.N. Blommel, R.P. Hammer, H. Chang, and D.J. Riese II. "Neuregulin isoforms exhibit distinct patterns of ErbB family receptor activation." *Oncogene* **21**:8442-8452 (2002).
5. Hobbs, S.S., E.M. Cameron, R.P. Hammer, A.T.D. Le, R.M. Gallo, E.N. Blommel, S.L. Coffing, H. Chang, and D.J. Riese II. "Five carboxyl-terminal residues of Neuregulin2 are critical for stimulation of signaling by the ErbB4 receptor tyrosine kinase." *Oncogene* **23**: 883-893 (2004).
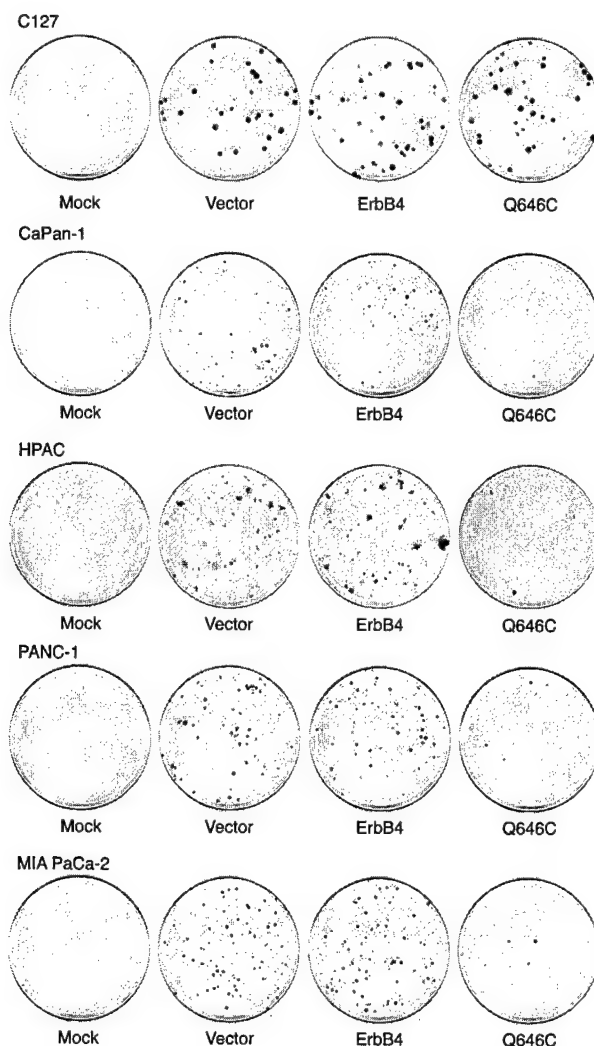
Appendices: List of Documents (48 pages total)

Figures – 8 pages

Journal Articles - 40 pages

1. Penington, D.J., I. Bryant, and D.J. Riese II. "Constitutively Active ErbB4 and ErbB2 Mutants Exhibit Distinct Biological Activity." *Cell Growth Differentiation 13*: 247-256 (2002).

2. Hobbs, S.S., S.L. Coffing, A.T.D. Le, E.M. Cameron, E.E. Williams, M. Andrew, E.N. Blommel, R.P. Hammer, H. Chang, and D.J. Riese II. "Neuregulin isoforms exhibit distinct patterns of ErbB family receptor activation." *Oncogene* 21:8442-8452 (2002).

3. Williams, E.E., L.J. Trout, R.M. Gallo, S.E. Pitfield, I. Bryant, D.J. Penington, and D.J. Riese II. "A Constitutively-Active ErbB4 Mutant Inhibits Drug-Resistant Colony Formation by the DU-145 and PC-3 Human Prostate Tumor Cell Lines." *Cancer Letters* 192: 67-74 (2003).

4. Hobbs, S.S., E.M. Cameron, R.P. Hammer, A.T.D. Le, R.M. Gallo, E.N. Blommel, S.L. Coffing, H. Chang, and D.J. Riese II. "Five carboxyl-terminal residues of Neuregulin2 are critical for stimulation of signaling by the ErbB4 receptor tyrosine kinase." *Oncogene* 23: 883-893 (2004).

Figure 1. *The constitutively active Q646C ErbB4 mutant inhibits drug-resistant colony formation by the CaPan-1, HPAC, PANC-1, and MIA PaCa-2 human pancreatic tumor cell lines.*

Human pancreatic tumor cell lines were infected with recombinant retroviruses that express the neomycin resistance gene along with the constitutively active Q646C ErbB4 mutant (Q646C). As controls, these cells were infected with a recombinant retrovirus that expresses only the neomycin resistance gene (Vector), or the neomycin resistance gene together with wild-type ErbB4 (ErbB4). Cells were also mock infected. Following infection, cells were incubated in G418 to select for infected, drug-resistant cells. After 10-30 days of selection, colonies of drug-resistant cells were visualized by staining the tissue culture plates with Giemsa. The plates were rinsed, dried, and digitized using a UMAX Astra 2400S flatbed scanner set for a resolution of 300 dots per inch (dpi). This composite figure was assembled using Adobe Photoshop. This figure is taken from unpublished data from my laboratory and is representative of at least three independent sets of infections.

Figure 2. *The constitutively active Q646C ErbB4 mutant inhibits drug-resistant colony formation by four human prostate tumor cell lines.*

Cell Line/Infection Virus	Retrovirus Titer (CFU/mL)	Colony Formation Efficiency (% of C127)	Inhibition of Colony Formation (% of vector)
C127			
Mock			
Vector	2.6×10^5	100	
ErbB4-WT	2.9×10^5	100	
ErbB4-Q646C	5.6×10^5	100	
CaPan-1			
Mock			
Vector	1.3×10^2	0.043 ± 0.021 (n=3)	
ErbB4-WT	1.9×10^2	0.061 ± 0.030 (n=4)	None (n=3)
ErbB4-Q646C	6.9×10^0	0.001 ± 0.001 (n=4)	99 ± 2.0 (n=3)
HPAC			
Mock			
Vector	1.6×10^5	65 ± 18 (n=5)	
ErbB4-WT	1.5×10^5	59 ± 15 (n=5)	6.6 ± 26 (n=5)
ErbB4-Q646C	4.1×10^4	7.0 ± 3.8 (n=5)	88 ± 9.0 (n=5)
PANC-1			
Mock			
Vector	1.0×10^4	4.3 ± 1.5 (n=4)	
ErbB4-WT	1.2×10^4	4.0 ± 1.1 (n=4)	None (n=4)
ErbB4-Q646C	6.0×10^3	1.1 ± 0.8 (n=4)	69 ± 25 (n=4)
MIA PaCa-2			
Mock			
Vector	4.7×10^4	20 ± 4.0 (n=4)	
ErbB4-WT	5.8×10^4	22 ± 10 (n=4)	None (n=4)
ErbB4-Q646C	3.6×10^4	5.6 ± 3.0 (n=4)	71 ± 16 (n=4)

Human prostate tumor cell lines were infected and the formation of drug-resistant colonies was visualized as described in the legend for Figure 1. The number of drug-resistant colonies was divided by the volume of virus used in the infection to determine the viral titer for each combination of virus stock and cell line. Colony formation efficiency for each combination of virus stock and cell line was calculated by dividing the viral titer in the cell lines of interest by the viral titer in mouse C127 cells. This ratio will be reduced for those stocks that are growth inhibitory in the cell lines of interest. In the figure shown above, the Q646C mutant inhibits drug-resistant colony formation by the HPAC cell lines by approximately 88%. This value is calculated by dividing 7.0% by 65% and by subtracting this result from 100%. This figure is taken from unpublished data from my laboratory and represents at least 3 independent sets of infections.

Figure 3. *The constitutively active Q646C ErbB4 mutant inhibits drug-resistant colony formation by the MCF10A human mammary epithelial cell line.*
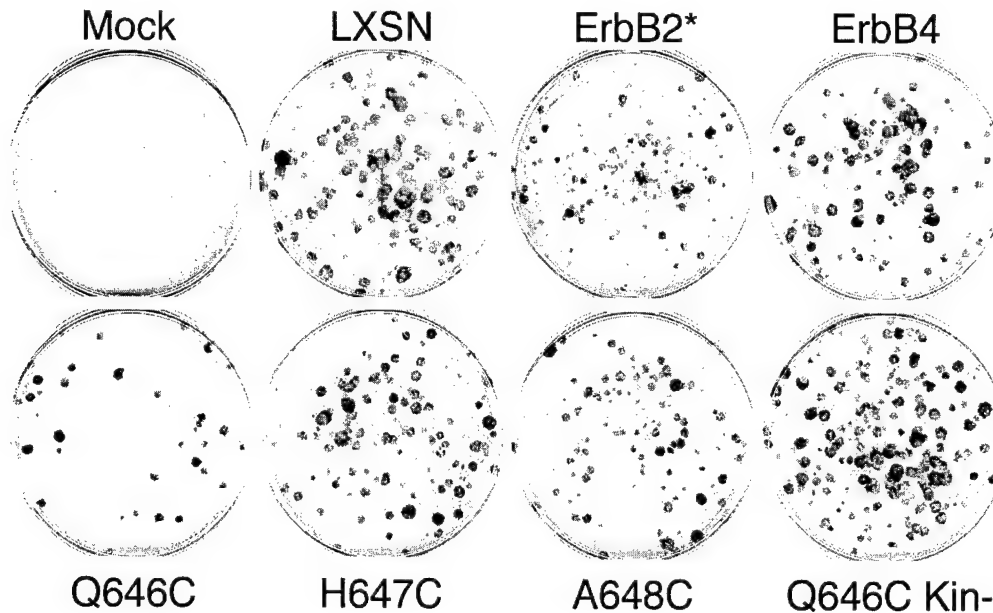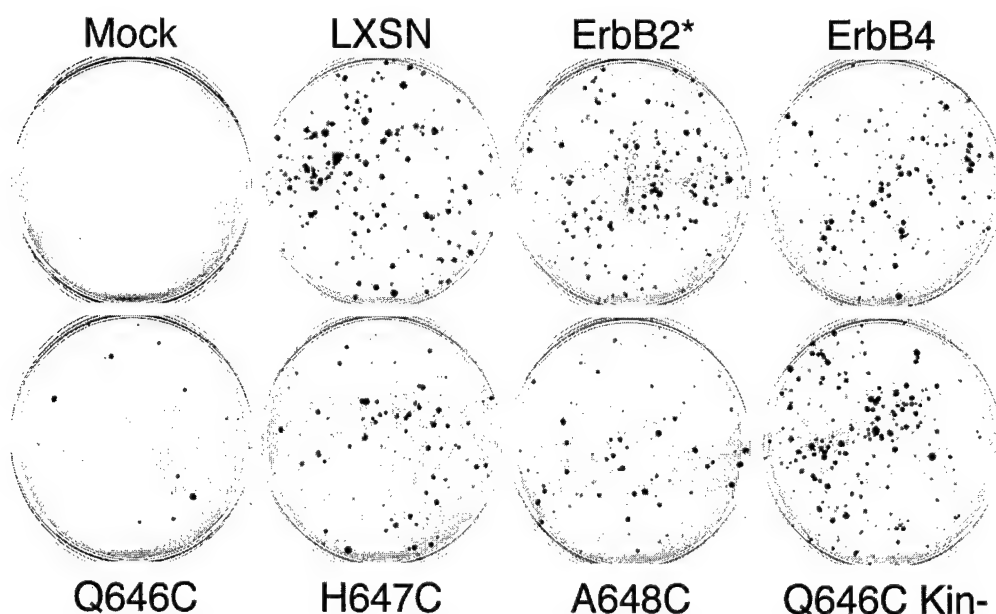

MCF-10A human mammary epithelial cells were infected with recombinant retroviruses that express the neomycin resistance gene along with one of the three constitutively active ErbB4 mutants (Q646C, H647C, and A648C). As controls, MCF-10A cells were infected with a recombinant retrovirus that expresses only the neomycin resistance gene (LXSN), or the neomycin resistance gene together with either wild-type ErbB4 (ErbB4) or a constitutively active ErbB2 mutant (ErbB2*). MCF-10A cells were also mock infected or infected with a recombinant retrovirus that expresses the neomycin resistance gene along with a kinase-deficient, Q646C ErbB4 double mutant (Q646C Kin-). Following infection, cells were incubated in 600 µg/mL G418 to select for infected, drug-resistant cells. After approximately 10 days of selection, colonies of drug-resistant cells were visualized by staining the tissue culture plates with Giemsa. The plates were rinsed, dried, and digitized using a UMAX Astra 2400S flatbed scanner set for a resolution of 300 dots per inch (dpi). This composite figure was assembled using Adobe Photoshop. This figure is taken from unpublished data from my laboratory and is representative of at least five independent sets of infections.

Figure 4. *The constitutively active Q646C ErbB4 mutant inhibits drug-resistant colony formation by the MCF7 human mammary tumor cell line.*

MCF-7 human mammary tumor cells were infected with recombinant retroviruses that express the neomycin resistance gene along with one of the three constitutively active ErbB4 mutants (Q646C, H647C, and A648C). As controls, MCF-7 cells were infected with a recombinant retrovirus that expresses only the neomycin resistance gene (LXSN), or the neomycin resistance gene together with either wild-type ErbB4 (ErbB4) or a constitutively active ErbB2 mutant (ErbB2*). MCF-7 cells were also mock infected or infected with a recombinant retrovirus that expresses the neomycin resistance gene along with a kinase-deficient, Q646C ErbB4 double mutant (Q646C Kin-). Following infection, cells were incubated in 600 µg/mL G418 to select for infected, drug-resistant cells. After approximately 10 days of selection, colonies of drug-resistant cells were visualized by staining the tissue culture plates with Giemsa. The plates were rinsed, dried, and digitized using a UMAX Astra 2400S flatbed scanner set for a resolution of 300 dots per inch (dpi). This composite figure was assembled using Adobe Photoshop. This figure is taken from unpublished data from my laboratory and is representative of at least five independent sets of infections.

Figure 4. *The constitutively active Q646C ErbB4 mutant inhibits drug-resistant colony formation by the MCF7 human mammary tumor cell line.*

MCF-7 human mammary tumor cells were infected with recombinant retroviruses that express the neomycin resistance gene along with one of the three constitutively active ErbB4 mutants (Q646C, H647C, and A648C). As controls, MCF-7 cells were infected with a recombinant retrovirus that expresses only the neomycin resistance gene (LXSN), or the neomycin resistance gene together with either wild-type ErbB4 (ErbB4) or a constitutively active ErbB2 mutant (ErbB2*). MCF-7 cells were also mock infected or infected with a recombinant retrovirus that expresses the neomycin resistance gene along with a kinase-deficient, Q646C ErbB4 double mutant (Q646C Kin-). Following infection, cells were incubated in 600 μg/mL G418 to select for infected, drug-resistant cells. After approximately 10 days of selection, colonies of drug-resistant cells were visualized by staining the tissue culture plates with Giemsa. The plates were rinsed, dried, and digitized using a UMAX Astra 2400S flatbed scanner set for a resolution of 300 dots per inch (dpi). This composite figure was assembled using Adobe Photoshop. This figure is taken from unpublished data from my laboratory and is representative of at least five independent sets of infections.

Figure 5. *The constitutively active Q646C ErbB4 mutant specifically inhibits drug-resistant colony formation by the MCF-10A human mammary epithelial cell line and the MCF-7 and SKBR3 human mammary tumor cell lines.*

Virus	Viral titers				Colony formation efficiency		
	Cell line				Ratios		
Stock	C127	MCF 7	MCF 10A	SKBR3	MCF 7/C127	MCF 10A/C127	SKBR3/C127
Vector	7.41E+05	6.89E+04	3.85E+04	5.64E+04	9.7% ± 1.4%	5.1% ± 0.8%	7.3% ± 1.3%
ErbB2*	3.22E+05	4.15E+04	1.63E+04	2.44E+04	15.2% ± 3.0%	5.1% ± 0.9%	7.0% ± 0.7%
ErbB4 WT	2.03E+05	2.49E+04	1.22E+04	1.51E+04	15.0% ± 3.2%	5.5% ± 0.5%	8.1% ± 1.7%
Q646C	7.18E+05	2.01E+04	1.43E+04	1.60E+04	* 3.0% ± 0.5%	* 1.7% ± 0.2%	* 2.2% ± 0.3%
H647C	9.79E+05	8.01E+04	7.10E+04	5.21E+04	9.6% ± 1.4%	7.6% ± 0.8%	5.5% ± 0.9%
A648C	2.41E+05	2.91E+04	2.17E+04	1.75E+04	13.3% ± 2.0%	8.6% ± 0.7%	6.8% ± 0.9%
Q646C Kin-	4.96E+05	5.92E+04	3.20E+04	4.05E+04	14.7% ± 2.6%	5.6% ± 0.7%	9.1% ± 2.1%

* $p \leq 0.05$ (Comparing Q646C to Vector)

MCF-7, MCF-10A, and SKBR3 cells were infected with recombinant retroviruses that express the neomycin resistance gene along with one of the three constitutively active ErbB4 mutants (Q646C, H647C, and A648C). As controls, these cells were infected with a recombinant retrovirus that expresses only the neomycin resistance gene (Vector), or the neomycin resistance gene together with either wild-type ErbB4 (ErbB4 WT) or a constitutively active ErbB2 mutant (ErbB2*). These cells were also mock infected or infected with a recombinant retrovirus that expresses the neomycin resistance gene along with a kinase-deficient, Q646C ErbB4 double mutant (Q646C Kin-). Following infection, cells were incubated in 600 μg/mL G418 to select for infected, drug-resistant cells. In parallel, mouse C127 cells were infected and 1 mg/mL G418 was used to select for infected cells. After 10-20 days of selection, colonies of drug-resistant cells were visualized by staining the tissue culture plates with Giemsa.

The number of drug-resistant colonies was divided by the volume of virus used in the infection to determine the viral titer for each combination of virus stock and cell line. Colony formation efficiency for each combination of virus stock and cell line was calculated by dividing the viral titer in the cell lines of interest by the viral titer in mouse C127 cells. This ratio will be reduced for those stocks that are growth inhibitory in the cell lines of interest. In the figure shown above, the Q646C mutant inhibits drug-resistant colony formation by the MCF-7 cell lines by approximately 70%. This value is calculated by dividing 3.0% by 9.7% and by subtracting this result from 100%. This figure is taken from unpublished data from my laboratory and represents at least 5 independent sets of infections.
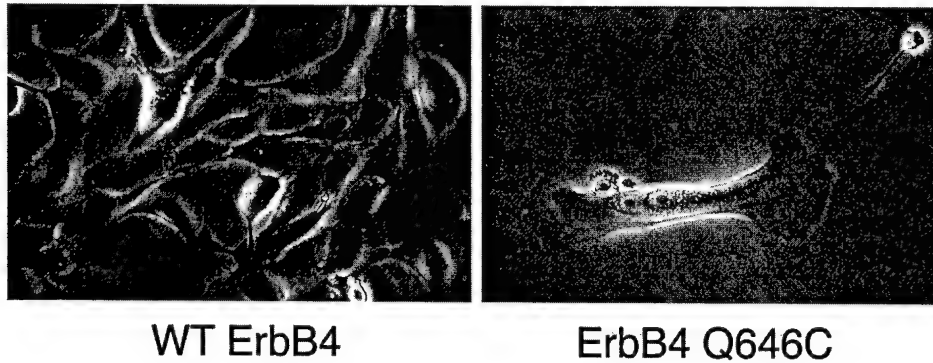
Figure 6. *ErbB4 Tyr1056 appears to be necessary and sufficient to couple ErbB4 to inhibition of colony formation in MCF-10A human mammary epithelial cells.*

Cell Line/ Infection	Retrovirus Titer	Colony Formation Efficiency	Inhibition of Colony Formation
C127			
ErbB4 WT	4.2×10^5	100%	
Q646C	7.8×10^5	100%	
Q646C/K751M	5.0×10^5	100%	
Q646C/TyrChg8	1.9×10^6	100%	
Q646C/TyrChg9-1056F	7.6×10^5	100%	
Q646C/Y1056F	4.7×10^5	100%	
MCF-10A			
ErbB4 WT	2.1×10^4	8.4%	
Q646C	7.9×10^3	1.4%	83%
Q646C/K751M	3.2×10^4	8.5%	0%
Q646C/TyrChg8	1.3×10^4	0.9%	89%
Q646C/TyrChg9-1056F	5.0×10^4	9.8%	0%
Q646C/Y1056F	5.5×10^4	11.7%	0%

MCF-10A cells were infected with recombinant retroviruses that express the neomycin resistance gene along with the Q646C constitutively active ErbB4 mutant as well as with a recombinant retrovirus that expresses the neomycin resistance gene together with wild-type ErbB4 (ErbB4 WT). These cells were also infected with a recombinant retrovirus that expresses the neomycin resistance gene along with a Q646C ErbB4 mutant that also has all nine of the putative sites of tyrosine phosphorylation (Tyr1022, Tyr1056, Tyr1150, Tyr1162, Tyr1188, Tyr1202, Tyr1242, Tyr1258, and Tyr1284) mutated to phenylalanine (Q646C TyrChg9-1056F). These cells were also infected with a recombinant retrovirus that expresses the neomycin resistance gene along with a Q646C ErbB4 mutant that has eight of the nine putative sites of tyrosine phosphorylation mutated to phenylalanine but retains Tyr1056. This mutant is designated Q646C TyrChg8. Finally, these cells were infected with a recombinant retrovirus that expresses the neomycin resistance gene along with a Q646C ErbB4 mutant in which Tyr1056 has been mutated to phenylalanine. Following infection, cells were incubated in 600 µg/mL G418 to select for infected, drug-resistant cells. In parallel, mouse C127 cells were infected and 1 mg/mL G418 was used to select for infected cells. After 10-20 days of selection, colonies of drug-resistant cells were visualized by staining the tissue culture plates with Giemsa.

The number of drug-resistant colonies was divided by the volume of virus used in the infection to determine the viral titer for each combination of virus stock and cell line. Colony formation efficiency for each combination of virus stock and cell line was calculated by dividing the viral titer in the cell lines of interest by the viral titer in mouse C127 cells. This ratio will be reduced for those stocks that are growth inhibitory in the cell lines of interest. In the figure shown above, the Q646C mutant inhibits drug-resistant colony formation by the MCF-10A cell line, as does the Q646C TyrChg8 mutant. However, the Q646C TyrChg9-1056F mutant and the Q646C Y1056F mutant, like the kinase-deficient Q646C/K751M mutant, both fail to inhibit drug-resistant colony formation, as the efficiency of colony formation with this mutant is similar to that observed following infection with the retrovirus that directs expression of wild-type ErbB4.

Figure 7. *The constitutively active Q646C ErbB4 mutant causes growth arrest of MCF-10A human mammary epithelial cells.*

WT ErbB4   ErbB4 Q646C

We infected 1000 MCF-10A or C127 cells with 10000 colony-forming units (cfu) of the recombinant retrovirus that expresses wild-type ErbB4 or with an equal amount of the recombinant retrovirus that expresses the Q646C ErbB4 mutant. At the time of infection, we circled 20 isolated cells using a permanent marker. Four to seven days after infection we examined the marked cells to determine whether they remained present as single cells, whether they were absent, or whether they had formed a colony of cells. Photomicrographs were taken of representative fields. This figure is taken from unpublished data from my laboratory and is representative of the results of three independent sets of experiments.

Figure 8. *The constitutively active Q646C ErbB4 mutant causes growth arrest, but not apoptosis, of MCF-10A human mammary epithelial cells.*

Cell Line	Virus	Cell Fate Following Infection		
		Present	Absent	Colony
C127	Mock	3.0	0.0	17.0
	ErbB4	5.0	0.5	14.5
	ErbB4 Q646C	5.5	0.0	14.5
	ErbB4 vs Q646C	**p=0.841**		**p=0.978**
MCF 10A	Mock	6.0	2.3	11.8
	ErbB4	4.5	2.8	12.8
	ErbB4 Q646C	13.3	1.3	5.5
	ErbB4 vs Q646C	**p=0.003**		**p=0.001**

We infected 1000 MCF-10A or C127 cells with 10000 colony-forming units (cfu) of the recombinant retrovirus that expresses wild-type ErbB4 or with an equal amount of the recombinant retrovirus that expresses the Q646C ErbB4 mutant. At the time of infection, we circled 20 isolated cells using a permanent marker. Four to seven days after infection we examined the marked cells to determine whether they remained present as single cells, whether they were absent, or whether they had formed a colony of cells. The results were tabulated and averages from three independent sets of infections were calculated. This enabled us to determine whether the Q646C ErbB4 mutant specifically couples to growth arrest (cell is present), apoptosis (cell is absent), or has no effect on cell behavior (cell forms a colony). This figure is taken from unpublished data from my laboratory and represents at least three independent infections.

Constitutively Active ErbB4 and ErbB2 Mutants Exhibit Distinct Biological Activities[1]

Desi J. Penington, Ianthe Bryant, and David J. Riese II[2]

Department of Medicinal Chemistry and Molecular Pharmacology,
Purdue University, West Lafayette, Indiana 47907-1333

Abstract

ErbB4 is a member of the epidermal growth factor receptor (EGFR) family of tyrosine kinases, which includes EGFR/ErbB1, ErbB2/HER2/Neu, and ErbB3/HER3. These receptors play important roles both in normal development and in neoplasia. For example, deregulated signaling by ErbB1 and ErbB2 is observed in many human malignancies. In contrast, the roles that ErbB4 plays in tumorigenesis and normal biological processes have not been clearly defined. To identify the biological responses that are coupled to ErbB4, we have constructed three constitutively active ErbB4 mutants. Unlike a constitutively active ErbB2 mutant, the ErbB4 mutants are not coupled to increased cell proliferation, loss of contact inhibition, or anchorage independence in a rodent fibroblast cell line. This suggests that ErbB2 and ErbB4 may play distinct roles in tumorigenesis *in vivo*.

Introduction

ErbB4 (HER4/p180erbB4) is a member of the EGFR[3] (EGFR/ErbB) family of receptor tyrosine kinases. These receptors play important roles in the embryonic development of heart, lung, and nervous tissues (1–4), and they have been implicated in the progression of metastatic disease. For example, EGFR/ErbB1 is overexpressed, amplified, or mutated in a number of human malignancies including breast, ovary, prostate, and lung cancers (5–7). ErbB2 overexpression cor-

relates with tumor aggressiveness and poor prognosis in node-positive breast cancer patients (reviewed in Ref. 8). Finally, ErbB3 overexpression is observed in a subset of human mammary and gastric cancers (9, 10).

Some reports indicate that increased ErbB4 expression or signaling is associated with tumorigenesis. ErbB4 overexpression has been observed in a variety of cancers, including tumors of the thyroid, breast, and gastrointestinal tract (11–14). However, the prognostic significance of ErbB4 expression in tumors may also depend on which ErbB family members are coexpressed with ErbB4. In the case of childhood medulloblastoma (one of the most common solid tumors of childhood), patients with tumors overexpressing both ErbB2 and ErbB4 have a significantly worse prognosis than patients with tumors that overexpress either receptor alone (15).

Other reports indicate that increased ErbB4 expression or signaling correlates with tumor cell differentiation and reduced aggressiveness. ErbB4 overexpression in breast tumors is associated with progesterone receptor and estrogen receptor expression and a more favorable prognosis (16–17). In contrast, ErbB2 overexpression varies inversely with progesterone receptor and estrogen receptor levels and indicates tumors that are more likely to be metastatic and fatal (18). In one survey of common solid human cancers, the loss of ErbB4 expression is seen in a significant percentage of breast, prostate, and head and neck malignancies (19). These findings raise the intriguing possibility that ErbB4 is unique to the ErbB family of receptors in that ErbB4 expression and signaling may couple to reduced tumorigenesis or tumor cell proliferation. However, in the face of the conflicting evidence we have summarized here, it remains unclear what general or specific roles ErbB4 plays in differentiation, tumor suppression, or proliferation.

Efforts to elucidate ErbB4 function have been hampered by many factors. There are no known agonists or antagonists specific to the ErbB4 receptor. All of the peptide hormones of the EGF family that are capable of binding ErbB4 also bind at least one other ErbB family member. For example, epiregulin and betacellulin bind and activate both ErbB1 and ErbB4 (20, 21). Furthermore, ligands that do not bind an ErbB family receptor can still activate signaling by that receptor in *trans* through ligand-induced receptor heterodimerization (reviewed in Refs. 22, 23). For example, EGF stimulates ErbB2 tyrosine phosphorylation when ErbB2 is coexpressed with ErbB1, whereas EGF will not stimulate ErbB2 tyrosine phosphorylation in the absence of ErbB1 (24). Consequently, ligands that bind and directly activate ErbB4 (neuregulin, betacellulin, and epiregulin) also stimulate ErbB1, ErbB2, and ErbB3 signaling (Refs. 20, 21, 25, 26; reviewed in Refs. 22, 23). Therefore, in most contexts it is virtually impossible to use an EGF family hormone to study the functional consequences of ErbB4 signaling.

To study ErbB4 function, we have opted to generate ErbB4 mutants that contain a cysteine substitution in the extracellular domain. This is predicted to result in constitutively dimerized and constitutively active ErbB4 mutants. Introducing cysteine residues to form covalently linked, dimeric, constitutively active receptor tyrosine kinases is not novel. This strategy has been used to generate dimeric, constitutively active mutants of EGFR/ErbB1 and ErbB2 (27, 28). Cysteine substitutions also lead to constitutively active mutants of the fibroblast growth factor receptors 2 and 3 (29, 30).

Here we report the generation and characterization of three constitutively active ErbB4 mutants. These mutants were generated through the introduction of a cysteine residue in the extracellular region of ErbB4. These mutants exhibit increased ligand-independent ErbB4 tyrosine phosphorylation, dimerization, and kinase activity. However, these constitutively active ErbB4 mutants do not induce increased proliferation, loss of contact inhibition, or anchorage-independent growth in FR3T3 fibroblasts. In contrast, a constitutively active ErbB2 mutant does induce increased proliferation, loss of contact inhibition, and anchorage-independent growth in FR3T3 fibroblasts. These results suggest that ErbB4 and ErbB2 couple to different signaling pathways and biological responses. These results also suggest that ErbB4 and ErbB2 may play distinct roles in tumorigenesis in vivo.

Results

ErbB4 Mutants Are Constitutively Tyrosine Phosphorylated.
We substituted a single cysteine for amino acids Pro-645, Gln-646, His-647, Ala-648, and Arg-649 in the juxtamembrane region of the ErbB4 extracellular domain. These ErbB4 mutants (P645C, Q646C, H647C, A648C, and R649C) were generated in the context of the pLXSN-ErbB4 recombinant retroviral expression vector (26). Because these cysteine substitutions might cause inappropriate protein folding and decreased protein stability, we assayed the ErbB4 mutants for stable expression. We transfected the recombinant retroviral vectors containing the ErbB4 mutant constructs into the Ψ2 ecotropic retrovirus packaging cell line, selected for stable transformants, and generated pooled cell lines. We harvested low-titer ecotropic retrovirus stocks from these cell lines, and we analyzed the expression and tyrosine phosphorylation of the ErbB4 mutants in these cell lines. Three ErbB4 mutants (Q646C, H647C, and A648C) exhibit abundant expression and ligand-independent tyrosine phosphorylation (data not shown). However, the R649C ErbB4 mutant is not efficiently expressed, and the P645C mutant does not display ligand-independent tyrosine phosphorylation (data not shown).

Previous studies indicate that transfection and subsequent overexpression of ErbB family receptors lead to ligand-independent receptor tyrosine phosphorylation (31–33). Consequently, we were concerned that the ligand-independent phosphorylation of the Q646C, H647C, and A648C ErbB4 mutants in the transfected Ψ2 cells was a consequence of overexpression. Therefore, we infected the PA317 amphotropic retrovirus packaging cell line with the ErbB4 mutant recombinant ecotropic retroviruses at low multiplicities of infection (<0.1), selected for infected cells, and generated
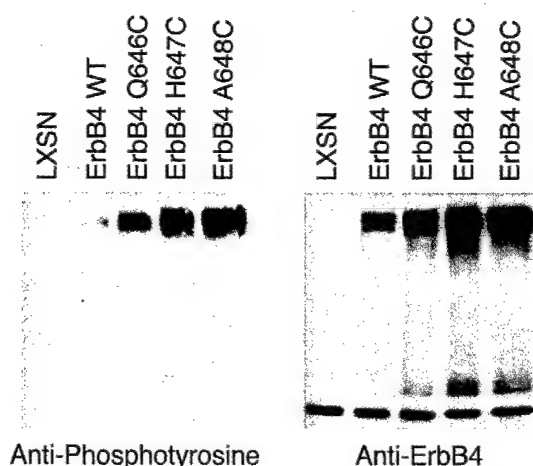

Fig. 1. ErbB4 mutants are constitutively tyrosine phosphorylated. ErbB4 expression and tyrosine phosphorylation were assayed in PA317 cells infected with retroviruses that direct the expression of wild-type ErbB4 or the ErbB4 mutants. Cells infected with the LXSN recombinant retrovirus vector control served as the negative control. Lysates were prepared from each of the cell lines, and ErbB4 was immunoprecipitated from 1000 μg of each lysate. Samples were resolved by SDS-PAGE, electroblotted to nitrocellulose, and immunoblotted with an anti-phosphotyrosine antibody (left panel). The blot was then stripped and probed with an anti-ErbB4 rabbit polyclonal antibody (right panel). The band at the top of the blots represents ErbB4.

pooled cell lines. Because these cell lines were generated by infection at low multiplicities of infection, it is likely that each cell contains only one or two copies of the ErbB4 expression construct. This reduces the likelihood of ErbB4 overexpression in these cell lines.

We analyzed ErbB4 expression and tyrosine phosphorylation in the PA317 cell lines by anti-ErbB4 immunoprecipitation and either anti-ErbB4 (Fig. 1, right panel) or anti-phosphotyrosine (Fig. 1, left panel) immunoblotting. As expected, cells infected with the LXSN vector control retrovirus do not exhibit ErbB4 expression (Fig. 1, right panel) or tyrosine phosphorylation (Fig. 1, left panel). Cells infected with the wild-type or mutant ErbB4 retroviruses exhibit ErbB4 expression (Fig. 1, right panel). However, cells infected with the mutant ErbB4 retroviruses exhibit abundant ErbB4 tyrosine phosphorylation, whereas cells infected with the wild-type ErbB4 retrovirus exhibit minimal ErbB4 tyrosine phosphorylation (Fig. 1, left panel).

Quantification of the chemilumigrams shown in Fig. 1 suggests that the expression levels of the three ErbB4 mutants is less than three times greater than the amount of wild-type ErbB4 expression (Table 1). In contrast, the amounts of tyrosine phosphorylation of the three ErbB4 mutants appear to be much greater than the amount of wild-type ErbB4 tyrosine phosphorylation. Moreover, the ratios of ErbB4 tyrosine phosphorylation to ErbB4 expression for the three ErbB4 mutants appear to be at least four times greater than the ratio for wild-type ErbB4. These data suggest that the three ErbB4 mutants exhibit greater amounts of tyrosine phosphorylation on a per-molecule basis than does wild-type ErbB4. Consequently, these data indicate that the Q646C, H647C, and A648C ErbB4 mutants are constitutively active for signaling.

Table 1 The Q646C, H647C, and A648C ErbB4 mutants exhibit increased normalized tyrosine phosphorylation

Cell line	ErbB4 tyrosine phosphorylation	ErbB4 expression	Ratio
Wild-type ErbB4	210000	1800000	0.12
ErbB4 Q646C	1900000	3300000	0.58
ErbB4 H647C	2900000	4700000	0.62
ErbB4 A648C	4000000	4500000	0.89

ErbB4 Mutants Have Increased *in Vitro* Kinase Activity.
Next, we assessed whether the increased tyrosine phosphorylation of the three ErbB4 mutants correlates with increased kinase activity. Equal amounts of the same lysates used for the experiments described in Fig. 1 were immunoprecipitated with an anti-ErbB4 polyclonal antibody. Kinase reactions were performed on the immunoprecipitates in the presence of [γ-^{32}P]ATP. The reaction products were resolved by SDS-PAGE on a 7.5% acrylamide gel. The gel was dried, and the reaction products were visualized by autoradiography.

In Fig. 2, we show that PA317 cells infected with the LXSN vector control retrovirus lack detectable ErbB4 kinase activity. Moreover, PA317 cells that express the three constitutively active ErbB4 mutants exhibit greater ErbB4 tyrosine kinase activity than cells that express wild-type ErbB4. Quantification of the bands on the autoradiogram indicates that the Q646C and H647C ErbB4 mutants exhibit approximately five times more kinase activity than does wild-type ErbB4, whereas the A648C ErbB4 mutant exhibits approximately nine times more kinase activity than does wild-type ErbB4. Given that the expression of the ErbB4 mutants (in these same lysates) is somewhat greater than the expression of wild-type ErbB4 (Fig. 1 and Table 1), it appears that the intrinsic kinase activity of the three ErbB4 mutants is three to four times greater than the intrinsic kinase activity of wild-type ErbB4.

Constitutively Active ErbB4 Mutants Do Not Induce a Loss of Contact Inhibition. Once we determined that the Q646C, H647C, and A648C ErbB4 mutants are constitutively active for signaling, we performed experiments using these mutants to identify the biological events coupled to ErbB4 signaling. A common assay for genes that encode growth control or signaling proteins involves introducing the gene into an established rodent fibroblast cell line and assaying for foci of piled-up cells. These foci indicate a loss of contact inhibition, a common attribute of malignant cells. Thus, this gene transfer assay is commonly used to identify genes that encode proteins that are coupled to malignant growth transformation.

Conflicting results have been obtained from assays for growth transformation by ErbB4. Transfection and consequent overexpression of ErbB4 induces foci (loss of contact inhibition) in NIH 3T3 clone 7 cells in the absence of ligand. Moreover, in these cells focus formation was stimulated by the ErbB4 ligand neuregulin 2β. In contrast, NIH 3T3 clone 7d cells (which lack EGFR expression) transfected with wild-type ErbB4 did not form foci in the presence or absence of neuregulin 1β; however, ErbB4 cotransfected with EGFR/ErbB1 or ErbB2 does induce foci in these cells (32, 33). One
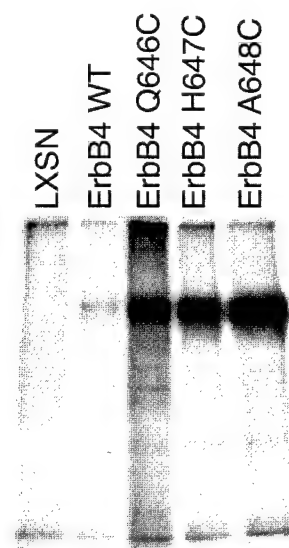

Fig. 2. Q646C, H647C, and A648C mutants exhibit increased *in vitro* kinase activity. Equal amounts of protein lysates (1000 μg) from PA317 cells that stably express wild-type ErbB4 or the ErbB4 mutants (Q646C, H647C, and A648C) were immunoprecipitated with an anti-ErbB4 rabbit polyclonal antibody. Lysates from PA317 cells that express the LXSN vector served as the negative control. Kinase reactions were performed on the immunoprecipitates in the presence of [γ-^{32}P]ATP. The products were resolved by SDS-PAGE. The gel was dried overnight and exposed to X-ray film for ~20 h to visualize the products of the kinase reactions.

possible explanation is that ErbB4 lacks intrinsic transforming activity but does permit EGFR/ErbB1 or ErbB2 signaling and coupling to growth transformation in the presence of an ErbB4 ligand.

To test whether ErbB4 signaling is sufficient to transform the growth of cultured rodent fibroblasts, FR3T3 fibroblasts were infected with 200 cfu of the ErbB4 mutant recombinant ecotropic retrovirus stocks and assayed for focus formation. Cells infected with 200 cfu of the LXSN vector control recombinant ecotropic retrovirus and with 200 cfu of the wild-type ErbB4 recombinant ecotropic retrovirus served as negative controls. Cells infected with 200 cfu of the constitutively active (V664E transmembrane domain) mutant ErbB2* retrovirus served as a positive control.

FR3T3 cells infected with the ErbB2* retrovirus had formed foci within 9 days after infection, whereas cells infected with the vector control retrovirus had not (Fig. 3). Furthermore, cells infected with the wild-type or mutant ErbB4 retroviruses had not formed foci within 9 days after infection. Within 18 days after infection, the foci arising from FR3T3 cells infected with the ErbB2* retrovirus had completely covered the surface of the tissue culture plate and had began to detach from the surface of the plate (data not shown). Within 18 days after infection, FR3T3 cells infected with the mutant ErbB4 retroviruses had formed relatively high-density clumps (data not shown). These high-density clumps did not exhibit the overlapping cell processes characteristic of foci (data not shown). The cells comprising these clumps were cloned and expanded into cell lines, as were cells from less dense regions of the cell monolayers. The cells from the clumps are morphologically indistinguishable from cells derived from the
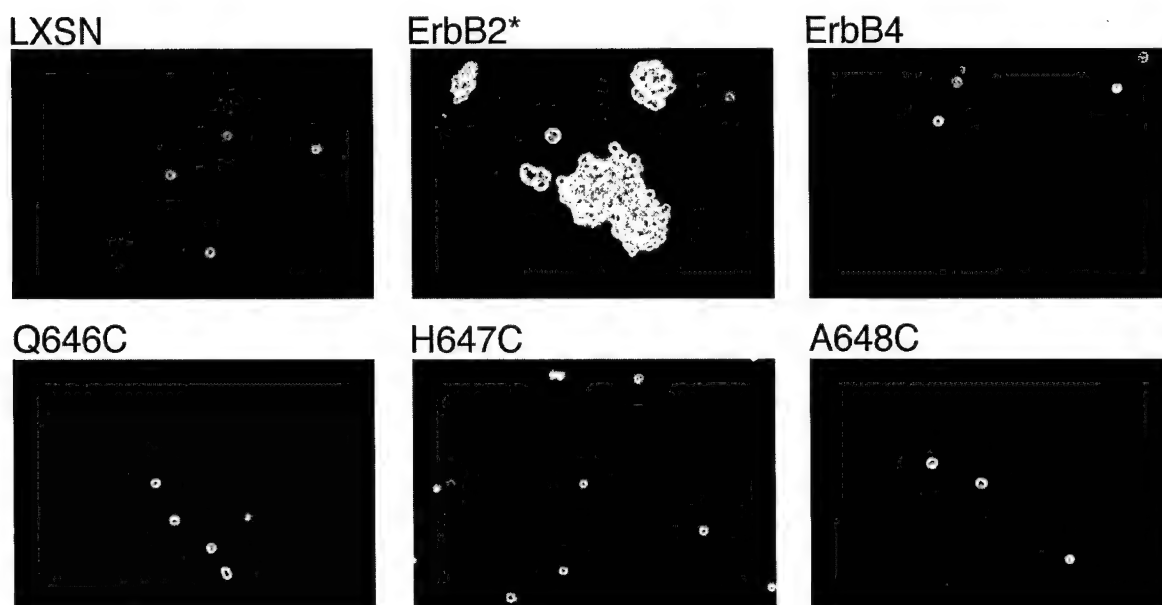
LXSN

ErbB2*

ErbB4

Q646C

H647C

A648C

Fig. 4.   Constitutively active ErbB4 receptors do not induce growth in semisolid medium. FR3T3 cells that stably express the LXSN vector control, the constitutively active ErbB2 mutant (ErbB2*), wild-type ErbB4, or the constitutively active ErbB4 mutants (Q646C, H647C, and A648C) were seeded in semisolid medium at a density of 2×10^4 cells/ml in 60-mm dishes. The cells were incubated for 10 days, after which images were recorded by photomicroscopy. Images shown are representative of those obtained in three independent experiments.

Fig. 5.   Constitutively active ErbB4 mutants do not increase the growth rate of FR3T3 fibroblasts. FR3T3 cells that express the LXSN vector control, the constitutively active ErbB2* mutant, wild-type ErbB4, or the constitutively active ErbB4 mutants (Q646C, H647C, and A648C) were plated at a density of 2×10^4 cells in 60-mm dishes (700 cells/cm²) and were incubated for 1–10 days. Cells were counted daily to assess growth rates and saturation densities. The means for three independent experiments; bars, SE.

FR3T3 Growth Curves

and selected for stable infection using G418. As controls, we also infected FR3T3 cells with 200 cfu of the vector control retrovirus, 200 cfu of the ErbB2* retrovirus, and with 200 cfu of the wild-type ErbB4 retrovirus. Drug-resistant colonies were pooled and expanded into stable cell lines. The cell lines were starved of serum in the presence of 500 μM Na$_3$VO$_4$ (34) to decrease the background level of tyrosine phosphorylation and to increase the phosphorylation of the

Table 2 Constitutively active ErbB4 mutants do not increase the saturation density of FR3T3 fibroblasts

Saturation Densities	
LXSN	$5.8 \pm 0.3 \times 10^5$
ErbB2*	$5.4 \pm 0.1 \times 10^6$
ErbB4	$6.1 \pm 0.5 \times 10^5$
Q646C	$6.6 \pm 0.6 \times 10^5$
H647C	$7.6 \pm 0.7 \times 10^5$
A648C	$6.6 \pm 0.4 \times 10^5$

constitutively active ErbB4 mutants. We prepared lysates and analyzed ErbB4 expression and tyrosine phosphorylation by precipitation with an anti-ErbB4 antibody and sequential anti-phosphotyrosine and anti-ErbB4 immunoblotting.

In Fig. 6, *lower panel,* we show that ErbB4 expression is detectable in the FR3T3 cell lines infected with the wild-type ErbB4 retrovirus or the constitutively active ErbB4 mutant retroviruses. However, ErbB4 tyrosine phosphorylation is observed only in the FR3T3 cell lines infected with the constitutively active ErbB4 mutant retroviruses (Fig. 6, *upper panel*). The amount of phosphorylation exhibited by the ErbB4 mutants is less than the amount of phosphorylation exhibited by the constitutively active ErbB2 mutant. Furthermore, the expression of wild-type ErbB4 appears to be less than the expression of the ErbB4 mutants. Nonetheless, these data suggest that the apparent failure of the constitutively active ErbB4 mutants to transform the growth of FR3T3 fibroblasts is not attributable to an absence of expression and tyrosine phosphorylation of these mutants in these cells.

Discussion

In this report, we describe the construction and initial characterization of three constitutively active ErbB4 mutants. These mutants display increased dimerization (data not shown) and ligand-independent tyrosine phosphorylation and kinase activity. In these respects, the ErbB4 mutants resemble constitutively active mutants of ErbB2 or EGFR. However, unlike constitutively active ErbB2 mutants, these mutants are not coupled to malignant growth transformation in FR3T3 fibroblasts; they do not induce foci, anchorage-independent growth, or increases in the growth rate or saturation density. These data suggest that ErbB2 and ErbB4 play distinct roles in tumorigenesis *in vivo*. This conclusion is supported by the observation that NIH3T3 clone 7d cells do not form foci after ErbB4 transfection and treatment with the ErbB4 ligand neuregulin but do form foci after ErbB2 and ErbB4 cotransfection and neuregulin treatment (32, 33).

Of course, another potential explanation is that the amounts of tyrosine phosphorylation displayed by the three constitutively active ErbB4 mutants are insufficient to couple to malignant growth transformation in fibroblasts. This is consistent with the observation that the three constitutively active ErbB4 mutants are less phosphorylated than the constitutively active ErbB2 mutant (Fig. 6). However, anti-phosphotyrosine immunoblotting is not a sensitive method for assessing ErbB family receptor signaling and coupling to biological responses. Indeed, the neuregulin concentration
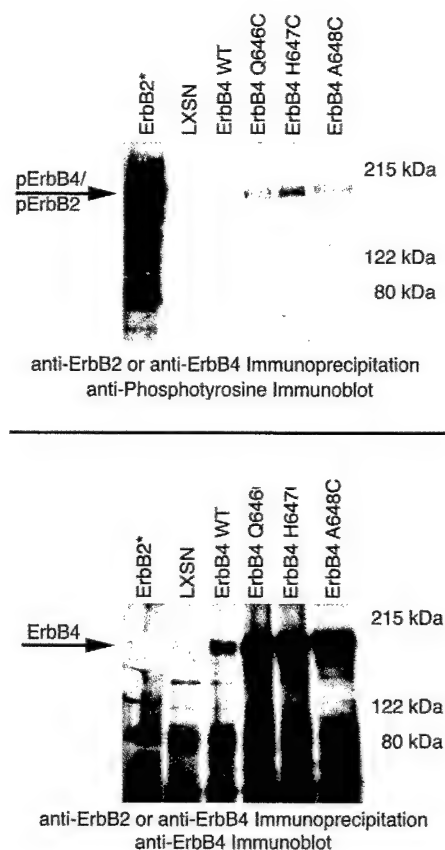

anti-ErbB2 or anti-ErbB4 Immunoprecipitation
anti-Phosphotyrosine Immunoblot

anti-ErbB2 or anti-ErbB4 Immunoprecipitation
anti-ErbB4 Immunoblot

Fig. 6. Constitutively active ErbB4 mutants are expressed and are constitutively tyrosine phosphorylated in FR3T3 cells. ErbB4 expression and tyrosine phosphorylation were assayed in FR3T3 cells infected with retroviruses that direct the expression of wild-type ErbB4 or the ErbB4 mutants. Cells infected with the LXSN recombinant retrovirus control or with the ErbB2* retrovirus served as controls. Lysates were prepared from each of the cell lines, and ErbB receptors were precipitated from 1.5 mg of each lysate using protein A-Sepharose and either an anti-ErbB4 rabbit polyclonal antibody or an anti-ErbB2 rabbit polyclonal antibody. Samples were resolved by SDS-PAGE, electroblotted to nitrocellulose, and immunoblotted with an anti-phosphotyrosine antibody (*upper panel*). The blot was then stripped and probed with an anti-ErbB4 rabbit polyclonal antibody (*lower panel*). *Arrows,* positions of ErbB2 and ErbB4 on the blots.

required for maximal ErbB4 tyrosine phosphorylation is ~10-fold greater than the neuregulin concentration sufficient for maximal ErbB family receptor coupling to biological responses. Furthermore, the neuregulin concentration sufficient for maximal ErbB family receptor coupling to biological responses stimulates, at most, only modest amounts of ErbB4 tyrosine phosphorylation (26). Thus, it is not likely that the failure of the constitutively active ErbB4 mutants to couple to malignant growth transformation in fibroblasts is attributable to insufficient ErbB4 tyrosine phosphorylation.

Clearly, additional work is necessary to define the roles that ErbB4 plays in tumorigenesis and in regulating cellular functions *in vivo*. However, important clues have emerged to guide these future studies. In a significant percentage of breast tumor samples, ErbB4 expression correlates with estrogen receptor expression, which indicates a favorable prognosis (16–17). Furthermore, ErbB4 expression is fre-

quently lost in tumors of the breast and prostate (19). Finally, ligands for ErbB4 can induce terminal differentiation and growth arrest of some mammary tumor cell lines (35–37). These data indicate that ErbB4 signaling may be coupled to differentiation, growth arrest, and tumor suppression. The ErbB4 mutants described in this study will enable us to evaluate this hypothesis. Indeed, preliminary data from our laboratory indicate that the Q646C ErbB4 mutant causes reduced colony formation in plastic dishes by a number of cultured human breast and prostate tumor cell lines.

We will also perform additional studies to characterize the biochemistry of signaling by the three ErbB4 mutants. Whereas these mutants exhibit greater ligand-independent tyrosine phosphorylation and autokinase activity than the wild-type receptor, it is unclear whether this is attributable to increased intrinsic kinase activity or attributable to increased availability of the substrate. Additional experiments are warranted to distinguish between these two possibilities.

Another area of future study will focus on identifying the mechanisms by which ErbB4 is coupled to biological responses. Initial studies will identify the sites of ErbB4 tyrosine phosphorylation for these mutants. If our preliminary studies indicating that the Q646C ErbB4 mutant is coupled to prostate and mammary tumor cell growth arrest hold true, then we will use genetic strategies to identify the sites of ErbB4 tyrosine phosphorylation that are sufficient and necessary to couple the Q646C ErbB4 mutant to this biological response. A similar strategy has been used to identify the sites of ErbB2 and platelet-derived growth factor receptor tyrosine phosphorylation that are critical for coupling these receptors to biological responses (38, 39).

Once we have identified the site(s) of tyrosine phosphorylation that is sufficient for coupling to biological responses, we will identify signaling proteins that bind this phosphorylation site and couple it to biological responses. Using this strategy, we will begin to characterize the ErbB4 signaling pathway. Our prediction is that the three constitutively active ErbB4 mutants are phosphorylated on different tyrosine residues and that these mutants differentially couple to biological responses. We have shown previously that different ErbB4 ligands cause phosphorylation on different sites on ErbB4 and differential coupling to biological responses (40). Moreover, one cysteine substitution mutation in the rat ErbB2 extracellular domain (V656C) results in low amounts of constitutive receptor tyrosine phosphorylation and efficient coupling to malignant growth transformation in rodent fibroblasts. In contrast, another rat ErbB2 extracellular domain cysteine substitution mutant (T657C) exhibits very high levels of constitutive receptor tyrosine phosphorylation but a relatively low amount of coupling to malignant growth transformation in rodent fibroblasts (28).

We were somewhat surprised to discover that the three constitutively active ErbB4 mutants failed to couple to malignant growth transformation in a rodent fibroblast cell line. Nonetheless, these mutants will enable us to assess ErbB4 function in a wide variety of cell, tissue, and organismal contexts. Given that ErbB4 appears to regulate diverse functions in a number of distinct contexts, much work remains to complete this story.

Materials and Methods

Cell Lines, Cell Culture, and Antibodies. The Ψ2, PA317, C127, and FR3T3 cell lines were generous gifts from Daniel DiMaio (Yale University New Haven, CT). All cell lines were propagated in DMEM supplemented with 10% FBS, 50 IU/ml penicillin, 50 μg/ml streptomycin (Mediatech), and 0.25 μg/ml Fungizone (Amphotericin B; Life Technologies, Inc.). Recombinant cell lines generated in the course of the experiments described in this report were propagated in the medium described above supplemented with 200 μg/ml G418 (Mediatech).

The anti-ErbB4 mouse monoclonal (SC-8050), anti-ErbB4 rabbit polyclonal (SC-283), and anti-ErbB2 rabbit polyclonal (C-18) antibodies were purchased from Santa Cruz Biotechnology. Goat antimouse and goat antirabbit horseradish peroxidase-conjugated antibodies were purchased from Pierce. Enhanced chemiluminescence (ECL) Western blotting reagents, Redivue adenosine 5'-[γ-^{32}P]triphosphate, and Protein-A Sepharose (CL-4B) were purchased from Amersham Pharmacia Biotech. The 4G10 anti-phosphotyrosine mouse monoclonal antibody was purchased from Upstate Biotechnology.

Plasmids. The recombinant retroviral vector pLXSN (41) was obtained from Daniel DiMaio (Yale University). This construct contains two recombinant LTRs derived from the Maloney murine leukemia virus and the Maloney murine sarcoma virus. These LTRs flank the Ψ packaging signal and the aminoglycoside 3'-phosphotransferase (Neo^R) gene under the transcriptional control of the SV40 early promoter. The Neo^R gene confers resistance to the aminoglycoside antibiotic G418 (geneticin; Life Technologies, Inc.).

The recombinant retroviral construct pLXSN-ErbB4 (26) was generated by subcloning the human ErbB4 cDNA into pLXSN. In this construct, the ErbB4 cDNA is under the transcriptional control of the upstream LTR. The recombinant retroviral construct pLXSN-ErbB2* (42) was a gift of Lisa Petti (Albany Medical College, Albany, NY). It was generated by subcloning the cDNA encoding the constitutively active rat ErbB2 mutant (V664E transmembrane domain mutant, ErbB2*) into pLXSN. In this construct, the ErbB2* cDNA is under the transcriptional control of the upstream LTR.

ErbB4 Mutagenesis. The plasmid pLXSN-ErbB4 was used as the template for site-directed mutagenesis (QuikChange Site Directed Mutagenesis kit; Stratagene) to construct the putative constitutively active ErbB4 mutants. The mutants were constructed by introducing mutations that substitute a cysteine residue for proline 645, glutamine 646, histidine 647, alanine 648, or arginine 649 in the ErbB4 extracellular juxtamembrane domain. These mutants are denoted as follows: P645C, Q646C, H647C, A648C, and R649C. A new restriction enzyme site was also engineered in each mutant to facilitate the identification of the mutants. The following primers were used for mutagenesis. "T" denotes the upper primer, whereas "B" denotes the lower primer. The novel cysteine codons and anticodons are indicated by bold type, the point mutations that create the novel cysteine residues are double underlined, and the novel restriction enzyme sites are singly underlined.

P645CT:5'-ATTTACTACCCATGG<u>ACCGGT</u>CATTCCACTT
TA<u>**TGC**</u>CAACATGCTAGAACTCCC-3'
P645CB:5'-GGGAGTTCTAGCATGTT**GGCA**TAAAGTGGA
ATG<u>ACCGGT</u>CCATGGGTAGTAAAT-3'
Q646CT:5'-TACTACCCATGG<u>ACCGGT</u>CATTCCACTTTAC
CA<u>**TGC**</u>CATGCTAGAACTCCCCTG-3'
Q646CB:5'-CAGGGGAGTTCTAGCATG**GGCA**TGGTAAAGT
GGAATG<u>ACCGGT</u>CCATGGGTAGTA-3'
H647CT:5'-CATTTACTACCCATGG<u>ACCGGT</u>CATTCCACT
TTACCACAA<u>**TGT**</u>GCTAGAACTCCCCT-3'
H647CB:5'-AGGGGAGTTCTAGC<u>**ACA**</u>TTGTGGTAAAGTG
GAATG<u>ACCGGT</u>CCATGGGTAGTAAATG-3'
A648CT:5'-TCCACTTTACCACAACAT<u>**TGT**</u>AGAA<u>CTCCTC</u>
TGATTGCAGCTGGA-3'
A648CB:5'-TCCAGCTGCAATCA<u>GAGGAG</u>TTCT<u>**ACA**</u>ATG
TTGTGGTAAAGTGGA-3'
R649CT:5'-ACTTTACCACAACATGC<u>**TTGC**</u>A<u>CTCCTC</u>TGA
TTGCAGCTGGA-3'
R649CB:5'-TCCAGCTGCAATCA<u>GAGGAG</u>T<u>**GCA**</u>AGCATG
TTGTGGTAAAGT-3'

The site-directed mutagenesis reactions were performed according to the manufacturer's instructions. Standard techniques (43) were used for bacterial transformations, small-scale plasmid DNA preparations, restriction enzyme analysis of the clones, and large-scale plasmid DNA preparations. Positive clones were sequenced by the University of Wisconsin-Madison Biotechnology Center to confirm their identity.

Production of Recombinant Retroviruses and Retroviral Infections. The ErbB4 mutant constructs were transfected using standard techniques (44, 45) into the ψ2 ecotropic retrovirus packaging cell line (46) to generate cell lines that express the ErbB4 mutants and to package the constructs into low-titer ecotropic retrovirus particles (44, 45). ψ2 cells were transfected with the pLXSN vector control plasmid, pLXSN-ErbB4, and pLXSN-ErbB2* to generate control cell lines and recombinant ecotropic retroviruses. The PA317 amphotropic packaging cell line (47) and the FR3T3 rat fibroblast cell line were infected with the ecotropic recombinant retroviruses using standard techniques (44, 45) to generate additional cell lines that express the ErbB4 mutants.

Immunoblot Assays for Receptor Tyrosine Phosphorylation and Expression. The analysis of ErbB4 and ErbB2 tyrosine phosphorylation by immunoprecipitation and anti-phosphotyrosine immunoblotting has been described previously (21, 26). Briefly, cell lysates were generated, and protein content was quantified using a Coomassie Protein Assay Reagent (Ref. 48; Pierce Chemical). ErbB2 or ErbB4 was immunoprecipitated from equal amounts of protein using specific antibodies. The immunoprecipitates were resolved by SDS-PAGE on a 7.5% acrylamide gel and were electrotransferred onto nitrocellulose. The blots were probed with the anti-phosphotyrosine monoclonal antibody 4G10. Antibody binding was detected and visualized using a goat antimouse horseradish peroxidase-coupled antibody and enhanced chemiluminescence. The blots were then stripped and probed with the anti-ErbB4 polyclonal antibody to as-

sess ErbB4 expression levels. Antibody binding was detected and visualized using a goat antimouse horseradish peroxidase-coupled antibody and enhanced chemiluminescence.

The amounts of receptor tyrosine phosphorylation and expression were quantified by digitizing the chemilumigrams using a Linotype-Hell Jade two-dimensional scanning densitometer set at 600-dpi resolution. The bands on the images were quantified using NIH Image for Macintosh v1.6 software. Values are expressed as arbitrary units. Background levels were computed using the vector control lanes and were subtracted from the gross values to produce net receptor expression and tyrosine phosphorylation values. The digitized images were also cropped and annotated using Adobe Photoshop for Macintosh v3.0.5 software.

In Vitro **Kinase Assay.** ErbB2 and ErbB4 were immunoprecipitated from protein extracts from PA317 cells as described previously (26). Immune complex kinase reactions were performed as described previously (31). Briefly, 35 μl of protein A-Sepharose and 5 μl of anti-ErbB2 or anti-ErbB4 rabbit polyclonal antibodies were used to immunoprecipitate the receptors from lysates containing the same amount of protein (1000 μg). Immunoprecipitates were washed five times in 500 μl of kinase buffer [20 mM Tris-HCl (pH 7.4), 5 mM MgCl$_2$, and 3 mM MnCl$_2$]. After the last wash, the samples were resuspended in 100 μl of kinase buffer supplemented with 10 μCi of [γ-^{32}P]ATP and were incubated for 10 min at room temperature to permit the kinase reaction to occur. The beads were then washed two times in NET-N buffer (49) and boiled for 5 min in SDS-PAGE protein sample buffer. The samples were resolved by SDS-PAGE on a 7.5% acrylamide gel. The gels were dried overnight and exposed to X-ray film for ~20 h. The autoradiograms were digitized using a Linotype-Hell Jade two-dimensional scanning densitometer set at 600-dpi resolution. The bands on the images were quantified using NIH Image for Macintosh v1.6 software. Values are expressed as arbitrary units. Background levels were computed using the vector control lanes and were subtracted from the gross values to produce net kinase activity values. The digitized images were also cropped and annotated using Adobe Photoshop for Macintosh v3.0.5 software.

Focus Formation Assay for Loss of Contact Inhibition. FR3T3 and C127 cells were infected with recombinant ecotropic retroviruses as described earlier and in reports published previously (44, 45). Briefly, 60-mm dishes of cells at ~70% confluence were infected with ecotropic retrovirus stocks. Approximately 24 h after infection, cells were passaged into three 60-mm dishes. Cells were maintained in DMEM supplemented with 10% FBS until foci appeared. During this period, the medium was changed every 3 days. Once robust foci appeared, cells were fixed in 100% methanol and stained with Giemsa (Fisher) to visualize the foci. The plates were digitized using a Linotype-Hell Jade two-dimensional scanning densitometer set at 600-dpi resolution. The digitized images were cropped and annotated using Adobe Photoshop for Macintosh v3.0.5 software.

Assay for Anchorage Independence. FR3T3 cells were seeded at a density of 2×10^4 cells in 60-mm dishes containing 2.5 ml of 0.3% LMP-agarose (Life Technologies, Inc.)

as described previously (50). Every 3 days, DMEM supplemented with 10% FBS and 0.3% LMP-agarose was added to each plate. The cells were incubated at 37°C for 10 days, and fields were photographed with an Olympus OM-10 camera attached to an Olympus CK-2 phase-contrast inverted microscope. The images were digitized by the photofinisher. These images were cropped and annotated using Adobe Photoshop for Macintosh v3.0.5 software. Images are representative of three independent experiments.

Growth Rate/Saturation Density Assay. Stable FR3T3 cell lines expressing the wild-type ErbB4 receptor, ErbB2*, or the ErbB4 mutants (Q646C, H647C, and A648C) were plated in 10 60-mm dishes at a density of 2×10^4 cells/dish. Cells were incubated from 1 to 10 days at 37°C. Cells were counted (Coulter Counter ZM) each day for a total of 10 days. The mean and SE are representative of three independent experiments.

Acknowledgments

References

1. Miettinen, P. J., Berger, J. E., Meneses, J., Werb, Z., and Derynck, R. Epithelial immaturity and multiorgan failure in mice lacking epidermal growth factor receptor. Nature (Lond.), 376: 337–344, 1995.

2. Lee, K., Simon, H., Chen, H., Bates, B., Hung, M., and Hauser, C. Requirement for neuregulin receptor ErbB2 in neuronal and cardiac development. Nature (Lond.), 378: 394–398, 1995.

3. Riethmacher, D., Sonnenberg-Riethmacher, E., Brinkmann, V., Yamaai, T., Lewin, G. R., and Birchmeier, C. Severe neuropathies in mice with targeted mutations in the ErbB3 receptor. Nature (Lond.), 389: 725–730, 1997.

4. Gassmann, M., Casagranda, F., Orioli, D., Simon, H., Lai, C., Klein, R., and Lemke, G. Aberrant neuronal and cardiac development in mice lacking the ErbB4 neuregulin receptor. Nature (Lond.), 378: 390–394, 1995.

5. Wong, A. J., Ruppert, J. M., Bigner, S. H., Grzeschik, C. H., Humphrey, P. A., Bigner, D. S., and Vogelstein, B. Structural alterations of the epidermal growth factor receptor gene in human gliomas. Proc. Natl. Acad. Sci. USA, 89: 2965–2969, 1992.

6. Moscatello, D. K., Holgado-Madruga, M., Godwin, A. K., Ramirez, G., Gunn, G., Zoltick, P. W., Biegel, J. A., Hayes, R. L., and Wong, A. J. Frequent expression of a mutant epidermal growth factor receptor in multiple human tumors. Cancer Res., 55: 5536–5539, 1995.

7. Gorgoulis, V., Aninos, D., Mikou, P., Kanavaros, P., Karameris, A., Joardanoglou, J., Rasidakis, A., Veslemes, M., Ozanne, B., and Spandidos, D. A. Expression of EGF, TGF-α, and EGFR in squamous cell lung carcinoma. Anticancer Res., 12: 1183–1187, 1992.

8. Hynes, N. E., and Stern, D. F. The biology of ErbB-2/Neu/HER-2 and its role in cancer. Biochem. Biophys. Acta, 1198: 165–184, 1994.

9. Kraus, M. H., Issing, W., Miki, T., Popescu, N. C., and Aaronson, S. A. Isolation and characterization of ERBB3, a third member of the ERBB/epidermal growth factor receptor family: evidence for overexpression in a subset of human mammary tumors. Proc. Natl. Acad. Sci. USA, 86: 9193–9197, 1989.

10. Sanidas, E. E., Filipe, M. I., Linehean, J., Lemoine, N. R., Gullick, W. J., Rajkumar, T., and Levinson, D. A. Expression of the c-ErbB-3 gene product in gastric cancer. Int. J. Cancer, 54: 935–940, 1993.

11. Haugen, D. R., Akslen, L. A., Varhaug, J. E., and Lillehaug, J. R. Expression of c-erbB-3 and c-erbB-4 proteins in papillary thyroid carcinomas. Cancer Res., 56: 1184–1188, 1996.

12. Kew, T. Y., Bell, J. A., Pinder, S. E., Denley, H., Srinivasan, R., Gullick, W. J., Nicholson, R. I., Blamey, R. W., and Ellis, I. O. c-ErbB-4 protein expression in human breast cancer. Br. J. Cancer, 82: 1163–1170, 2000.

13. Kato, T. Expression of mRNA for heregulin and its receptor, ErbB-3 and ErbB-4, in human upper gastrointestinal mucosa. Life Sci., 63: 553–564, 1998.

14. Bacus, S. S, Zelnick, C. R., Plowman, G., and Yarden, Y. Expression of the ErbB-2 family of growth factor receptors and their ligands in breast cancer: implications for tumor biology and clinical behavior. Am. J. Clin. Pathol., 102: S13–S24, 1994.

15. Gilbertson, R. J., Perry, R. H., Kelly, P. J., Pearson, A. D. J., and Lunec, J. Prognostic significance of HER2 and HER4 coexpression in childhood medulloblastoma. Cancer Res., 57: 3272–3280, 1997.

16. Knowlden, J. M., Gee, J. W., Seery, L. T., Farrow, L., Gullick, W. J., Ellis, I. O., Blamey, R. W., Robertson, J. R., and Nicholson, R. I. c-ErbB3 and c-ErbB4 expression is a feature of the endocrine responsive phenotype in clinical cancer. Oncogene, 17: 1949–1957, 1998.

17. Bacus, S. S., Chin, D., Yarden, Y., Zelnick, C. R., and Stern, D. F. Type 1 receptor tyrosine kinases are differentially phosphorylated in mammary carcinoma and differentially associated with steroid receptors. Am. J. Pathol., 148: 549–558, 1996.

18. Borg, A., Tandon, A. K., Sigurdsson, H., Clark, G. M., Ferno, M., Fuqua, S. A. W., Killander, D., and McGuire, W. L. HER-2/neu amplification predicts poor survival in node-positive breast cancer. Cancer Res., 50: 4332–4337, 1990.

19. Srinivasan, R., Poulsom, R., Hurst, H. C., and Gullick, W. J. Expression of the c-erbB4/HER4 protein and mRNA in normal human fetal and adult tissues and in a survey of nine solid tumor types. J. Pathol., 185: 236–245, 1998.

20. Riese, D. J., II, Bermingham, Y., van Raaij, T. M., Buckley, S., Plowman, G. D., and Stern, D. F. Betacellulin activates the epidermal growth factor receptor and erbB-4 and induces cellular response patterns distinct from those stimulated by epidermal growth factor or neuregulin-β. Oncogene, 12: 345–353, 1996.

21. Riese, D. J., II, Komurasaki, T., Plowman, G. D., and Stern, D. F. Activation of ErbB4 by the bifunctional epidermal growth factor family hormone epiregulin is regulated by ErbB2*. J. Biol. Chem., 273: 11288–11294, 1998.

22. Alroy, I., and Yarden, Y. The ErbB signaling network in embryogenesis and oncogenesis: signal diversification through combinatorial ligand-receptor interactions. FEBS Lett., 410: 83–86, 1997.

23. Riese, D. J., II, and Stern, D. F. Specificity within the EGF family/ErbB receptor family signaling network. Bioessays, 20: 41–48, 1998.

24. Stern, D. F., and Kamps, M. EGF-stimulated tyrosine phosphorylation of p185neu: a potential model for receptor interactions. EMBO J., 7: 995–1001, 1988.

25. Riese, D. J., II, Kim, E. D., Elenius, K., Buckley, S., Klagsbrun, M., Plowman, G. D., and Stern, D. F. The epidermal growth factor receptor couples transforming growth factor-α, heparin-binding epidermal growth factor-like factor, and amphiregulin to Neu, ErbB-3, and ErbB-4. J. Biol. Chem., 271: 20047–20052, 1996.

26. Riese, D. J., II, Van Raaij, T. M., Plowman, G. D., Andrews, G. C., and Stern, D. F. The cellular response to neuregulins is governed by complex interactions of the erbB receptor family. Mol. Cell. Biol., 15: 5770–5776, 1995.

27. Moriki, T., Maruyama, H., and Maruyama, I. N. Activation of preformed EGF receptor dimers by ligand-induced rotation of the transmembrane domain. J. Mol. Biol., 311: 1011–1025, 2001.

28. Burke, C. L., and Stern, D. F. Activation of Neu (ErbB-2) mediated by disulfide bond-induced dimerization reveals a receptor tyrosine kinase dimer interface. Mol. Cell. Biol., 18: 5371–5379, 1998.

29. d'Avis, P. Y., Robertson, S. C., Meyer, A. N., Bardwell, W. M., Webster, M. K., and Donoghue, D. J. Constitutive activation of fibroblast growth factor receptor 3 by mutations responsible for the lethal skeletal dysplasia thanatophoric dysplasia type I. Cell Growth Differ., 9: 71–78, 1998.

30. Galvin, B. D., Hart, K. C., Meyer, A. N., Webster, M. K., and Donoghue, D. J. Constitutive receptor activation by Crouzon syndrome mutations in fibroblasts growth factor receptor (FGFR) 2 and FGFR2/Neu chimeras. Proc. Natl. Acad. Sci. USA, 93: 7894–7899, 1996.

31. Cohen, B. D., Green, J. M., Foy, L., and Fell, H. P. HER4 mediated biological and biochemical properties in NIH 3T3 cells. J. Biol. Chem., *271:* 4813–4818, 1996.

32. Cohen, B. D., Kiener, P. A., Green, J. M., Foy, L., Perry Fell, H., and Zhang, K. The relationship between human epidermal growth-like factor receptor expression and cellular transformation in NIH3T3 cells. J. Biol. Chem., *271:* 30897–30903, 1996.

33. Zang, K., Sun, J., Liu, N., Wen, D., Chang, D., Thomason, A., and Yoshinaga, S. K. Transformation of NIH3T3 cells by HER3 or HER4 receptors requires the presence of HER1 or HER2*. J. Biol. Chem., *271:* 3884–3890, 1996.

34. DiGiovanna, M. P., and Stern, D. F. Activation state-specific monoclonal antibody detects tyrosine phosphorylated $p185^{neu/erbB2}$ in a subset of human breast tumors overexpressing this receptor. Cancer Res., *55:* 1946–1955, 1995.

35. Peles, E., Bacus, S. S., Koski, R. A., Lu, H. S., Wen, D., Ogden, S. G., Ben Levy, R., and Yarden, Y. Isolation of the Neu/HER-2 stimulatory ligand: a 44 Kd glycoprotein that induces differentiation of mammary tumor cells. Cell, *69:* 205–216, 1992.

36. Jones, F. E., Jerry, D. J., Guarino, B. C., Andrews, G. C., and Stern, D. F. Heregulin induces *in vivo* proliferation and differentiation of mammary epithelium into secretory lobuloalveoli. Cell Growth Differ., *7:* 1031–1038, 1996.

37. Sartor, C. I., Zhou, H., Kozlowska, E., Guttridge, K., Kawata, E., Caskey, L., Harrelson, J., Hynes, N., Ethier, S., Calvo, B., and Earp, H. S., III. HER4 mediates ligand-dependent antiproliferative and differentiation responses in human breast cancer cells. Mol. Cell. Biol., *21:* 4265–4275, 2001.

38. Dankort, D. L., Wang, Z., Blackmore, V., Moran, M. F., and Muller, W. J. Distinct tyrosine autophosphorylation sites negatively and positively modulate Neu-mediated transformation. Mol. Cell. Biol., *17:* 5410–5425, 1997.

39. Drummond-Barbosa, D., Vaillancourt, R. R., Kazlauskas, A., and Di-Maio, D. Ligand-independent activation of the platelet-derived growth factor β receptor: requirements for bovine papillomavirus E5-induced mitogenic signaling. Mol. Cell. Biol., *15:* 2570–2581, 1995.

40. Sweeney, C., Lai, C., Riese, D. J., II, Diamonti, A. J., Cantley, L. C., and Carraway, K. L., III. Ligand discrimination in signaling through an ErbB4 receptor homodimer. J. Biol. Chem., *275:* 19803–19807, 2000.

41. Miller, D. A., and Rosman, G. J. Improved retroviral vectors for gene transfer and expression. BioTechniques, *7:* 980–990, 1989.

42. Petti, L. M., and Ray, F. A. Transformation of mortal human fibroblasts and activation of a growth inhibitory pathway by the bovine papillomavirus E5 oncoprotein. Cell Growth Differ., *11:* 395–408, 2000.

43. Sambrook, J., and Russell, D. W. Molecular Cloning: A Laboratory Manual, pp. 1.31–1.170. Cold Spring Harbor, NY: Cold Spring Harbor Laboratory, 2001.

44. Leptak, C., Ramon y Cajal, S., Kulke, R., Horwitz, B. H., Riese, D. J., II, Dotto, G. P., and DiMaio, D. Tumorigenic transformation of murine keratinocytes by the *E5* genes of bovine papillomavirus type I and human papillomavirus type 16. J. Virol., *65:* 7078–7083, 1991.

45. Riese, D. J., II, and DiMaio, D. An intact PDGF signaling pathway is required for efficient growth transformation of mouse C127 cells by the bovine papillomavirus E5 protein. Oncogene, *10:* 1431–1439, 1999.

46. Mann, R., Mulligan, R. C., and Baltimore, D. Construction of a retrovirus packaging mutant and its use to produce helper-free defective retrovirus. Cell, *33:* 153–159, 1983.

47. Miller, D. A., and Buttimore, C. Redesign of retrovirus packaging cell lines to avoid recombination leading to helper virus production. Mol. Cell. Biol., *6:* 2895–2902, 1986.

48. Bradford, M. A rapid and sensitive method for the quantification of microgram quantities of protein utilizing the principle of protein dye-binding. Anal. Biochem., *72:* 248–254, 1976.

49. Petti, L., Nilson, L. A., and DiMaio, D. Activation of the platelet-derived growth factor receptor by the bovine papillomavirus E5 transforming protein. EMBO J., *10:* 845–855, 1991.

50. Hwang, E., Riese, D. J., II, Settleman, J., Nilson, L. A., Honig, J., Flynn, S., and Dimaio, D. Inhibition of cervical carcinoma cell line proliferation by the introduction of a bovine papillomavirus regulatory gene. J. Virol., *67:* 3720–3729, 1993.

Neuregulin isoforms exhibit distinct patterns of ErbB family receptor activation

Stuart S Hobbs[1], Stephanie L Coffing[1], Ann TD Le[1], Elizabeth M Cameron[1], Eric E Williams[1], Michelle Andrew[1], Erika N Blommel[1], Robert P Hammer[2], Han Chang[3] and David J Riese II*,[1]

[1]Department of Medicinal Chemistry and Molecular Pharmacology, Purdue University School of Pharmacy, West Lafayette, Indiana, IN 7907-1333, USA; [2]Department of Chemistry, Louisiana State University, Baton Rouge, Louisiana, LA 70803-1804, USA; [3]Bristol-Myers Squibb Pharmaceutical Research Institute, P.O. Box 5400, Princeton, New Jersey, NJ 08543-5400, USA

During the last decade, several novel members of the Epidermal Growth Factor family of peptide growth factors have been identified. Most prominent among these are the Neuregulins or Heregulins. To date, four different Neuregulin genes have been identified (Neuregulin1-4) and several different splicing isoforms have been identified for at least two of these genes (Neuregulin1 and Neuregulin2). While Neuregulin1 isoforms have been extensively studied, comparatively little is known about Neuregulin3, Neuregulin4, or the Neuregulin2 isoforms. Indeed, there has been no systematic comparison of the activities of these molecules. Here we demonstrate that Neuregulin2alpha and Neuregulin2beta stimulate ErbB3 tyrosine phosphorylation and coupling to biological responses. In contrast, Neuregulin3 and Neuregulin4 fail to activate ErbB3 signaling. Furthermore, Neuregulin2beta, but not Neuregulin2alpha, stimulates ErbB4 tyrosine phosphorylation and coupling to biological responses. Finally, both Neuregulin3 and Neuregulin4 stimulate modest amounts of ErbB4 tyrosine phosphorylation. However, whereas Neuregulin3 stimulates a modest amount of ErbB4 coupling to biological responses, Neuregulin4 fails to stimulate ErbB4 coupling to biological responses. This suggests that there are qualitative as well as quantitative differences in ErbB family receptor activation by Neuregulin isoforms.
Oncogene (2002) **21,** 8442–8452. doi:10.1038/sj.onc. 1205960

Keywords: heregulins; neuregulins; ErbB3; ErbB4; HER3; HER4

Introduction

The Epidermal Growth Factor (EGF) family of peptide hormones consists of approximately 20 different proteins encoded by at least 10 different genes (Reviewed in Kumar and Vadlamudi, 2000; Gullick, 2001; Yarden and Sliwkowski, 2001). These peptide growth factors are agonists for the four ErbB family receptors, including the Epidermal Growth Factor Receptor (EGFR), ErbB2 (HER2/Neu), ErbB3 (HER3), and ErbB4 (HER4) (Reviewed in Schlessinger, 2000; Gullick, 2001; Yarden and Sliwkowski, 2001). Deregulated signaling by this network has been implicated in the genesis and progression of several types of human malignancies, including tumors of the breast, ovary, prostate, pancreas, lung, and brain (Reviewed in Stern, 2000; Normanno *et al.*, 2001; Ozawa *et al.*, 2001; Yarden and Sliwkowski, 2001).

During the last decade, several novel members of the EGF family have been identified and characterized. Most notable among these proteins are the Neuregulins (NRGs), also known as the Heregulins (HRGs) or Neu Differentiation Factors (NDFs) (Holmes *et al.*, 1992; Wen *et al.*, 1992; Carraway *et al.*, 1997; Chang *et al.*, 1997; Zhang *et al.*, 1997; Harari *et al.*, 1999). Currently, there are four known Neuregulin genes, NRG1 through NRG4. NRG1 and NRG2 encode multiple splicing isoforms; these are denoted as either alpha or beta isoforms depending on the sequence of the EGF homology domain.

Difficulties in the expression and purification of Neuregulin isoforms have hampered efforts to characterize the functions of these ligands. Nonetheless, several fundamental principles have emerged: (1) both the alpha and beta isoforms of NRG1 are ErbB3 ligands (Kita *et al.*, 1994; Lu *et al.*, 1995; Pinkas-Kramarski *et al.*, 1996; Jones *et al.*, 1999); (2) the NRG1 beta isoform is a higher affinity ligand for ErbB4 than is the NRG1 alpha isoform (Tzahar *et al.*, 1994; Jones *et al.*, 1999); (3) NRG3 and NRG4 are ErbB4 ligands (Zhang *et al.*, 1997; Harari *et al.*, 1999). However, some of these experiments have been performed *in vitro* using recombinant receptor fragments and synthetic hormones or hormones expressed from bacteria. Other experiments have been performed using a variety of cultured cell lines. Thus, it has been difficult to compare the results that appear in different reports. Indeed, there has been no report of a

systematic functional comparison of NRG2 alpha, NRG2 beta, NRG3, and NRG4.

Thus, a careful analysis of the published literature reveals a number of fundamental questions concerning NRG function: (1) Do the alpha and beta isoforms of NRG2 behave similarly to the corresponding NRG1 isoforms? (2) Are NRG3 and NRG4 agonists for ErbB3? (3) Given the large number of ErbB4 agonists among the NRGs, are the different agonists for ErbB4 functionally distinct? In this study we describe a novel method for easily expressing and purifying recombinant, bioactive NRGs. We present data indicating that NRG2 alpha (NRG2α) and NRG2 beta (NRG2β) are functionally distinct. We also present data indicating that NRG3 and NRG4 are ErbB4 agonists but do not appear to be ErbB3 agonists. Finally, we present data indicating that the different NRG ErbB4 agonists cause differential coupling of ErbB4 to biological responses. This is some of the most compelling evidence to date that different direct agonists for the same ErbB family receptor may be functionally distinct.

Results

Recombinant NRGs can be expressed in insect cells

Several groups have expressed recombinant EGF family peptide hormones in *E. coli*. Advantages of this strategy include yield and suitability of the protein for structural analysis by NMR or X-ray crystallography. One disadvantage of this strategy is that the purification and refolding strategies may be cumbersome. Another is that the proteins lack the glycosylation present in proteins expressed in eukaryotic cells. Other groups have generated synthetic EGF family peptide hormones. A significant disadvantage of this strategy is the expense. Thus, we sought to produce recombinant NRG2α, NRG2β, NRG3, and NRG4 using an insect cell expression system (Invitrogen). The advantages of this system are that the yield is reasonable (∼300 μg purified protein/liter of insect cell culture), the expense is modest (∼$200/mg purified protein), the purification strategy is straightforward, there is no need to refold the protein following purification, and the protein is glycosylated.

We began by subcloning a portion of the NRG cDNAs into the insect cell vector pMT-BiP-V5HisB (Invitrogen). Others and we have previously reported the cloning of the NRG2α and NRG2β cDNAs (Carraway et al., 1997; Chang et al., 1997). We isolated the NRG3 cDNA (Zhang et al., 1997) from a human cDNA library and we isolated the NRG4 cDNA (Harari et al., 1999) from a mouse cDNA library. The regions of these cDNAs encoding the EGF homology domain and surrounding sequences (NRG2α: Ser247 to Asp328; NRG2β: Ser247 to Lys314; NRG3: Ser284 to Gln360; NRG4: Thr3 to Asn60) were subcloned into the conditional insect cell expression vector pMT-BiP-V5HisB (Invitrogen). The inserts were cloned in frame with the vector sequences that encode the upstream BiP secretion signal and the downstream V5 and poly-

histidine epitope tags (Figure 1a). The predicted sequences of the recombinant NRGs encoded by these expression constructs are shown in Figure 1b. The amino acid sequences of the NRG3 and NRG4 regions are identical to those reported in the literature (Zhang et al., 1997; Harari et al., 1999).

We cotransfected the S2 Schneider insect cell line (American Type Culture Collection) with the NRG constructs and pCoHygro, a plasmid that directs the expression of the hygromycin resistance gene (Invitrogen). Transfected S2 cells were selected using hygromycin and were pooled to generate stable cell lines. A one liter culture of each cell line was expanded to a density of 10^7 cells/ml and resuspended in serum-free insect cell medium (Gibco/BRL/Life Technologies) supplemented with 1 mM $CuSO_4$ to induce recombinant NRG expression from the pMT-BiP-V5His constructs. The recombinant NRGs were purified and concentrated by ultrafiltration, dialysis, and chromatography using ProBond Ni^{2+} beads.

We quantified the absolute concentrations of the NRG preparations by immunoblotting using an anti-V5 antibody (Invitrogen). A 53-kDa positive control peptide (Positope–Invitrogen) was used as the standard (Figure 2). Each NRG appeared as a heterogeneous mixture of at least three isoforms with distinct mobilities. Overall, the apparent molecular weights of the NRG isoforms is a little less than those predicted from the amino acid sequences (NRG2α – 12 500 Da; NRG2β – 10 900 Da; NRG3 – 12 200 Da; NRG4 – 9700 Da); however, the relative apparent molecular weights are in agreement with those predicted from the amino acid sequences. (NRG2α and NRG3 have higher apparent molecular weights than NRG2β and NRG2β has a higher apparent molecular weight than NRG4). Finally, the multiple isoforms of each NRG were resolved to a single, tightly focused band by treatment with peptide N-glycosidase F (data not shown). This suggests that these isoforms represent differentially glycosylated species.

We digitized the immunoblots and quantified the bands for each NRG. We quantified all of the bands for those NRGs that exhibited multiple isoforms. We used these values to construct a dose response curve of best fit for each NRG. These curves were used in conjunction with the dose response curve of best fit for the Positope control to calculate the concentration of each NRG stock. We also quantified the relative concentrations of the NRG preparations by ELISA using an anti-V5 antibody (Invitrogen) and the ABC ELISA kit (Pierce). Recombinant NRG yields were typically 300 μg from a one liter culture of insect cells.

Recombinant NRGs differentially stimulate ErbB3 tyrosine phosphorylation

We assessed the interactions of the recombinant NRGs with ErbB family receptors by first assaying induction of ErbB3 tyrosine phosphorylation by the NRG isoforms. ErbB3 lacks tyrosine kinase activity and ErbB2 is an orphan receptor for which there is no

a.

```
BiP                        NRG Insert      V5 Epitope      His6
MKLCILLAVVAFVGLSLGRS ..........  PRFEGKPIPNPLLGLDSTRTGHHHHHH
```

b.

```
NRG2α  SGHARKCNETAKSYCVNGGVCYYIEGINQLS...CKCPNGFFGQRCLEKLPLRLYMPDPKQSVLWDTPGTGVSSSQWSTSPSTLDLN

NRG2β  SGHARKCNETAKSYCVNGGVCYYIEGINQLS...CKCPVGYTGDRCQQFAMVNFSKHLGFELKEAEELYQK

NRG3   SEHFKPCRDKDLAYCLNDGECFVIETLTGSHKHCRCKEGYQGVRCDQFLPKTDSILSDPTDHLGIEFMESEEVYQRQ

NRG4   TDHEQPCGPRHRSFCLNGGICYVIPTIPSPF...CRCIENYTGARCEEVFLPSSSIPSESN
```

Figure 1 The NRG cDNAs were subcloned into the conditional insect cell expression vector pMT-BiP-V5-His. (**a**) The inserts were cloned in frame with the regions of the vector that encode the BiP signal sequence and the V5 and polyhistidine epitope tags. (**b**) The amino acid sequences of the NRG inserts are noted. The consensus EGF homology domain of each NRG is underlined. The six conserved cysteine residues are denoted by larger type
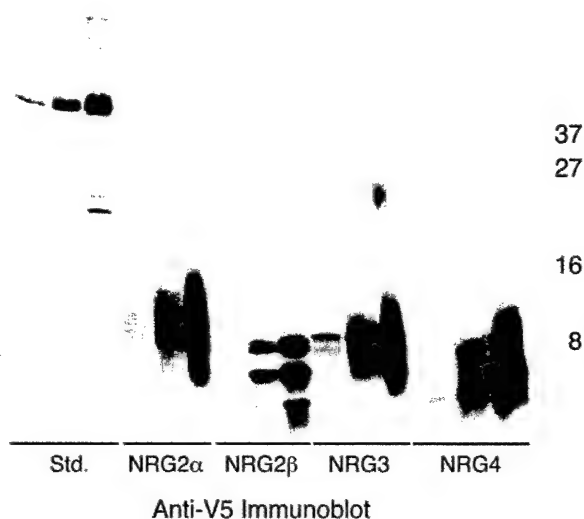

Figure 2 Anti-V5 immunoblotting can be used to assess the relative concentrations of the NRG isoforms. Dilutions were prepared for each recombinant NRG stock. Various volumes were resolved by SDS–PAGE using a 20% acrylamide gel. The resolved proteins were electroblotted onto nitrocellulose and the resulting blot was probed using an anti-V5 monoclonal antibody. Antibody binding was visualized using an HRP-conjugated anti-mouse secondary antibody and chemiluminescence. Defined amounts (10, 30, and 100 ng) of the Positope recombinant peptide (Invitrogen) were used as a positive control for V5 immunoblotting and as a standard for quantification. Positions of molecular weight markers are indicated

known ligand. Consequently, we assayed ligand induction of ErbB3 tyrosine phosphorylation in mouse BaF3 lymphoid cells (which lack endogenous EGFR, ErbB2, and ErbB4 expression) that we had engineered to express ErbB2 and ErbB3 (BaF3/ErbB2 + ErbB3) (Riese et al., 1995). The recombinant NRG1β positive control (EGF homology domain; R&D Systems) stimulates abundant ErbB2 and ErbB3 tyrosine phosphorylation (Figure 3). Both NRG2α and NRG2β stimulate more modest amounts of ErbB3 tyrosine phosphorylation, nonetheless indicating that these growth factors are ligands for ErbB3. In contrast, neither NRG3 nor NRG4 stimulate detectable ErbB3 tyrosine phosphorylation.

Recombinant NRGs differentially stimulate ErbB4 tyrosine phosphorylation

We assayed induction of ErbB4 tyrosine phosphorylation by the NRG isoforms using a human CEM lymphoid cell line (which lacks endogenous ErbB receptor expression) engineered to express ErbB4 (Plowman et al., 1993). The NRG1β positive control and NRG2β stimulate abundant ErbB4 tyrosine phosphorylation, whereas NRG4 stimulates a moderate amount of ErbB4 tyrosine phosphorylation and NRG3 stimulates a modest amount of ErbB4 tyrosine phosphorylation (Figure 4). NRG2α fails to stimulate any detectable ErbB4 tyrosine phosphorylation (Figure 4).

Increasing NRG2α concentrations fail to stimulate ErbB4 tyrosine phosphorylation (Figure 4). We were concerned that the failure of NRG2α to stimulate ErbB4 tyrosine phosphorylation was due to a relatively modest difference in the affinities of NRG2α and NRG2β for ErbB4. Consequently, we stimulated CEM/ErbB4 cells with greater concentrations of NRG2α. In Figure 5 we show that 1000 ng/ml NRG2α stimulates little ErbB4 tyrosine phosphorylation. In contrast, ErbB4 tyrosine phosphorylation reaches saturation at a NRG2β concentration of approximately 30 ng/mL and a NRG3 and NRG4 concentration of approximately 300 ng/ml. Thus, the dissociation constant (K_d) of NRG3 and NRG4 for ErbB4 appears to be approximately 10 times greater than the K_d of NRG2β for ErbB4. Furthermore, if the failure of NRG2α to stimulate abundant ErbB4 tyrosine phosphorylation is due to the decreased affinity of NRG2α for ErbB4, the K_d of NRG2α for ErbB4 must be more than 30 times greater than the K_d of NRG2β for ErbB4.

Recombinant NRGs differentially stimulate ErbB family receptor coupling to biological responses

We assayed induction of ErbB3 coupling to biological responses in the BaF3/ErbB2 + ErbB3 cell line and the BaF3/EGFR + ErbB4 cell line. BaF3 cells are dependent upon interleukin-3 (IL3) for survival and proliferation. However, we have previously shown that ligands for ErbB3 induce IL3-independent survival, but not proliferation, in BaF3/ErbB2 + ErbB3 cells (Riese
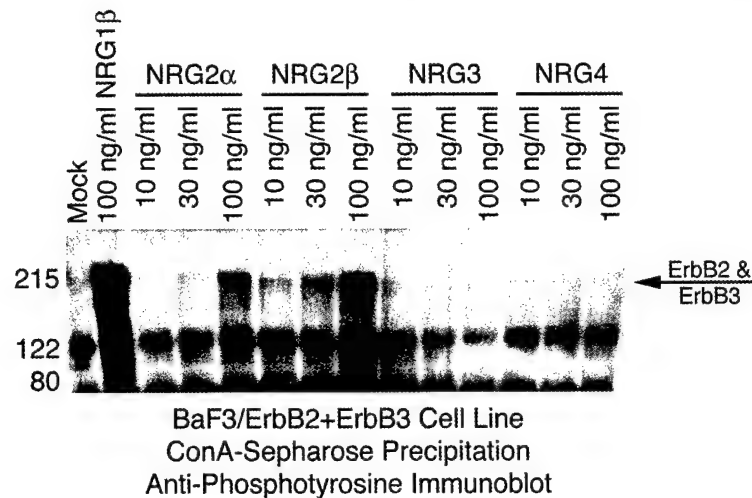
Figure 3 NRG2α and NRG2β, but not NRG3 and NRG4, stimulate ErbB2 and ErbB3 tyrosine phosphorylation in BaF3/Erb-B2 + ErbB3 cells. BaF3/ErbB2 + ErbB3 cells were stimulated with NRG2α, NRG2β, NRG3, and NRG4 as noted below. NRG1β was used as a positive control and the NRG solvent (PBS) was used as a negative (Mock) control. Cells were lysed and the ErbB receptors were precipitated using ConcanavalinA-sepharose. Precipitates were resolved by SDS–PAGE and the resolved proteins were electroblotted onto nitrocellulose. The blot was probed with an anti-phosphotyrosine monoclonal antibody. Antibody binding was visualized using an HRP-conjugated anti-mouse secondary antibody and chemiluminescence. Positions of molecular weight markers are indicated

Figure 4 NRG isoforms stimulate distinct levels of ErbB4 tyrosine phosphorylation in CEM/ErbB4 cells. CEM/ErbB4 cells were stimulated with NRG2α, NRG2β, NRG3, and NRG4 as noted below. NRG1β was used as a positive control and the NRG solvent (PBS) was used as a negative (mock) control. Cells were lysed and ErbB4 was precipitated using ConcanavalinA-sepharose. Precipitates were resolved by SDS–PAGE and the resolved proteins were electroblotted onto nitrocellulose. The blot was probed with an anti-phosphotyrosine monoclonal antibody. Antibody binding was visualized using an HRP-conjugated anti-mouse secondary antibody and chemiluminescence. Positions of molecular weight markers are indicated
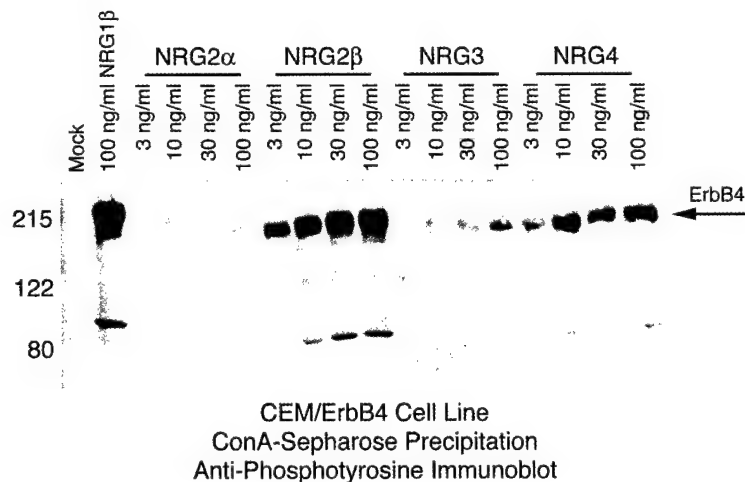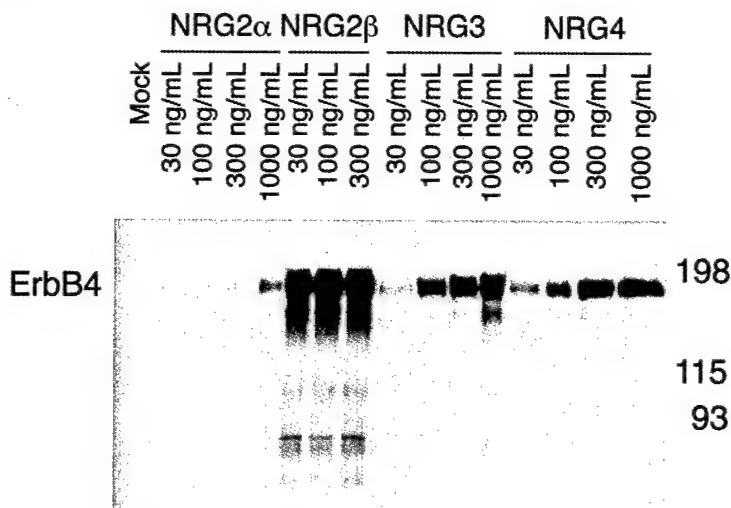
et al., 1995). Furthermore, we have previously shown that ligands for EGFR or ErbB4 induce IL3-independent proliferation in BaF3/EGFR + ErbB4 cells (Riese et al., 1995, 1996a).

Here we demonstrate that NRG2α and NRG2β, as well as the NRG1β positive control, induce IL3-independent survival in BaF3/ErbB2 + ErbB3 cells (Figure 6). Furthermore, NRG3 fails to induce IL3 independence in BaF3/ErbB2 + ErbB3 cells and NRG4 induces minimal IL3 independence in these cells. These results are largely consistent with the ErbB3 tyrosine

phosphorylation data that suggest that NRG2α and NRG2β are ligands for ErbB3, whereas NRG3 and NRG4 are not ligands for ErbB3 (Figure 3).

We also demonstrate that NRG2β and the NRG1β positive control induce IL3-independent proliferation in BaF3/EGFR + ErbB4 cells (Figure 6). In contrast, NRG3 induces IL3-independent survival (not proliferation) in BaF3/EGFR + ErbB4 cells and both NRG2α and NRG4 induce minimal IL3 independence in these cells. The results of the IL3 independence assays indicate that NRG2β, but not NRG2α, is an

NRG2α NRG2β   NRG3   NRG4

ErbB4 — 198

115

93

CEM/ErbB4 Cell Line
Anti-ErbB4 Immunoprecipitation
Anti-Phosphotyrosine Immunoblot

Figure 5 Increased NRG2α concentrations fail to stimulate ErbB4 tyrosine phosphorylation in CEM/ErbB4 cells. CEM/ErbB4 cells were stimulated with NRG2α, NRG2β, NRG3, and NRG4 as noted below. NRG1β was used as a positive control and the NRG solvent (PBS) was used as a negative (mock) control. Cells were lysed and ErbB4 was precipitated using an antibody specific for ErbB4. Precipitates were resolved by SDS–PAGE and the resolved proteins were electroblotted onto nitrocellulose. The blot was probed with an anti-phosphotyrosine monoclonal antibody. Antibody binding was visualized using an HRP-conjugated anti-mouse secondary antibody and chemiluminescence. Positions of molecular weight markers are indicated

Figure 6 The recombinant NRGs induce distinct patterns of IL3 independence in BaF3/ErbB2 + ErbB3 and BaF3/EGFR + ErbB4 cell lines. Cells were seeded in 24-well dishes at a density of 1×10^5 cells/ml in medium lacking interleukin3 (IL3), in medium containing IL3, or in media lacking IL3 but supplemented with the NRGs indicated below (100 ng/ml). Cells were incubated for 96 h, after which viable cells were counted using a hemacytometer

ErbB4 agonist, which is in line with the ErbB4 tyrosine phosphorylation data with NRG2α and NRG2β (Figures 4 and 5).

NRG3 and NRG4 fail to stimulate ErbB4 tyrosine phosphorylation in BaF3/EGFR + ErbB4 cell lines

Despite the fact that 100 ng/ml NRG3 or NRG4 stimulates ErbB4 tyrosine phosphorylation (Figures 4 and 5), 100 ng/ml NRG3 or NRG4 fail to stimulate ErbB4 coupling to biological responses to the extent that NRG2β does (Figure 6). Furthermore, despite the fact that identical concentrations of NRG3 and NRG4 stimulate similar levels of ErbB4 tyrosine phosphorylation (Figure 5), NRG3 stimulates a greater level of IL3 independence in the BaF3/EGFR + ErbB4 cell line than does NRG4 (Figure 6). In an attempt to resolve these discrepancies, we stimulated BaF3/EGFR + ErbB4 cells with the various NRG isoforms and assayed both EGFR and ErbB4 tyrosine phosphorylation by receptor immunoprecipitation and antiphosphotyrosine immunoblotting. In Figure 7 we show that 100 ng/ml NRG1β or NRG2β stimulates EGFR and ErbB4 tyrosine phosphorylation, but 100 ng/ml NRG2α, NRG3, or NRG4 does not. Indeed, even 1000 ng/ml NRG3 or NRG4 does not stimulate EGFR or ErbB4 tyrosine phosphorylation (Figure 8). These data are consistent with the IL3 independence data (Figure 6) and suggest that EGFR inhibits stimulation of ErbB4 tyrosine phosphorylation and coupling to downstream signaling events by NRG3 and NRG4.

**BaF3/EGFR+ErbB4 Cell Line
Anti-EGFR or Anti-ErbB4 Immunoprecipitation
Anti-phosphotyrosine Immunoblot**

Figure 7 Different NRG isoforms induce distinct patterns of EGFR and ErbB4 tyrosine phosphorylation in the BaF3/EG-FR + ErbB4 cell line. BaF3/EGFR + ErbB4 cells were stimulated with NRG isoforms (100 ng/ml) as noted below. The NRG solvent (PBS) was used as a negative (mock) control. Cells were lysed and receptors were precipitated using proteinA-sepharose and either an anti-EGFR monoclonal antibody or an anti-ErbB4 rabbit polyclonal antibody. A rabbit anti-mouse secondary antibody was used as a bridge between the anti-EGFR monoclonal antibody and the proteinA sepharose. Precipitates were resolved by SDS–PAGE and the resolved proteins were electroblotted onto nitrocellulose. The blots were probed with an anti-phosphotyrosine monoclonal antibody. Antibody binding was visualized using an HRP-conjugated anti-mouse secondary antibody and chemiluminescence. Positions of molecular weight markers are indicated
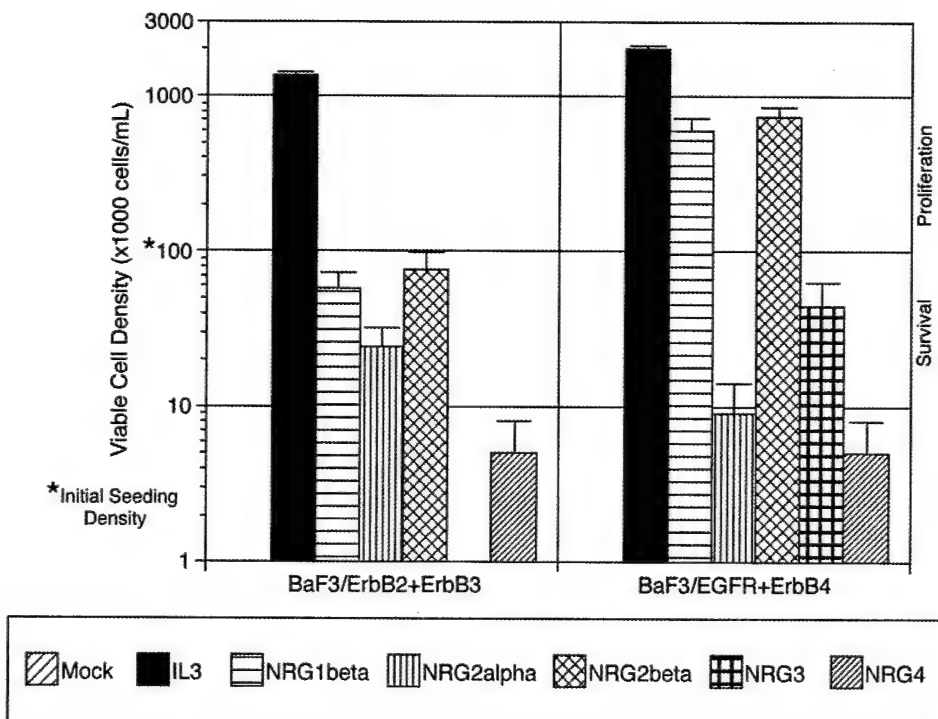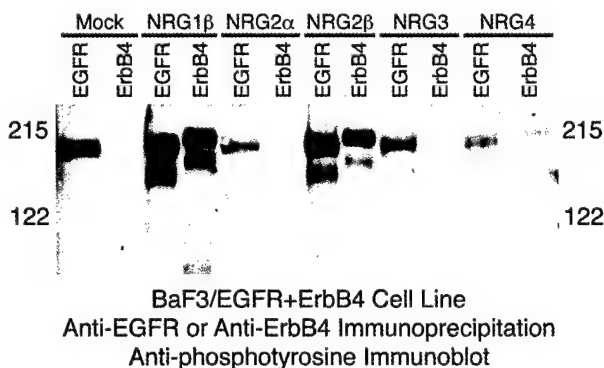
Discussion

In this study we demonstrate that recombinant NRGs can be expressed in insect cells and that these molecules retain biological and biochemical activities. This is a significant advance since methods traditionally used to generate EGF family peptide hormones are cumbersome or expensive. Indeed, this methodology will facilitate functional analyses of NRGs by site-directed mutagenesis. While this strategy has been used to analyse the function of some EGF family hormones, most notably EGF itself (Reviewed in Groenen *et al.*, 1994; Boonstra *et al.*, 1995), such analysis of NRGs have been limited to binding studies done using NRGs expressed in phage display systems (Jones *et al.*, 1998; Ballinger *et al.*, 1999). Undoubtedly, studies facilitated by the ready availability of NRG mutants will reveal new insights into the nature of the interactions between EGF family peptide growth factors and their cognate ErbB family receptor tyrosine kinases.

The studies presented here also represent the initial systematic functional comparison of NRG2α, NRG2β, NRG3, and NRG4. Here we show that NRG2α and NRG2β stimulate ErbB3 tyrosine phosphorylation (in the context of ErbB2 and ErbB3 coexpression), whereas NRG3 and NRG4 do not. These results are consistent with the published observation that NRG alpha and beta isoforms are ligands for ErbB3 (Tzahar *et al.*, 1994; Pinkas-Kramarski *et al.*, 1996, 1998, 1999; Jones *et al.*, 1999). However, these results contrast the observation that a recombinant NRG2α fusion protein fails to compete with radiolabeled NRG1β for binding to recombinant ErbB2-ErbB3 heterodimers (Jones *et al.*, 1999). Of course the physiologic relevance of preformed recombinant ErbB2-ErbB3 heterodimers is unclear and it was noted by the authors that the NRG fusion proteins have reduced affinity for their native receptors (Jones *et al.*, 1998). Our results are consistent with the published observation that a recombinant NRG3 fusion protein fails to compete with radiolabeled NRG1β for binding to a recombinant ErbB3 fusion protein (Jones *et al.*, 1999). However, the observation that NRG3 stimulates ErbB2 and ErbB3 tyrosine phosphorylation in 32D cells devoid of endogenous ErbB family receptors (Hijazi *et al.*, 1998) contrasts our results. Of course, coexpression of ErbB2 and ErbB3 in 32D cells permits EGF stimulation of receptor coupling to IL3 independence and mitogenesis (Pinkas-Kramarski *et al.*, 1998). This calls into question the utility of the 32D model system for defining ligand-receptor interactions. Regardless, we conclude that NRG2α and NRG2β are functionally distinct from NRG3 and NRG4.

We also show that NRG2β is a potent agonist of ErbB4 tyrosine phosphorylation, whereas NRG3 and NRG4 stimulate modest levels of ErbB4 tyrosine phosphorylation and NRG2α fails to stimulate ErbB4 tyrosine phosphorylation (Figures 4 and 5). These results are consistent with the observation that NRG beta isoforms are more potent and higher affinity ligands for ErbB4 than are NRG alpha isoforms
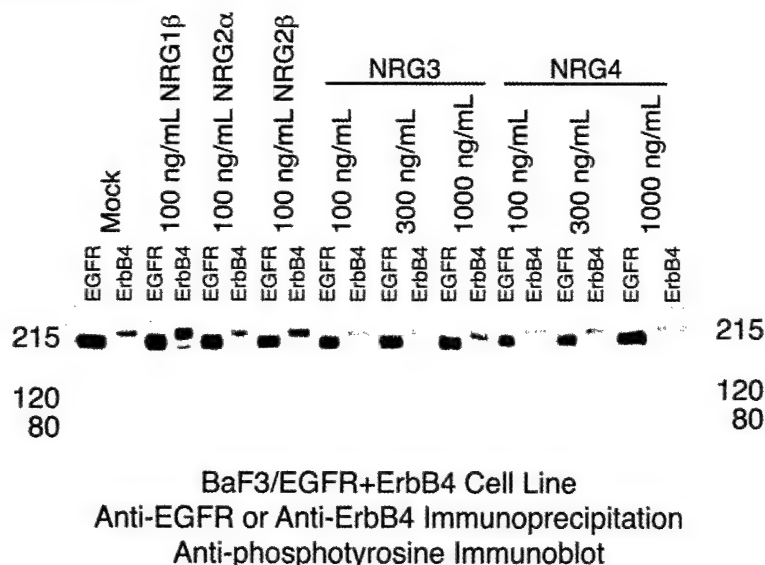
Figure 8 Increased NRG3 and NRG4 concentrations fail to stimulate EGFR or ErbB4 tyrosine phosphorylation in the BaF3/EG-FR + ErbB4 cell line. BaF3/EGFR + ErbB4 cells were stimulated with NRG isoforms as noted below. The NRG solvent (PBS) was used as a negative (mock) control. Cells were lysed and receptors were precipitated using proteinA-sepharose and either an anti-EGFR monoclonal antibody or an anti-ErbB4 rabbit polyclonal antibody. A rabbit anti-mouse secondary antibody was used as a bridge between the anti-EGFR monoclonal antibody and the proteinA sepharose. Precipitates were resolved by SDS–PAGE and the resolved proteins were electroblotted onto nitrocellulose. The blots were probed with an anti-phosphotyrosine monoclonal antibody. Antibody binding was visualized using an HRP-conjugated anti-mouse secondary antibody and chemiluminescence. Positions of molecular weight markers are indicated

(Tzahar *et al.*, 1994; Lu *et al.*, 1995; Pinkas-Kramarski *et al.*, 1998, 1999; Jones *et al.*, 1999). These data are also consistent with the observation that NRG3 and NRG4 are both ErbB4 ligands (Zhang *et al.*, 1997; Harari *et al.*, 1999; Jones *et al.*, 1999). However, these data also suggest that NRG2β is a more potent ligand for ErbB4 than are NRG4 and NRG3. It should be noted that ErbB4 tyrosine phosphorylation reaches saturation following stimulation with 30 ng/ml NRG2β, 300 ng/ml NRG3, or 300 ng/ml NRG4. Thus, some of the functional difference between NRG2β and NRG3 or NRG4 appears to be due to the higher affinity of NRG2β for ErbB4. Indeed, the affinity of NRG3 for ErbB4 is reported to be less than one-tenth the affinity of NRG2β for ErbB4 (Jones *et al.*, 1999). Similarly, the affinity of NRG4 for ErbB4 is reported to be approximately one-tenth the affinity of NRG1β for ErbB4 (Harari *et al.*, 1999).

NRG2α and NRG2β stimulate IL3 independent survival in BaF3/ErbB2 + ErbB3 cells, whereas NRG3 and NRG4 do not stimulate IL3 independence in these cells (Figure 6). These results are consistent with the observation that NRG alpha and beta isoforms stimulate coupling of ErbB2 and ErbB3 to biological responses (Pinkas-Kramarski *et al.*, 1996, 1998, 1999). These results are also consistent with the tyrosine phosphorylation data shown in Figure 3. NRG3 does not stimulate any IL3 independence in the BaF3/ErbB2 + ErbB3 cells (Figure 6), consistent with the tyrosine phosphorylation data shown in Figure 3. NRG4 also fails to stimulate ErbB3 tyrosine phosphorylation in the BaF3/ErbB2 + ErbB3 cells (Figure

3). However, NRG4 stimulates a modest amount of IL3 independence in these cells (Figure 6). It is possible that the IL3 independence assay is a more sensitive measure of ligand-induced receptor signaling than is antiphosphotyrosine immunoblotting. Indeed, we have previously shown that the ligand concentration required for saturated levels of ErbB receptor tyrosine phosphorylation in BaF3 cells is approximately 10-fold greater than the ligand concentration required for saturated levels of IL3 independence in the same cell lines (Riese *et al.*, 1995).

NRG2β stimulates IL3-independent proliferation in BaF3/EGFR + ErbB4 cell lines, whereas NRG2α stimulates minimal IL3 independence (Figure 6). This is consistent with the tyrosine phosphorylation data shown in Figures 4 and 5. More intriguing are the observations that 100 ng/ml NRG3 stimulates only IL3-independent survival and that 100 ng/ml NRG4 stimulates minimal IL3 independence (Figure 6). We were concerned that we were not using a sufficient concentration of NRG3 or NRG4 in these IL3 independence assays. However, even 1000 ng/ml NRG3 or NRG4 failed to stimulate IL3-independent proliferation in the BaF3/EGFR + ErbB4 cells (data not shown). Thus, we attempted to explain these results by assaying ligand-induced receptor tyrosine phosphorylation in the BaF3/EGFR + ErbB4 cell (Figures 7 and 8). These experiments reveal that NRG2α, NRG3, and NRG4 stimulate minimal receptor tyrosine phosphorylation in the BaF3/EGFR + ErbB4 cells. This is consistent with the relative inactivity of these ligands in the IL3 independence assay using these cells.

Furthermore, the high basal (ligand-independent) level of receptor tyrosine phosphorylation in these cells (Figures 7 and 8) may account for the small amount of IL3-independence stimulated by NRG2α (which is presumably not a potent ErbB4 agonist).

We are left trying to explain why NRG3 and NRG4 stimulate much lower levels of ErbB4 tyrosine phosphorylation (Figures 7 and 8) and ErbB receptor coupling to biological responses in the BaF3/EGFR + ErbB4 cells (Figure 6) than would be expected from the ErbB4 tyrosine phosphorylation data obtained from the CEM/ErbB4 cells (Figures 4 and 5). A simple, non-mechanistic explanation is that EGFR inhibits ligand-induced ErbB4 tyrosine phosphorylation. However, we have previously shown that ErbB2 or ErbB3 expression does not quantitatively modulate ErbB4 tyrosine phosphorylation stimulated by betacellulin or NRG1β (Feroz et al., 2002). Nonetheless, it is possible that inhibition of ligand-induced ErbB4 signaling is specific for EGFR, NRG3, or NRG4.

A more attractive, mechanistic explanation is that the EGFR-ErbB4 heterodimers stimulated by NRG3 and NRG4 treatment are in a different conformation that results in less receptor tyrosine phosphorylation than the EGFR-ErbB4 heterodimers stimulated by NRG2β. There are precedents for differential receptor tyrosine kinase dimerization, tyrosine phosphorylation, and coupling to downstream events. The bovine papillomavirus (BPV) E5 protein is a membrane-bound agonist for the platelet derived growth factor receptor (PDGFR) and stimulates PDGFR dimerization, tyrosine phosphorylation, and PDGFR-dependent malignant growth transformation of fibroblasts (Reviewed in Drummond-Barbosa and DiMaio, 1997). However, there are BPV E5 mutants that stimulate PDGFR tyrosine phosphorylation yet fail to couple to PDGFR-dependent growth transformation (Nilson et al., 1995; Klein et al., 1998). Similarly, mutation of different ErbB2 extracellular juxtamembrane amino acids residues to cysteine results in ErbB2 disulfide-linked dimers that exhibit high levels of ErbB2 tyrosine phosphorylation yet fail to cause malignant growth transformation of fibroblasts (Burke and Stern, 1998).

Thus, we hypothesize that in BaF3/EGFR + ErbB4 cells, NRG3 and NRG4 stimulate EGFR and ErbB4 phosphorylation on different or a smaller number of tyrosine residues than does NRG2β. These hypotheses are consistent with several published observations. In the MDA-MB-453 breast tumor cell line, NRG1β and NRG2β stimulate ErbB2 and ErbB3 tyrosine phosphorylation to similar extents, but only NRG1β causes differentiation of these cells and the two growth factors cause differential recruitment of SH2 domain-containing proteins to the phosphorylated ErbB2 and ErbB3 and differential activation of gene transcription (Sweeney-Crovello et al., 1998; Sweeney et al., 2001). Similarly, betacellulin, NRG1β, NRG2β, and NRG3 induce qualitatively different patterns of ErbB4 tyrosine phosphorylation, as revealed by 2-dimensional peptide mapping (Sweeney et al., 2000).

Our data suggest that regulation of ErbB family receptor signaling by EGF family hormones occurs at multiple levels. NRG2α and NRG2β are more potent ErbB3 agonists than are NRG3 and NRG4 (Figures 3 and 6). Furthermore, NRG2β is a potent ErbB4 agonist, whereas NRG3 and NRG4 are less potent ErbB4 agonists and NRG2α directly stimulates minimal ErbB4 signaling (Figures 4–8). To a first approximation, these differences in activity of the various NRGs and other EGF family hormones (Figure 9) reflect the different affinities of these hormones for ErbB family receptors (Jones et al., 1999; Reviewed in Riese and Stern, 1998; Kumar and Vadlamudi 2000; Gullick, 2001; Yarden and Sliwkowski, 2001). Consequently, differential ligand activation of signaling by a specific ErbB family receptor is in part a function of quantitative differences in the affinities of the various ligands for the particular receptor.

However, this quantitative model cannot explain all of the data presented here. The dissociation constant (K_d) of NRG2α and ErbB4 is reported to be 20–50-fold greater than the K_d of NRG2β and ErbB4 (Jones et al., 1999; Pinkas-Kramarski et al., 1998, 1999). Yet, whereas 3 ng/ml NRG2β stimulates a modest amount of ErbB4 tyrosine phosphorylation, 300 ng/ml NRG2α fails to stimulate ErbB4 tyrosine phosphorylation and 1000 ng/ml NRG2α stimulates only a very small amount of ErbB4 tyrosine phosphorylation (Figures 4 and 5). Furthermore, whereas NRG3 and NRG4 stimulate detectable amounts of ErbB4 tyrosine phosphorylation in CEM/ErbB4 cells, at the same ligand concentrations they fail to stimulate detectable amounts of ErbB4
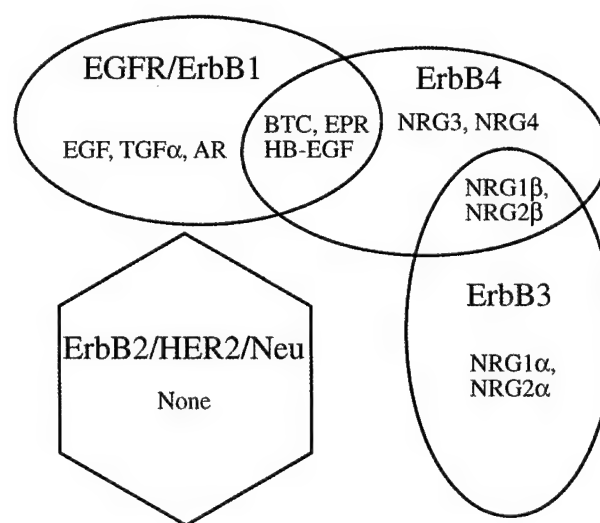

Figure 9 A Venn diagram illustrates the interactions of the four ErbB family receptors with the following EGF family hormones: Transforming Growth Factor alpha (TGFα), Amphiregulin (AR), Heparin-binding Epidermal Growth Factor-like Factor (HB-EGF), Betacellulin (BTC), Epiregulin (EPR), Neuregulin1 beta (NRG1β), Neuregulin2 beta (NRG2β), Neuregulin1 alpha (NRG1α), Neuregulin2 alpha (NRG2α), Neuregulin3 (NRG3), and Neuregulin4 (NRG4). This figure summarizes data presented here and published previously (Reviewed in Riese and Stern, 1998)

tyrosine phosphorylation in BaF3/EGFR + ErbB4 cells. In contrast, NRG2β stimulates abundant ErbB4 tyrosine phosphorylation in both cell lines. These observations suggest that there are qualitative differences in activation of ErbB4 signaling and coupling to downstream signaling events by the various NRG isoforms. Published data suggest that these qualitative differences between the NRG isoforms reflect ligand-induced ErbB4 tyrosine phosphorylation on different tyrosine residues and consequent differential receptor coupling to downstream signaling pathways. This would explain the functional differences of the NRG isoforms seen in this study. One of our future challenges will be to formally test whether there are qualitative differences in the activities of the ErbB4 ligands and to identify the mechanism for these differences. Another challenge will be to develop a model that explains the interactions of EGF family hormones with ErbB family receptors and that accounts for these qualitative differences in the activities of the ErbB4 ligands.

Materials and methods

Cell lines and cell culture

The S2 Schneider insect cells were purchased from the American Type Culture Collection. The CEM/ErbB4 cells (Plowman *et al.*, 1993) are a generous gift from Dr Gregory D Plowman, Exelixis Pharmaceuticals. The BaF3/ErbB2 + ErbB3 and BaF3/EGFR + ErbB4 cell lines have been described previously (Riese *et al.*, 1995). All cell lines were maintained according to vendor instructions or published procedures (Plowman *et al.*, 1993; Riese *et al.*, 1995; Feroz *et al.*, 2002).

Plasmids and plasmid construction

The insect cell conditional expression vector pMT-BiP-V5HisB and the pCoHygro plasmid were purchased from Invitrogen. We isolated NRG2α, NRG2β, NRG3, and NRG4 clones from human, rat, and mouse cDNA libraries. The regions of the cDNA clones that encode the EGF homology domain of the NRG isoforms were amplified by PCR and were subcloned by standard molecular biology techniques into the *Bgl*II and *Sac*II sites of pMT-BiP-V5HisB. The upstream primer used to amplify the rat NRG2α sequences has the following sequence: 5'-CTCGAGAGATC-TTCGGGGCACGCCCGGAAGTG-3'. The downstream primer has the following sequence: 5'-CTCGAGCCG-CGGATTCAAATCCAAGGTGCTTGG-3'. The amplified sequences encode Ser247 to Asp328 (Carraway *et al.*, 1997; Chang *et al.*, 1997). The upstream primer used to amplify the rat NRG2β sequences has the following sequence: 5'-CTCGAGAGATCTTCGGGGCACGCCCGGAAGTG-3'. The downstream primer has the following sequence: 5'-CTCGAGCCGCGGCTTCTGGTACAGCTCCTC-3'. The amplified sequences encode Ser247 to Lys314 (Carraway *et al.*, 1997; Chang *et al.*, 1997). The upstream primer used to amplify the human NRG3 sequences has the following sequence: 5'-CTCGAGAGATCTTCCGAGCACTTCAAAC-CCTG-3'. The downstream primer has the following sequence: 5'-CTCGAGCCGCGGCTGCCTTTGATAAAC-TTCTTCACTCTCC-3'. The amplified sequences encode Ser284 to Gln360 (Zhang *et al.*, 1997). The upstream primer used to amplify the mouse NRG4 sequences has the following sequence: 5'-CTCGAGAGATCTACAGATCAC-

GAGCAGCC-3'. The downstream primer has the following sequence: 5'-CTCGAGCCGCGGATTACTTTCGCTTGGG-ATGCTGG-3'. The amplified sequences encode Thr3 to Asn60 (Harari *et al.*, 1999). The inserts were subcloned in frame with the upstream BiP secretion signal encoded by pMT-BiP-V5HisB and in frame with the downstream V5 and polyhistidine epitope tags encoded by pMT-BiP-V5HisB.

Generation and purification of recombinant NRGs

The NRG clones were co-transfected into the S2 cells along with the plasmid pCoHygro, which carries the hygromycin resistance gene. Transfections were performed using a calcium phosphate transfection kit (Invitrogen) according to vendor instructions. Transfected cells were selected using 300 U/ml hygromycin B (Cellgro) and stably transfected cells appeared approximately 14 days after the beginning of selection.

Hygromycin-resistant cells were pooled, expanded, and frozen for archival purposes. Transfected cells were seeded in a one liter culture at a density of 2×10^6 cells/ml. Cells were maintained until they reached a density of 1×10^7 cells/ml. At that point cells were collected by centrifugation and seeded at a density of 2×10^7 cells/ml in serum-free medium (Gibco/BRL/Life Technologies) supplemented with 1 mM $CuSO_4$. Cells were maintained for 5 days in serum-free medium to permit recombinant NRG expression and secretion into the culture medium.

The insect cells were collected from the culture media by centrifugation. The conditioned media supernatants were transferred into a fresh container and clarified by filtration through a 0.22 μM filter. The NRGs present in the conditioned medium were concentrated approximately 30-fold by ultrafiltration using a 5000 M.W.C.O. filter (Amicon). The concentrated NRGs were dialyzed against PBS using a 5000 M.W.C.O. membrane (Pierce) to remove low-molecular weight impurities. The NRGs were purified by incubating the samples with ProBond Ni^{2+} beads (Invitrogen), which bind proteins tagged with polyhistidine. The NRGs were eluted from the beads using 500 mM imidazole. We removed the imidazole from the eluates by dialysis against PBS using a 500 M.W.C.O. membrane (Pierce). The dialyzed proteins were then concentrated to a final volume of 2–5 ml by ultrafiltration using a 5000 M.W.C.O. filter (Amicon).

Anti-V5 immunoblotting

Anti-V5 immunoblotting was used to quantify the concentrations of the recombinant NRG samples. Samples were resolved by SDS–PAGE using a 20% acrylamide gel. Resolved samples were electroblotted onto nitrocellulose. The blots were probed using an anti-V5 mouse monoclonal antibody (Invitrogen). Primary antibody binding was detected using a goat anti-mouse antibody conjugated to horseradish peroxidase (Pierce). Secondary antibody binding was visualized by chemiluminescence (Amersham). The positope recombinant protein (Invitrogen) was analysed in parallel as a control for V5 immunoblotting and as a standard for quantification.

The resulting immunoblot was digitized using a UMAX Astra 2400S flatbed scanner and the image was cropped using Adobe Photoshop. The bands were quantified using NIH Image for Macintosh software. We generated a dose-response line of best fit for each recombinant NRG using Microsoft Excel. The coefficients of correlation exceeded 0.96. These curves were used to calculate the concentration of each recombinant NRG stock.

Anti-V5 ELISA

The concentration of the NRG2α, NRG3, and NRG4 preparations were determined relative to the concentration of the NRG2β preparation by ELISA using an anti-V5 monoclonal antibody (Invitrogen) and the ABC ELISA kit (Pierce). Polyvinyl chloride (PVC) 96-well assay plates were seeded with 1, 3, and 10 ng/well of NRG2β and 3, 10, and 30 μl/well of several dilutions of the other NRGs in a total volume of 100 μl/well. The plates were incubated for 1 h at room temperature to allow for protein binding to the wells. The wells were then washed three times with 200 μl tris-buffered saline supplemented with 0.05% Tween-20 (TBS-T). Non-specific binding of the antibody to the wells was blocked by incubating the wells for 1 h at room temperature with 100 μl TBS/1% bovine serum albumin (Sigma). Next, 100 μl of the mouse-anti-V5 monoclonal antibody (0.2 μg/ml – Invitrogen) was added to each well and the plates were incubated for 30 min at room temperature. The wells were then washed three times with 200 μl TBS-T and 100 μl of a biotinylated anti-mouse antibody (1.5 μg/ml – Pierce) was added to each well. The plates were incubated for 30 min at room temperature. The wells were washed three times with 200 μl TBS-T. An avidin/biotinylated alkaline phosphatase complex (100 μl) was added to each well and the plates were incubated for 30 min at room temperature. The wells were washed three times with 200 μl TBS-T, after which 100 μl of TBS-T was added to each well and the plates were incubated for 5 min at room temperature. The TBS-T was removed and 100 μl of the alkaline phosphatase substrate, p-nitrophenyl phosphate (1 mg/ml solution dissolved in diethanolamine – Pierce), was added to each well. The plates were incubated until the appropriate amount of substrate had been dephosphorylated, which is evident from the yellow color of the product. The reactions were terminated by adding 25 μl 2 M NaOH to each well. Finally, the amount of product in each well was determined by measuring absorbance at 405 nm using a SpectrFluor Plus plate reader (Tecan).

The amount of product was plotted as a function of sample stock volume for NRG2α, NRG3, and NRG4. These dose-response curves were compared to a standard dose-response curve generated using NRG2β to determine the relative concentration of the NRG2α, NRG3, and NRG4 stocks.

Stimulation and analysis of ErbB family receptor tyrosine phosphorylation

We analysed ligand-induced ErbB family receptor tyrosine phosphorylation in CEM/ErbB4, BaF3/ErbB2 + ErbB3, and BaF3/EGFR + ErbB4 cells using procedures published previously (Riese et al., 1995, 1996a,b, 1998; Chang et al., 1997; Feroz et al., 2002). Briefly, approximately 10^7 cells were stimulated for 7 min on ice with ligand, after which the cells were lysed in an isotonic lysis buffer supplemented with the nonionic detergent NP40. Nuclei and debris were collected from the lysates by centrifugation and the supernatants were transferred to a fresh tube. The protein content of the lysates was analysed using a modified Bradford assay (Pierce). ErbB family receptors were precipitated from the lysates using Concanavlin A-sepharose, which binds to glycoproteins. ErbB family receptors were also precipitated from the lysates using an anti-EGFR mouse monoclonal antibody (Santa Cruz Biotechnology), or an anti-ErbB4 rabbit polyclonal antibody (Santa Cruz Biotechnology).

The precipitates were resolved by SDS–PAGE using a 7.5% acrylamide gel. The resolved samples were electroblotted onto nitrocellulose. The blots were probed using an anti-phosphotyrosine mouse monoclonal antibody (Upstate Biotechnology). Primary antibody binding was detected using a goat anti-mouse antibody conjugated to horseradish peroxidase (Pierce). Secondary antibody binding was visualized by chemiluminescence (Amersham).

Stimulation and analysis of ErbB family receptor coupling to IL3 independence

We analysed ligand-induced ErbB family receptor coupling to IL3 independence in BaF3/ErbB2 + ErbB3 and BaF3/EGFR + ErbB4 cells using procedures published previously (Riese et al., 1995, 1996a,b, 1998; Chang et al., 1997). Briefly, cells were seeded in 24-well dishes at a density of 10^5 cells/ml in medium lacking interleukin3 (IL3), in medium supplemented with IL3, or in medium lacking IL3 but supplemented with a recombinant NRG. Cells were incubated for 96 h, after which viable cells were counted using a hemacytometer. If the viable cell density was greater than 10^5 cells/ml, the cells were judged to be proliferating. If the viable cell density was between 10^4 and 10^5 cells/ml, the cells were judged to be surviving. If the viable cell density was below 10^4 cells/ml, the cells were judged to be dying.

References

Ballinger MD, Jones JT, Lofgren JA, Fairbrother WJ, Akita RW, Sliwkowski MX and Wells JA. (1998). *J. Biol. Chem.*, **273**, 11675–11684.

Boonstra J, Rijken P, Humbel B, Cremers F, Verkeij A and van Bergen en Henegouwen P. (1995). *Cell Biol. Intl.*, **19**, 413–430.

Burke CL and Stern DF. (1998). *Mol. Cell. Biol.*, **18**, 5371–5379.

Carraway III KL, Weber JL, Unger MJ, Ledesma J, Yu N, Gassmann M and Lai C. (1997). *Nature*, **387**, 512–516.

Chang H, Riese II DJ, Gilbert W, Stern DF and McMahan UJ. (1997). *Nature*, **387**, 509–512.

Drummond-Barbosa D and DiMaio D. (1997). *Biochim. Biophys. Acta,* **1332,** M1–M17.

Feroz K, Williams E and Riese II DJ. (2002). *Cell. Signal.,* **14,** 793–798.

Groenen LC, Nice EC and Burgess AW. (1994). *Growth Factors,* **11,** 235–237.

Gullick WJ. (2001). *Endocrine-Related Cancer,* **8,** 75–82.

Harari D, Tzahar E, Romano J, Shelly M, Pierce JH, Andrews GC and Yarden Y. (1999). *Oncogene,* **18,** 2681–2689.

Hijazi MM, Young PE, Dougherty MK, Bressette DS, Cao TT, Pierce JH, Wong LM, Alimandi M and King CR. (1998). *Int. J. Oncol.,* **13,** 1061–1067.

Holmes WE, Sliwkowski MX, Akita RW, Henzel WJ, Lee J, Park JW, Yansura D, Abadi N, Raab H, Lewis GD, Shepard HM, Kuang W-J, Wood WI, Goeddel DV and Vandlen RL. (1992). *Science,* **256,** 1205–1210.

Jones JT, Akita RW and Sliwkowski MX. (1999). *FEBS Lett.,* **447,** 227–231.

Jones JT, Ballinger MD, Pisacane PI, Lofgren JA, Fitzpatrick VD, Fairbrother WJ, Wells JA and Sliwkowski MX. (1998). *J. Biol. Chem.,* **273,** 11667–11674.

Kita YA, Barff J, Luo Y, Wen D, Brankow D, Hu S, Liu N, Prigent SA, Gullick WJ and Nicolson M. (1994). *FEBS Lett.,* **349,** 139–143.

Klein O, Polack GW, Surti T, Kegler-Ebo D, Smith SO and DiMaio D. (1998). *J. Virol.,* **72,** 8921–8932.

Kumar R and Vadlamudi RK. (2000). *J. Clin. Ligand Assay,* **23,** 233–237.

Lu HS, Chang D, Philo JS, Zhang K, Narhi LO, Liu N, Zhang M, Sun J, Wen J, Yanagihara D, Karunakaran D, Yarden Y and Ratzkin B. (1995). *J. Biol. Chem.,* **270,** 4784–4791.

Nilson LA, Gottlieb RL, Polack GW and DiMaio D. (1995). *J. Virol.,* **69,** 5869–5874.

Normanno N, Bianco C, DeLuca A and Salomon DS. (2001). *Frontiers Biosci.,* **6,** D685–D707.

Ozawa F, Friess H, Tempia-Caliera A, Kleeff J and Buchler MW. (2001). *Teratogen. Carcinogen. Mutagen.,* **21,** 27–44.

Pinkas-Kramarski R, Shelly M, Glathe S, Ratzkin BJ and Yarden Y. (1996). *J. Biol. Chem.,* **271,** 19029–19032.

Pinkas-Kramarski R, Shelly M, Guarino BC, Wang LM, Lyass L, Alroy I, Alamandi M, Kuo A, Moyer JD, Lavi S, Eisenstein M, Ratzkin BJ, Seger R, Bacus SS, Pierce JH, Andrews GC and Yarden Y. (1998). *Mol. Cell. Biol.,* **18,** 6090–6091.

Pinkas-Kramarski R, Shelly M, Guarino BC, Wang LM, Lyass L, Alroy I, Alamandi M, Kuo A, Moyer JD, Lavi S, Eisenstein M, Ratzkin BJ, Seger R, Bacus SS, Pierce JH, Andrews GC and Yarden Y. (1999). *Mol. Cell. Biol.,* **19,** 8695.

Plowman GD, Green JM, Culouscou J-M, Carlton GW, Rothwell VM and Buckley S. (1993). *Nature,* **366,** 473–475.

Riese II DJ, Bermingham Y, van Raaij TM, Buckley S, Plowman GD and Stern DF. (1996a). *Oncogene,* **12,** 345–353.

Riese II DJ, Kim ED, Elenius K, Buckley S, Klagsbrun M, Plowman GD and Stern DF. (1996b). *J. Biol. Chem.,* **271,** 20047–20052.

Riese II DJ, Komurasaki T, Plowman GD and Stern DF. (1998). *J. Biol. Chem.,* **273,** 11288–11294.

Riese II DJ and Stern DF. (1998). *Bioessays,* **20,** 41–48.

Riese II DJ, van Raaij TM, Plowman GD, Andrews GC and Stern DF. (1995). *Mol. Cell. Biol.,* **15,** 5770–5776.

Schlessinger J. (2000). *Cell,* **103,** 211–225.

Stern DF. (2000). *Breast Cancer Res.,* **2,** 176–183.

Sweeney C, Fambrough D, Huard C, Diamonti AJ, Lander ES, Cantley LC and Carraway III KL. (2001). *J. Biol. Chem.,* **276,** 22685–22698.

Sweeney C, Lai C, Riese II DJ, Diamonti AJ, Cantley LC and Carraway III KL. (2000). *J. Biol. Chem.,* **275,** 19803–19807.

Sweeney-Crovello C, Lai C, Cantley LC and Carraway III KL. (1998). *J. Biol. Chem.,* **273,** 26954–26961.

Tzahar E, Levkowitz G, Karungaran D, Yi L, Peles E, Lavi S, Chang D, Liu N, Yayon A, Wen D and Yarden Y. (1994). *J. Biol. Chem.,* **269,** 25226–25233.

Wen D, Peles E, Cupples R, Suggs SV, Bacus SS, Luo Y, Trail G, Hu S, Silbiger SM, Ben Levy R, Koski RA, Lu HS and Yarden Y. (1992). *Cell,* **69,** 559–572.

Yarden Y and Sliwkowski MX. (2001). *Nature Revs. Mol. Cell. Biol.,* **2,** 127–137.

Zhang D, Sliwkowski MX, Mark M, Frantz G, Akita R, Sun Y, Hillan K, Crowley C, Brush J and Godowski PJ. (1997). *Proc. Natl. Acad. Sci. USA,* **94,** 9562–9567.

A constitutively active ErbB4 mutant inhibits drug-resistant colony formation by the DU-145 and PC-3 human prostate tumor cell lines

Eric E. Williams, Laurie J. Trout, Richard M. Gallo, Sarah E. Pitfield, Ianthe Bryant, Desi J. Penington, David J. Riese II*

Department of Medicinal Chemistry and Molecular Pharmacology, Purdue University School of Pharmacy, 575 Stadium Mall Drive, Room 224D, West Lafayette, IN 47907-1333, USA

Abstract

ErbB4 (HER4) is a member of the ErbB family of receptor tyrosine kinases, a family that also includes the Epidermal Growth Factor Receptor (EGFR/ErbB1/HER1), Neu/ErbB2/HER2, and ErbB3/HER3. Several groups have hypothesized that signal transduction by the ErbB4 receptor tyrosine kinase is coupled to differentiation, growth arrest, and tumor suppression in mammary and prostate epithelial cells. In this report we demonstrate that a constitutively active ErbB4 mutant inhibits the formation of drug-resistant colonies by the DU-145 and PC-3 human prostate tumor cell lines. This is consistent with our hypothesis that ErbB4 signaling is growth inhibitory and may be coupled to tumor suppression in prostate cells.
© 2002 Elsevier Science Ireland Ltd. All rights reserved.

Keywords: ErbB4; Receptor tyrosine kinase; Growth inhibition; Tumor suppression; Prostate cancer

1. Introduction

ErbB4 is a member of the ErbB family of receptor tyrosine kinases, a family that also includes the epidermal growth factor (EGF) receptor (EGFR/ErbB1/HER1), ErbB2/HER2/Neu, and ErbB3/HER3 [1–3]. The agonists for these receptors are members of the EGF family of peptide hormones, which includes more than 20 different growth factors (reviewed in [2–4]. The signaling network comprised of these hormones and receptors regulates cell proliferation and differentiation, as well as other cellular functions. Moreover, deregulated signaling by this network, typically due to inappropriate receptor or ligand (over)expression, plays a significant role in many human tumors [3,5–7]. For example, EGFR or ErbB2 overexpression is detected in a significant percentage of human breast tumors and this overexpression correlates with increased metastatic potential, chemoresistance, and poorer patient prognosis.

In contrast, relatively little is known about the roles that ErbB4 plays in tumorigenesis. ErbB4 overexpression is much less common in mammary tumor samples than is EGFR or ErbB2 overexpression. Moreover, ErbB4 overexpression in mammary tumor samples correlates with a more favorable prognosis,

* Corresponding author. Tel.: +1-765-494-6091; fax: +1-765-494-1414.
E-mail address: driese@purdue.edu (D.J. Riese).

not a less favorable prognosis [8–11]. The expression of ErbB4 and its ligands in the developing mouse mammary epithelium is highest late in pregnancy and during lactation, and corresponds with a period of terminal differentiation of the mammary epithelium and only limited proliferation [12,13]. Finally, the normal human prostate epithelium exhibits abundant ErbB4 expression; in contrast, ErbB4 expression has not been detected in any cultured human prostate tumor cell line studied to date [14,15]. These data have led investigators to hypothesize that ErbB4 signaling is coupled to terminal differentiation, growth arrest, and tumor suppression in the mammary and prostate epithelia.

A typical strategy for studying the function of a given ErbB family receptor involves assessing the effect of an EGF family hormone that binds to the ErbB family receptor of interest. These studies can be done either in cells that endogenously express the receptor of interest or in cells that overexpress the appropriate receptor. However, EGF family hormones stimulate heterodimerization of the cognate (binding) ErbB family receptor with any other ErbB family receptor present. This results in tyrosine phosphorylation and signaling by both the cognate ErbB family receptor as well as any other ErbB receptor. Thus, in human breast and prostate tumor cell lines, which frequently express EGFR, ErbB2, and ErbB3, ligands for ErbB4 stimulate not only ErbB4 signaling, but signaling by the other ErbB family receptors as well. Consequently, stimulation with ErbB4 ligands has been of limited value in studying ErbB4 function. Nonetheless, the ErbB4 ligand Neuregulin1beta (NRG1β) stimulates differentiation of mammary epithelium to lobuloalveoli in vivo [16] and stimulates in vitro differentiation of the AU-565 human tumor cell line [17,18]. Furthermore, ErbB4 expression in the SUM102 human mammary tumor cell lines permits the induction of differentiation and growth inhibition by NRG1β [19]. However, efforts by our laboratory to extend these results to other human breast tumor cell lines and to prostate tumor cell lines have failed.

In response, we have embarked on a genetic strategy to study ErbB4 function. We have previously reported the construction of three constitutively active human ErbB4 mutants. These mutants are the result of a single cysteine substitution for Gln646, His647, or Ala648 of the ErbB4 extracellular, juxtamembrane domain. Our initial analyses of these mutants revealed that these mutants, unlike a constitutively active ErbB2 mutant, fail to malignantly transform the growth of rodent fibroblast cell lines [20]. In this report we show that one of these mutants inhibits drug-resistant colony formation by two human prostate tumor cell lines. These data suggest that ErbB4 may indeed be coupled to differentiation, growth arrest, and tumor suppression in the prostate epithelium.

2. Materials and methods

2.1. Cell lines and cell culture

Mouse C127 fibroblasts and the ψ2 and PA317 recombinant retrovirus packaging cell lines are generous gifts of Dr Daniel DiMaio (Yale University, New Haven, Connecticut, USA). These cells were cultured essentially as described previously [21,22]. PC-3 and DU-145 human prostate tumor cell lines were obtained from American Type Culture Collection and were cultured in accordance with vendor recommendations. Cell culture media and supplements were obtained from GIBCO/BRL/Life Technologies. Fetal bovine serum and G418 were obtained from Gemini Bioproducts. Plasticware and Giemsa stain were obtained from Fisher Scientific.

2.2. Retrovirus infections and drug-resistant colony formation assays

Recombinant amphotropic retroviruses were produced essentially as described earlier [22]. Briefly, the recombinant retroviral constructs pLXSN (vector) [23], pLXSN-ErbB4 (ErbB4 WT) [24], pLXSN-ErbB2 V664E (ErbB2*) [25], pLXSN-ErbB4 Q646C, pLXSN-ErbB4 H647C, and pLXSN-ErbB4 A648C [20] were transfected into the ψ2 ecotropic retrovirus packaging cell line [26]. Transfected cells were selected using G418 and drug-resistant colonies were pooled and expanded into stable cell lines. Recombinant ecotropic retroviruses were recovered from the conditioned media of the recombinant ψ2 cell lines. These stocks were used to infect the PA317 amphotropic retrovirus packaging cell line [27].

Infected cells were selected using G418 and drug-resistant colonies were pooled and expanded into stable cell lines. Recombinant amphotropic retroviruses were recovered from the conditioned media of the recombinant PA317 cell lines. pLXSN is a generous gift of Dr Daniel DiMaio (Yale University, New Haven, Connecticut, USA). pLXSN-ErbB2* is a generous gift of Dr Lisa Petti (Albany Medical College, Albany, New York, USA).

C127, DU-145, and PC-3 infections with the recombinant amphotropic retroviruses were performed essentially as described earlier [20–22]. Infected cells were selected using G418. Approximately 12 days after infection, drug-resistant colonies were stained using Giemsa. The tissue culture plates were digitized using an Epson flatbed scanner set for 600 dpi. The digital images were cropped, annotated and combined into composite images. The contrast of the images was enhanced and the background was minimized to maximize the signal–noise ratio. Manipulations of the digital images were performed using Adobe Photoshop.

Drug-resistant colonies were counted manually and the retrovirus titer for each combination of retrovirus and cell line was determined by dividing the number of colonies by the volume of retrovirus used in the infection. The average viral titers were calculated from at least ten independent sets of infections. The efficiency of drug-resistant colony formation was calculated for each retrovirus stock in the DU-145 cell line by dividing the retroviral titers in the DU-145 cells by the corresponding retroviral titers in the C127 cells. These values are expressed as mean percentages calculated from at least ten independent sets of infections. The standard error was also calculated for each mean percentage. Analogous calculations were performed to calculate the efficiency of drug-resistant colony formation for each retrovirus stock in the PC-3 cell lines.

2.3. Immunoprecipitation and immunoblotting

Anti-ErbB4 immunoprecipitations and anti-phosphotyrosine immunoblotting were performed essentially as described earlier [20]. Briefly, C127 cells were starved overnight in serum-free medium, then lysed using an ice-cold isotonic lysis buffer supplemented with the non-ionic detergent NP-40 (Sigma). Nuclei and cellular debris were cleared from the lysates by centrifugation. The protein content of the lysate supernatants was determined using a modified Bradford protein assay (Pierce). ErbB4 was immunoprecipitated from equal amounts of lysate using protein A sepharose (Amersham/Pharmacia) and an anti-ErbB4 rabbit polyclonal antibody (Santa Cruz Biotechnology). The precipitates were washed with an isotonic lysis buffer and the proteins were released from the sepharose beads by boiling in a reducing SDS sample buffer. The samples were resolved by SDS-PAGE using a 7.5% acrylamide gel and were electroblotted onto nitrocellulose. The resulting blot was probed with an anti-phosphotyrosine mouse monoclonal antibody (Upstate Biotechnology). Primary antibody binding was detected and visualized using a goat anti-mouse antibody conjugated to horseradish peroxidase (Pierce) and enhanced chemiluminescence (Amersham/Pharmacia). The chemilumigram was digitized using an Epson flatbed scanner set for 600 dpi resolution. The digital images were cropped and annotated using Adobe Photoshop.

3. Results

3.1. The ErbB4 Q646C mutant inhibits drug-resistant colony formation by the DU-145 human prostate tumor cell line

We previously described the construction and packaging of recombinant retroviral vectors that express the neomycin resistance gene as well as the constitutively active ErbB4 mutants [20]. We infected DU-145 cells with these retroviruses and selected for drug-resistant colonies using G418 to assess whether any of the constitutively active ErbB4 mutants inhibits drug-resistant colony formation. As controls we also infected DU-145 cells with recombinant retroviruses that carry only the neomycin resistance gene (Vector), with recombinant retroviruses that express a constitutively active (V664E) mutant of the rat ErbB2 gene (ErbB2*) [25], and with recombinant retroviruses that express the wild-type ErbB4 gene. To control for differences in absolute viral titers, we infected C127 mouse fibroblasts in parallel and

assayed the formation of drug-resistant colonies of infected cells.

As shown in Fig. 1, DU-145 cells infected with the recombinant retrovirus that expresses the ErbB4 Q646C mutant form fewer drug-resistant colonies than do DU-145 cells infected with the other recombinant retroviruses. Furthermore, the titer of the ErbB4 Q646C recombinant retrovirus in the DU-145 cells is less than the titers of the other recombinant retroviruses (Table 1). However, the titer of the ErbB4 Q646C recombinant retrovirus in C127 fibroblasts is not less than the titer of most of the other recombinant retroviruses (Table 1). Thus, the

ratio of the ErbB4 Q646C retroviral titers in DU-145 and C127 cells is much less than the corresponding ratios of the other retrovirus titers (Table 1). Indeed, it appears that the ErbB4 Q646C mutant inhibits drug-resistant colony formation by DU-145 cells by approximately 90%.

3.2. The ErbB4 Q646C mutant inhibits drug-resistant colony formation by the PC-3 human prostate tumor cell line

We infected PC-3 cells in parallel with the DU-145 and C127 infections. The results of these infections
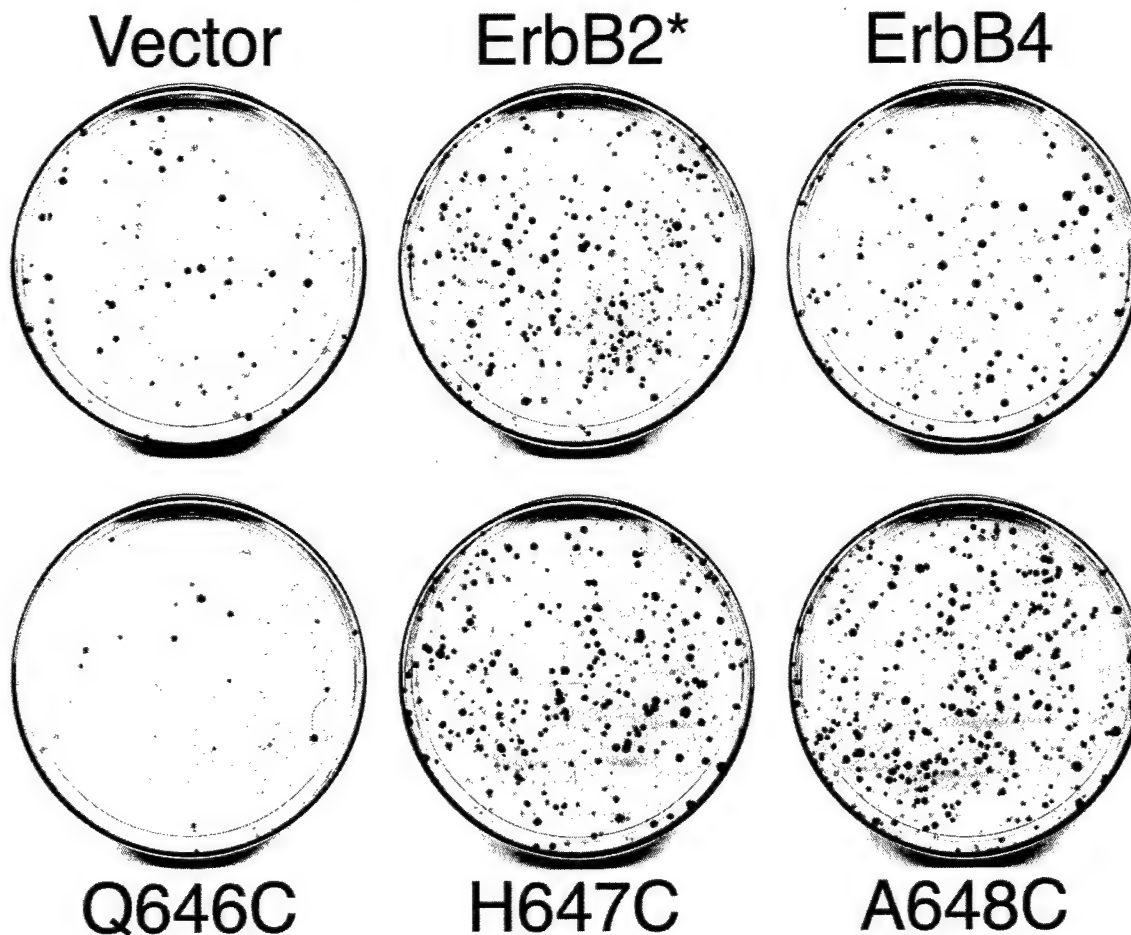

Fig. 1. The ErbB4 Q646C mutant inhibits drug-resistant colony formation by the DU-145 human prostate tumor cell line. DU-145 human prostate cells were infected with recombinant amphotropic retroviruses that carry the neomycin resistance gene (Vector) or with retroviruses that carry the neomycin resistance gene along with a constitutively active ErbB2 mutant (ErbB2*), wild-type ErbB4 (ErbB4), or constitutively active ErbB4 mutants (Q646C, H647C, A648C). Infected cells were selected using 600 µg/ml G418. Colonies of drug-resistant cells were stained using Giemsa and counted.

Table 1
The ErbB4 Q646C mutant specifically inhibits drug-resistant colony formation by the DU-145 and PC-3 human prostate tumor cell lines[a]

| Virus | Viral titers | | | Colony formation efficiency | |
| | Cell line | | | Ratios | |
Stock	C127	DU-145	PC-3	DU-145/C127	PC-3/C127
Vector	1.14E + 06	7.88E + 04	1.21 E + 05	10.7 ± 2.7	19.4 ± 5.7
ErbB2*	2.92E + 05	3.23E + 04	3.09E + 04	11.9 ± 1.8	15.6 ± 3.9
ErbB4 WT	1.55E + 05	1.44E + 04	2.27E + 04	12.0 ± 3.1	25.3 ± 7.5
Q646C	6.17E + 05	3.42E + 03	1.56E + 04	0.6 ± 0.1	3.1 ± 0.8
H647C	8.65E + 05	4.59E + 04	6.27E + 04	7.2 ± 1.2	17.3 ± 6.3
A648C	1.49E + 05	1.46E + 04	1.67E + 04	11.8 ± 2.1	15.0 ± 2.8

[a] We counted the number of colonies on each plate of infected DU-145, PC-3, and C127 cells and divided by the volume of retrovirus used to infect the cells to determine the titer of each retrovirus stock in each of the three cell lines. To compare the relative efficiency of each retrovirus stock at inducing drug-resistant colony formation in the DU-145 cell line, we divided the titer of each retrovirus stock in the DU-145 cell line by the titer of the same retrovirus stock in the C127 cell line. This value is expressed as a mean percentage calculated from at least ten independent sets of infections. The standard error for each mean was calculated and is reported. We performed analogous calculations to determine the efficiency of drug-resistant colony formation of each retrovirus stock in the PC-3 cell lines.

are similar to the results of the DU-145 infections. PC-3 cells infected with the recombinant retrovirus that expresses the ErbB4 Q646C mutant form fewer drug-resistant colonies than do PC-3 cells infected with the recombinant retroviruses that express the other ErbB4 constructs (Fig. 2). Furthermore, the titer of the ErbB4 Q646C recombinant retrovirus in the PC-3 cells is less than the titers of the other recombinant retroviruses (Table 1). Finally, the ratio of the ErbB4 Q646C retroviral titers in PC-3 and C127 cells is much less than the corresponding ratios of the other retrovirus titers (Table 1). Indeed, it appears that the ErbB4 Q646C mutant inhibits drug-resistant colony formation by PC-3 cells by approximately 75%.

3.3. The constitutively active ErbB4 mutants are expressed and tyrosine phosphorylated in the mouse C127 fibroblast cell line

We were concerned that the failure of the ErbB4 H647C and A648C mutants to inhibit drug-resistant colony formation by the DU-145 and PC-3 human prostate tumor cell lines may be due to an absence of expression and/or tyrosine phosphorylation of these ErbB4 mutants. Consequently, we pooled drug-resistant colonies that resulted from infections of C127 cells and generated stable cell lines. We assayed ErbB4 expression and tyrosine phosphorylation in

these cell lines by ErbB4 immunoprecipitation and anti-phosphotyrosine immunoblotting.

In Fig. 3 we show that all three constitutively active ErbB4 mutants are expressed and display ligand-independent tyrosine phosphorylation in the appropriate C127 cell lines. Indeed, it appears that the ErbB4 Q646C mutant exhibits less tyrosine phosphorylation than the ErbB4 H647C and A648C mutants. This suggests that the failure of the ErbB4 H647C and A648C mutants to inhibit drug-resistant colony formation by the DU-145 and PC-3 cell lines is not due to an absence of expression and/or tyrosine phosphorylation of these ErbB4 mutants.

4. Discussion

Here we demonstrate that the Q646C constitutively active ErbB4 mutant inhibits drug-resistant colony formation by the DU-145 and PC-3 human prostate tumor cell lines. This suggests that ErbB4 signaling is coupled to prostate cell growth arrest and tumor suppression. Several issues remain to be resolved in future experiments.

The phenotype that underlies ErbB4 coupling to inhibition of drug resistant colony formation has yet to be determined. For example, it is possible that ErbB4 couples to specific cell cycle arrest. However, it is also possible that ErbB4 is coupling to apoptosis rather than
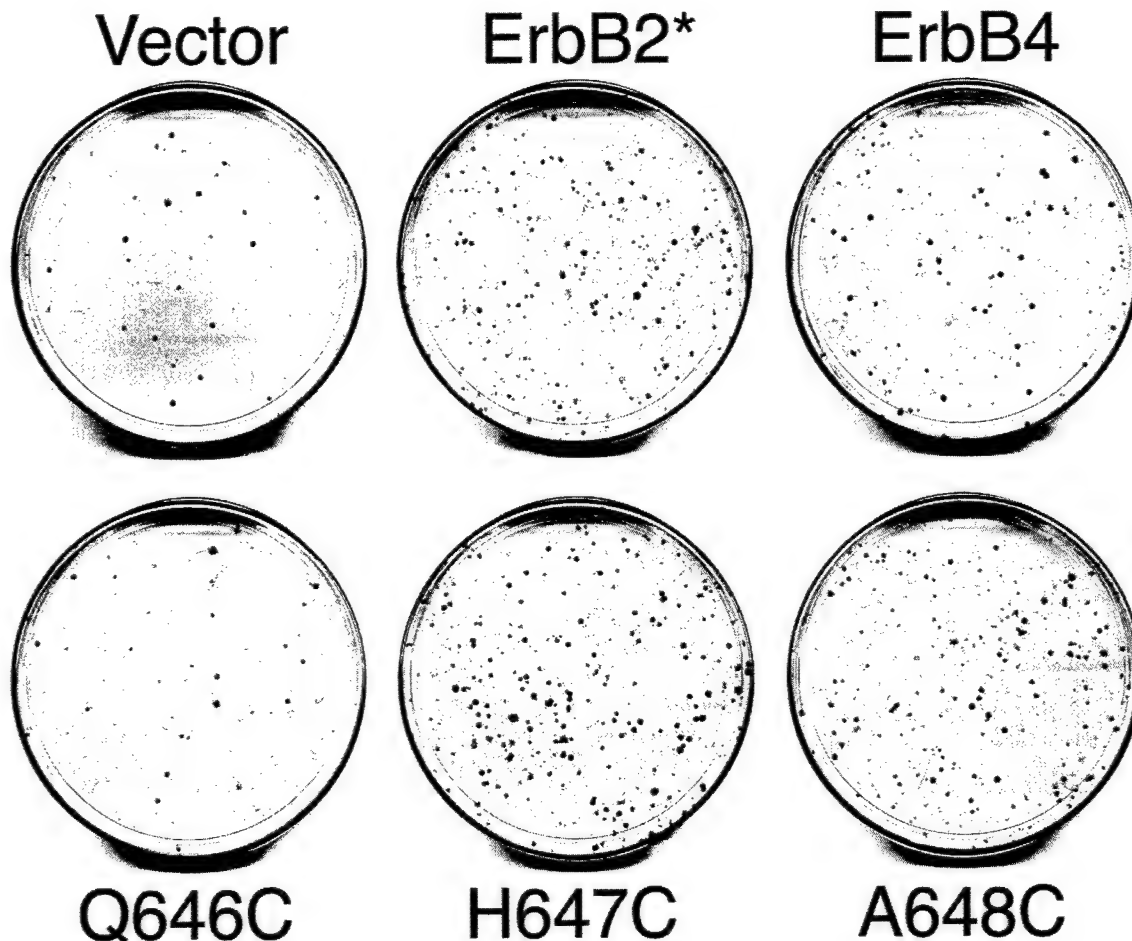
Fig. 2. The ErbB4 Q646C mutant inhibits drug-resistant colony formation by the PC-3 human prostate tumor cell line. PC-3 human prostate cells were infected with recombinant amphotropic retroviruses that carry the neomycin resistance gene (Vector) or with retroviruses that carry the neomycin resistance gene along with a constitutively active ErbB2 mutant (ErbB2*), wild-type ErbB4 (ErbB4), or constitutively active ErbB4 mutants (Q646C, H647C, A648C). Infected cells were selected using 600 μg/ml G418. Colonies of drug-resistant cells were stained using Giemsa and counted.

growth arrest. Since it is impossible to evaluate these hypotheses with the experimental system described in this report, we are developing a conditional expression system that should enable us to determine whether ErbB4 signaling is coupled to cell cycle arrest, apoptosis, or non-specific growth arrest.

Another goal for future experiments is to determine why the Q646C ErbB4 mutant is coupled to inhibition of drug-resistant colony formation by prostate tumor cell lines, whereas the H647C and A648C ErbB4 mutants are not. The differential coupling of these ErbB4 mutants is analogous to the differential coupling of constitutively phosphorylated rat ErbB2

mutants to growth transformation of rodent fibroblasts [28]. It is also analogous to the differential coupling of mutants of the bovine papillomavirus (BPV) E5 protein to malignant growth transformation of rodent fibroblasts. This differential coupling is in marked contrast to the fact that several of these BPV E5 mutants stimulate abundant platelet-derived growth factor receptor tyrosine phosphorylation [29,30]. In both of these examples, it is believed that the constitutively phosphorylated receptor tyrosine kinases are phosphorylated on different individual tyrosine residues, resulting in differential coupling to downstream signaling proteins and biological
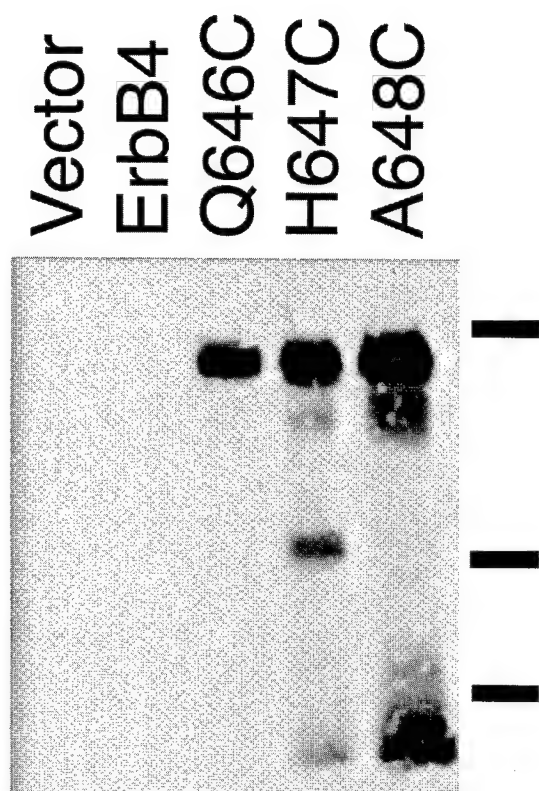
Fig. 3. The constitutively active ErbB4 mutants are expressed and tyrosine phosphorylated in the mouse C127 fibroblast cell line. C127 fibroblasts were infected with recombinant amphotropic retroviruses that express the neomycin resistance gene (Vector) or with retroviruses that express the neomycin resistance gene along with wild-type ErbB4 (ErbB4) or constitutively active ErbB4 mutants (Q646C, H647C, A648C). Infected cells were selected using 1000 µg/ml G418. Colonies of drug-resistant cells were pooled and expanded into stable cell lines. Confluent 100 mm plates of each cell line were incubated in serum-free medium for 24 h, after which cells were lysed. ErbB4 was precipitated using specific antibodies and the precipitates were resolved by SDS-PAGE and electroblotted onto nitrocellulose. The blot was probed with an anti-phosphotyrosine mouse monoclonal antibody. Antibody binding was detected and visualized using a goat anti-mouse secondary antibody coupled to horseradish peroxidase and enhanced chemiluminescence. Bars indicate the positions of the molecular weight markers (198 kDa, 115 kDa, and 93 kDa). Tyrosine phosphorylated ErbB4 is represented by the band with apparent mobility of approximately 190 kDa.

responses. Indeed, different ErbB4 ligands cause different patterns of ErbB4 phosphorylation and differential coupling to downstream signaling effectors and biological responses [31]. Thus, we hypoth-

esize that the functional differences between the ErbB4 Q646C mutant and the other constitutively active ErbB4 mutants are due to phosphorylation on different ErbB4 tyrosine residues. Mapping the sites of ErbB4 tyrosine phosphorylation for the three constitutively active ErbB4 mutants and genetic studies to identify the sites of ErbB4 tyrosine phosphorylation that couple ErbB4 to inhibition of drug resistant colony formation will enable us to formally address this hypothesis.

Finally, additional experiments will be necessary to formally test the hypothesis that ErbB4 is a prostate tumor suppressor. Male transgenic mice that exhibit tissue specific ectopic expression of the Q646C ErbB4 mutant in the prostate gland would be an appropriate in vivo model system for assessing whether constitutive ErbB4 signaling is sufficient to suppress prostate tumorigenesis.

References

[1] J. Schlessinger, Cell signaling by receptor tyrosine kinases, Cell 103 (2000) 211–225.

[2] W.J. Gullick, The type I growth factor receptors and their ligands considered as a complex system, Endocrine-Related Cancer 8 (2001) 75–82.

[3] Y. Yarden, M.X. Sliwkowski, Untangling the ErbB signalling network, Nat. Rev. Mol. Cell Biol. 2 (2001) 127–137.

[4] R. Kumar, R.K. Vadlamudi, The EGF family of growth factors, J. Clin. Ligand Assay 23 (2001) 233–237.

[5] D.F. Stern, Tyrosine kinase signalling in breast cancer: ErbB family receptor tyrosine kinases, Breast Cancer Res. 2 (2000) 176–183.

[6] N. Normanno, C. Bianco, A. DeLuca, D.S. Salomon, The role of EGF-related peptides in tumor growth, Frontiers Biosci. 6 (2001) d685–d707.

[7] F. Ozawa, H. Friess, A. Tempia-Caliera, J. Kleeff, M.W. Buchler, Growth factors and their receptors in pancreatic cancer, Teratogen. Carcinogen. Mutagen. 21 (2001) 27–44.

[8] S.S. Bacus, D. Chin, Y. Yarden, C.R. Zelnick, D.F. Stern, Type 1 receptor tyrosine kinases are differentially phosphorylated in mammary carcinoma and differentially associated with steroid receptors, Am. J. Pathol. 148 (1996) 549–558.

[9] J.M. Knowlden, J.W. Gee, L.T. Seery, L. Farrow, W.J. Gullick, I.O. Ellis, R.W. Blamey, J.R. Robertson, R.I. Nicholson, c-ErbB3 and c-ErbB4 expression is a feature of the endocrine responsive phenotype in clinical cancer, Oncogene 17 (1998) 1949–1957.

[10] V. Pawlowski, F. Revillion, M. Hebbar, L. Hornez, J-P. Peyrat, Prognostic value of the type I growth factor receptors in a large series of human primary breast cancers quantified with a real-time reverse transcription-polymerase chain reaction assay, Clin. Cancer Res. 6 (2000) 4217–4225.

[11] Z. Suo, B. Risberg, M.G. Kaisson, K. Willman, A. Tierens, E. Skovlund, J.M. Nesland, EGFR family expression in breast carcinomas, c-erbB2 and c-erbB4 receptors have different effects on survival, J. Pathol. 196 (2002) 17–25.

[12] J.A. Schroeder, D.C. Lee, Dynamic expression and activation of ErbB receptors in the developing mouse mammary gland, Cell Growth Differ. 9 (1998) 451–464.

[13] K.L. Troyer, D.C. Lee, Regulation of mammary gland development and tumorigenesis by the ErbB signaling network, J. Mammary Gland Biol. Neoplasia 6 (2001) 7–21.

[14] D. Robinson, F. He, T. Pretlow, H-J. Kung, A tyrosine kinase profile of prostate carcinoma, Proc. Natl. Acad. Sci. USA 93 (1996) 5958–5962.

[15] A.W. Grasso, D. Wen, C.M. Miller, J.S. Rhim, T.G. Pretlow, H.-J. Kung, ErbB kinases and NDF signaling in human prostate cancer cells, Oncogene 15 (1997) 2705–2716.

[16] F.E. Jones, D.J. Jerry, B.C. Guarino, G.C. Andrews, D.F. Stern, Heregulin induces in vivo proliferation and differentiation of mammary epithelium into secretory lobuloalveoli, Cell Growth Differ. 7 (1995) 1031–1038.

[17] E. Peles, S.S. Bacus, R.A. Koski, H.S. Lu, D. Wen, S.G. Ogden, R. Ben Levy, Y. Yarden, Isolation of the Neu/HER-2 stimulatory ligand: a 44 kd glycoprotein that induces differentiation of mammary tumor cells, Cell 69 (1992) 205–216.

[18] D. Wen, E. Peles, R. Cupples, S.V. Suggs, S.S. Bacus, Y. Luo, G. Trail, S. Hu, S.M. Silbiger, R. Ben Levy, R.A. Koski, H.S. Lu, Y. Yarden, Neu differentiation factor: a transmembrane glycoprotein containing an EGF domain and an immunoglobulin homology unit, Cell 69 (1992) 559–572.

[19] C.I. Sartor, H. Zhou, E. Kozlowska, K. Guttridge, E. Kawata, L. Caskey, J. Harrelson, N. Hynes, S. Ethier, B. Calvo, H.S. Earp III, HER4 mediates ligand-dependent antiproliferative and differentiation responses in human breast cancer cells, Mol. Cell Biol. 21 (2001) 4265–4275.

[20] D.J. Penington, I. Bryant, D.J. Riese II, Constitutively active ErbB4 and ErbB2 mutants exhibit distinct biological activities, Cell Growth Differ. 13 (2002) 247–256.

[21] D.J. Riese II, D. DiMaio, An intact PDGF signaling pathway is required for efficient growth transformation of mouse C127 cells by the bovine papillomavirus E5 protein, Oncogene 10 (1995) 1431–1439.

[22] C. Leptak, S. Ramon y Cajal, R. Kulke, B.H. Horwitz, D.J. Riese, G.P. Dotto, D. DiMaio, Tumorigenic transformation of murine keratinocytes by the E5 genes of bovine papillomavirus type 1 and human papillomavirus type 16, J. Virol. 65 (1991) 7078–7083.

[23] D.A. Miller, G.J. Rosman, Improved retroviral vectors for gene transfer and expression, BioTechniques 7 (1989) 980–990.

[24] D.J. Riese II, T.M. Van Raaij, G.D. Plowman, G.C. Andrews, D.F. Stern, The cellular response to neuregulins is governed by complex interactions of the ErbB receptor family, Mol. Cell Biol. 15 (1995) 5770–5776.

[25] L.M. Petti, F.A. Ray, Transformation of mortal human fibroblasts and activation of a growth inhibitory pathway by the bovine papillomavirus E5 oncoprotein, Cell Growth Differ. 11 (2000) 395–408.

[26] R. Mann, R.C. Mulligan, D. Baltimore, Construction of a retrovirus packaging mutant and its use to produce helper-free defective retrovirus, Cell 33 (1983) 153–159.

[27] D.A. Muller, C. Buttimore, Redesign of retrovirus packaging cell lines to avoid recombination leading to helper virus production, Mol. Cell Biol. 6 (1986) 2895–2902.

[28] C.L. Burke, D.F. Stern, Activation of Neu (ErbB2) mediated by disulfide bond-induced dimerization reveals a receptor tyrosine kinase dimer interface, Mol. Cell Biol. 18 (1998) 5371–5379.

[29] L.A. Nilson, R.A. Gottlieb, G.W. Pollack, D. DiMaio, Mutational analysis of the interaction between the bovine papillomavirus E5 transforming protein and the endogenous β receptor for platelet derived growth factor, J. Virol. 72 (1998) 5869–5874.

[30] O. Klein, G.W. Pollack, T. Surti, D. Kegler-Ebo, S.O. Smith, D. DiMaio, Role of glutamine 17 of the bovine papillomavirus E5 protein in platelet-derived growth factor β receptor activation and cell transformation, J. Virol. 72 (1998) 8921–8932.

[31] C. Sweeney, C. Lai, D.J. Riese II, A.J. Diamonti, L.C. Cantley, K.L. Carraway III, Ligand Discrimination in Signaling through an ErbB4 Receptor Homodimer, J. Biol. Chem. 276 (2000) 19803–19807.

npg

Five carboxyl-terminal residues of neuregulin2 are critical for stimulation of signaling by the ErbB4 receptor tyrosine kinase

Stuart S Hobbs[1], Elizabeth M Cameron[1], Robert P Hammer[2], Ann TD Le[1], Richard M Gallo[1], Erika N Blommel[1], Stephanie L Coffing[1], Han Chang[3] and David J Riese II*,[1]

[1]Department of Medicinal Chemistry and Molecular Pharmacology, Purdue University School of Pharmacy, West Lafayette, IN 47907-2064, USA; [2]Department of Chemistry, Louisiana State University, Baton Rouge, LA 70803-1804, USA; [3]Bristol-Myers Squibb Pharmaceutical Research Institute, PO Box 5400, Princeton, NJ 08543-5400, USA

The neuregulins (NRGs) are members of the epidermal growth factor (EGF) family of peptide growth factors. These hormones are agonists for the ErbB family of receptor tyrosine kinases, a family that includes the epidermal growth factor receptor (EGFR/ErbB1), ErbB2/Neu/HER2, ErbB3/HER3, and ErbB4/HER4. We recently observed that the EGF family hormone NRG2β is a potent agonist for ErbB4. In contrast, NRG2α, a splicing isoform of the same gene that encodes NRG2β, is a poor ErbB4 agonist. We hypothesized that carboxyl-terminal residues of NRG2β are critical for stimulation of ErbB4 tyrosine phosphorylation and coupling to downstream signaling events. Here, we demonstrate that the substitution of a lysine residue for Phe45 in NRG2β results in reduced ligand potency. We also demonstrate that substitution of a phenylalanine for Lys45 in NRG2α results in increased ligand potency. Finally, analyses of the gain-of-function NRG2α Chg5 mutant demonstrate that Gln43, Met47, Asn49, and Phe50 regulate ligand efficacy. Thus, these data indicate that carboxyl-terminal residues of NRG2β are critical for activation of ErbB4 signaling. Moreover, these NRG2α and NRG2β mutants reveal new insights into models for ligand-induced ErbB family receptor tyrosine phosphorylation and coupling to downstream signaling events.

Introduction

Neuregulins (NRGs) are members of the epidermal growth factor (EGF) family of peptide hormones (reviewed in Buonanno and Fischbach, 2001; Gullick, 2001), a family that includes EGF itself as well as transforming growth factor alpha (TGFα), betacellulin (BTC), amphiregulin (AR), heparin-binding EGF-like growth factor (HB-EGF), and epiregulin (EPR). NRGs are agonists for the four members of the ErbB family of receptor tyrosine kinases, a family that includes the epidermal growth factor receptor (EGFR/ErbB1), ErbB2/HER2/Neu, ErbB3/HER3, and ErbB4/HER4. There are four NRG genes; at least two of these genes encode multiple ligands through differential transcriptional splicing. Thus, there are more than 10 different NRG isoforms; many of these isoforms display different patterns of ErbB family receptor activation. For example, we recently demonstrated that NRG2β is a potent, direct ErbB4 agonist; in contrast, NRG2α, which is encoded by the same gene as NRG2β, fails to stimulate ErbB4 tyrosine phosphorylation directly (Hobbs et al., 2002).

Thus, an obvious question is: What is the mechanism underlying the difference in activation of ErbB4 signaling by NRG2α and NRG2β? Here, we demonstrate that Phe45 of NRG2β regulates the potency of this ligand. Moreover, we demonstrate that Gln43, Met47, Asn49, and Phe50 of NRG2β may regulate the efficacy of this ligand. In the discussion, we attempt to put these results in the context of existing models for activation of ErbB family receptor signaling by EGF family hormones. Given these models, we will discuss potential mechanisms by which the carboxyl-terminal amino acids of NRG2β may regulate its activity.

*Correspondence: DJ Riese II, Department of Medicinal Chemistry and Molecular Pharmacology, Purdue University, 201 S University Street, HANS 114, West Lafayette, IN 47907-2064, USA; E-mail: driese@purdue.edu

Results

Construction of NRG2 mutants

We have previously reported that NRG2β is a potent agonist for ErbB4 and that NRG2α is not (Hobbs et al., 2002). Consequently, we hypothesized that there is a domain present in NRG2β and absent in NRG2α that is critical for activation of ErbB4 signaling. A comparison of the sequences of NRG1α, NRG1β, NRG2α, NRG2β, NRG3, and NRG4 suggests that five amino acids near the carboxyl terminus of NRG2β are critical for activation of ErbB4 signaling (Figure 1): Gln43, Phe45, Met47, Asn49, and Phe50. The amount of conservation

	42	43	44		45	46	47	48	49	50	51	Activates ErbB4
NRG1α	Cys	Thr	Glu	---	Asn	Val	Pro	Met	Lys	Val	Gln	+/-
NRG1β	Cys	Gln	Asn	---	Tyr	Val	Met	Ala	Ser	Phe	Tyr	++++
NRG2α	Cys	Leu	Glu	---	Lys	Leu	Pro	Leu	Arg	Leu	Tyr	+/-
NRG2β	Cys	Gln	Gln	---	Phe	Ala	Met	Asn	Phe	Ser		++++
NRG3	Cys	Asp	Gln	---	Phe	Leu	Pro	Lys	Thr	Asp	Ser	+
NRG4	Cys	Glu	Glu	Val	Phe	Leu	Pro	Ser	Ser	Ser	Ile	++

Figure 1 The carboxyl terminus and activity of six NRG isoforms. The carboxyl-terminal amino-acid sequence of six NRG isoforms (NRG1α, NRG1β, NRG2α, NRG2β, NRG3, and NRG4) is given. Activation of ErbB4 tyrosine phosphorylation by the six NRG isoforms is indicated (Culouscou et al., 1993; Plowman et al., 1993; Tzahar et al., 1994; Carraway et al., 1997; Chang et al., 1997; Zhang et al., 1997; Harari et al., 1999; Hobbs et al., 2002). Five NRG residues appear to correlate with activation of ErbB4 tyrosine phosphorylation: Gln43, Phe45, Met47, Ser49, and Phe50. Solid underlining indicates identity with this sequence. Dotted underlining indicates conservation with this sequence

	43	44	45	46	47	48	49	50
NRG2α	Leu	Glu	Lys	Leu	Pro	Leu	Arg	Leu
NRG2β	Gln	Gln	Phe	Ala	Met	Val	Asn	Phe
NRG2α Chg5	Gln	Glu	Phe	Leu	Met	Leu	Asn	Phe
NRG2α L43Q	Gln	Glu	Lys	Leu	Pro	Leu	Arg	Leu
NRG2α K45F	Leu	Glu	Phe	Leu	Pro	Leu	Arg	Leu
NRG2α P47M	Leu	Glu	Lys	Leu	Met	Leu	Arg	Leu
NRG2α R49N	Leu	Glu	Lys	Leu	Pro	Leu	Asn	Leu
NRG2α L50F	Leu	Glu	Lys	Leu	Pro	Leu	Arg	Phe
NRG2β Q43L	Leu	Gln	Phe	Ala	Met	Val	Asn	Phe
NRG2β F45K	Gln	Gln	Lys	Ala	Met	Val	Asn	Phe
NRG2β M47P	Gln	Gln	Phe	Ala	Pro	Val	Asn	Phe
NRG2β N49R	Gln	Gln	Phe	Ala	Met	Val	Arg	Phe
NRG2β F50L	Gln	Gln	Phe	Ala	Met	Val	Asn	Leu

Figure 2 Putative loss-of-function NRG2β mutants and putative gain-of-function NRG2α mutants. Five NRG2β mutants were constructed by replacing one of the five 'critical' amino acids in NRG2β with the corresponding amino acids of NRG2α. Five NRG2α mutants were constructed by replacing one of the five 'critical' amino acids of NRG2α with the corresponding amino acid of NRG2β. An additional NRG2α mutant, NRG2α Chg5, was constructed by replacing all of the five 'critical' amino acids with the corresponding amino acids of NRG2β. Shaded text indicates the mutated amino acid

of these five amino acids in a NRG molecule correlates with stimulation of ErbB4 signaling. We tested this hypothesis by generating five putative loss-of-function NRG2β mutants (Figure 2) in which we substituted the corresponding NRG2α residue (Leu43, Lys45, Pro47, Arg49, and Leu50) for one of the five 'critical' residues in NRG2β. These mutants are designated NRG2β Q43L, F45K, M47P, N49R, and F50L. We generated five putative gain-of-function NRG2α mutants by substituting one of the five 'critical' residues in NRG2β for the corresponding residue in NRG2α. These mutants are designated NRG2α L43Q, K45F, P47 M, R49N, and L50F. We also generated a putative gain-of-function NRG2α mutant by substituting all five 'critical residues' in NRG2β for the corresponding residues in NRG2α. This mutant is designated NRG2α Chg5. These mutants were generated by site-directed mutagenesis and were expressed, purified, and quantified as described elsewhere in this report.

The NRG2β F45K mutant is no longer a potent ErbB4 agonist

We first assessed whether any of the putative loss-of-function ErbB4 mutants had lost some of their capacity to stimulate ErbB4 tyrosine phosphorylation. CEM cells, which lack endogenous ErbB family receptor expression, had been previously engineered to express human ErbB4 ectopically, resulting in CEM/ErbB4 cells (Plowman et al., 1993; Riese et al., 1998; Feroz et al., 2002). We treated CEM/ErbB4 cells with 10 nM NRG2α, NRG2β, or the five putative loss-of-function NRG2β mutants. Cells treated with 10 nM NRG1β served as a positive control. We assayed ErbB4 tyrosine phosphorylation by ErbB4 immunoprecipitation and antiphosphotyrosine immunoblotting (Figure 3a, top panel). As a control for ErbB4 expression levels, we stripped the blot and probed it with an anti-ErbB4 antibody (Figure 3a, bottom panel). Both NRG1β and NRG2β stimulate abundant ErbB4 tyrosine phosphorylation, whereas NRG2α does not. Four of the five NRG2β mutants (Q43L, M47P, N49R, and F50L) stimulate abundant ErbB4 tyrosine phosphorylation, but the NRG2β F45K mutant fails to stimulate ErbB4 tyrosine phosphorylation strongly. Thus, Phe45 appears to be necessary for stimulation of ErbB4 tyrosine phosphorylation by NRG2β.
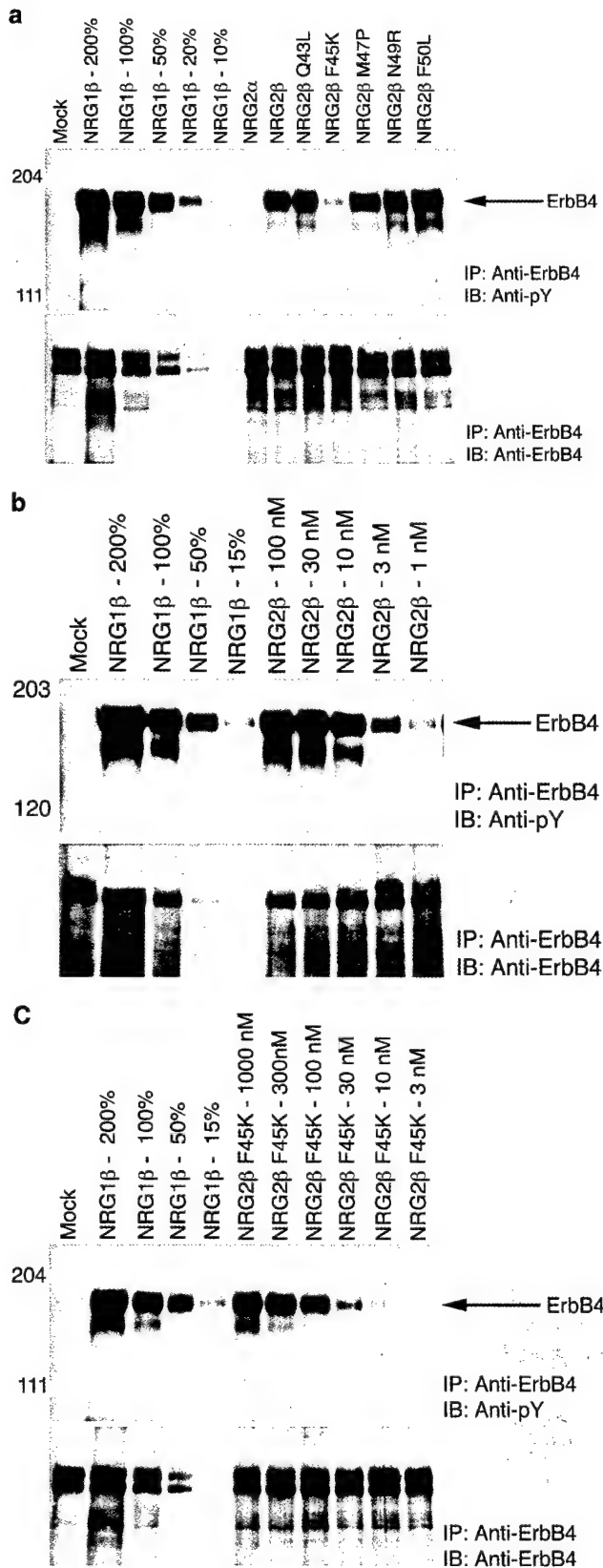
To further characterize the NRG2β F45K mutant we performed dose–response experiments using CEM/ErbB4 cells. We stimulated CEM/ErbB4 cells with varying amounts of NRG2β and NRG2β F45K. In parallel, we constructed an ErbB4 tyrosine phosphorylation standard curve by analysing varying amounts of ErbB4 immunoprecipitates generated from CEM/ErbB4 cells that had been stimulated with NRG1β. In multiple independent experiments, wild-type NRG2β displayed an average ErbB4 tyrosine phosphorylation EC_{50} of 7.0 ± 1.0 nM (Figure 3b). The NRG2β F45K mutant is a much less potent ErbB4 agonist, displaying an average ErbB4 tyrosine phosphorylation EC_{50} of 90 ± 15 nM over multiple experiments (Figure 3c).

The maximal amount of ErbB4 tyrosine phosphorylation (ErbB4 S_{max}) stimulated by wild-type NRG2β is $114 \pm 17\%$ of the ErbB4 S_{max} stimulated by NRG1β (Figure 3b). The ErbB4 S_{max} stimulated by the NRG2β F45K mutant is $120 \pm 10\%$ of the ErbB4 S_{max} stimulated by NRG1β (Figure 3c). Thus, at saturation, wild-type NRG2β and the NRG2β F45K mutant display similar efficacy. Altogether, the results of the dose–response experiments suggest that Phe45 regulates activation of ErbB4 tyrosine phosphorylation by NRG2β by regulating the affinity of NRG2β for ErbB4.

The NRG2α K45F mutant is a more potent ErbB4 agonist than NRG2α

We then stimulated CEM/ErbB4 cells with the six putative gain-of-function NRG2α mutants at a final concentration of 10 nM. Cells stimulated with 10 nM NRG2α, NRG2β, or NRG1β served as controls. We assayed ErbB4 tyrosine phosphorylation by ErbB4 immunoprecipitation and antiphosphotyrosine immu-

noblotting (Figure 4a, top panel). As a control for ErbB4 expression levels, we stripped the blot and probed it with an anti-ErbB4 antibody (Figure 4a,

bottom panel). NRG2α and four of the NRG2α mutants (L43Q, P47M, R49N, and L50F) stimulated much less ErbB4 tyrosine phosphorylation than did NRG1β and NRG2β. In contrast, the NRG2α Chg5 and K45F mutants stimulated at least modest amounts of ErbB4 tyrosine phosphorylation. This suggests that Phe45 of NRG2β is sufficient to enable NRG2α to stimulate ErbB4 tyrosine phosphorylation. However, because the NRG2α Chg5 mutant stimulates a greater amount of ErbB4 tyrosine phosphorylation than does the NRG2α K45F mutant, the Gln43, Met47, Asn49, and Phe50 residues may contribute to activation of ErbB4 by NRG2β, despite the fact that none of these residues are individually necessary for activation of ErbB4 by NRG2β or sufficient for activation of ErbB4 by NRG2α.

To further characterize the activity of the NRG2α Chg5 and K45F gain-of-function mutants, we performed dose–response experiments using CEM/ErbB4 cells and methodologies analogous to those described earlier in this report. Over multiple experiments, we failed to stimulate a saturated amount of ErbB4 tyrosine phosphorylation using wild-type NRG2α (Figure 4b). However, we conservatively estimate that NRG2α exhibits an average ErbB4 tyrosine phosphorylation EC_{50} of greater than 300 nM (Figure 4b). In contrast, the NRG2α K45F (Figure 4b) and NRG2α Chg5 (Figure 4c) mutants are much more potent. The average ErbB4 tyrosine phosphorylation EC_{50} values for these mutants are 73 ± 7 and 39 ± 9 nM, respectively.

Over multiple experiments, the average maximal amount of ErbB4 tyrosine phosphorylation (ErbB4 S_{max}) stimulated by the NRG2α Chg5 mutant is $141 \pm 23\%$ of the ErbB4 S_{max} stimulated by NRG1β. However, the ErbB4 S_{max} stimulated by the NRG2α K45F mutant is only $77 \pm 7\%$ of the ErbB4 S_{max} stimulated by NRG1β. Because of the limited potency of wild-type NRG2α, we are not able to determine the ErbB4 S_{max} for that ligand.

The lower ErbB4 tyrosine phosphorylation EC_{50} values of the NRG2α K45F and Chg5 mutants relative to NRG2α may reflect a higher affinity of these mutants for ErbB4. This suggests that the Phe45 residue plays an important role in conferring high-affinity binding to ErbB4. The ErbB4 tyrosine phosphorylation EC_{50} value

Figure 3 Phenylalanine 45 is necessary for stimulation of ErbB4 tyrosine phosphorylation by NRG2. CEM/ErbB4 cells were stimulated with the NRGs and NRG mutants as indicated. ErbB4 tyrosine phosphorylation (anti-pY IB) and expression (anti-ErbB4 IB) were analysed by immunoblotting following ErbB4 immunoprecipitation. Tyrosine phosphorylated ErbB4 is represented by the single band that has slightly greater mobility than the 204 kDa marker. On the ErbB4 blots, ErbB4 is present as a higher molecular weight band that represents the fully processed, mature form of the receptor and a lower molecular weight band that represents the immature form of the receptor. (a) ErbB4 tyrosine phosphorylation and expression following stimulation with 10 nM of the five putative loss-of-function NRG2β mutants. (b) ErbB4 tyrosine phosphorylation and expression following stimulation with increasing concentrations of NRG2β. (c) ErbB4 tyrosine phosphorylation and expression following stimulation with increasing concentrations of the NRG2β F45K loss-of-function mutant

of the NRG2α Chg5 mutant is somewhat lower than that of the NRG2α K45F mutant. This may reflect an increased affinity of NRG2α Chg5 for ErbB4 compared to the affinity of NRG2α K45F for ErbB4. Thus, it appears that the Gln43, Met47, Asn49, and Phe50 residues also play a limited role in regulating the affinity of NRG molecules for ErbB4. The ErbB4 S_{max} stimulated by the NRG2α Chg5 mutant is higher than the ErbB4 S_{max} stimulated by the NRG2α K45F

mutant. This suggests that there is an intrinsic difference between the two gain-of-function NRG2α mutants that is independent of their apparent differences in potency or affinity for ErbB4. Again, this highlights the potential role that the Gln43, Met47, Asn49, and Phe50 residues play in defining the function of NRG molecules.

Phe45 is not critical for NRG2-induced coupling of EGFR–ErbB4 heterodimers to IL3 independence

We have previously shown that in the IL3-dependent BaF3 mouse lymphoid cell line, ectopic EGFR and ErbB4 coexpression permits ligands for either EGFR or ErbB4 to stimulate EGFR–ErbB4 heterodimerization and coupling to interleukin-3 (IL3)-independent proliferation (Riese et al., 1995, 1996a). In BaF3/ EGFR + ErbB4 cells, 10 nM of NRG1β, NRG2β or the NRG2α Chg5 mutant all stimulate IL3-independent proliferation, whereas 10 nM NRG2α stimulates, at best, a modest level of IL3 independence (Figure 5). Thus, NRG2α is a much weaker stimulus of EGFR and ErbB4 coupling to downstream signaling events than are NRG1β, NRG2β, and the NRG2α Chg5 mutant. These results are consistent with the ErbB4 tyrosine phosphorylation data shown earlier (Figures 3a and 4a).

At a concentration of 10 nM, the NRG2α K45F mutant, which stimulates slightly less ErbB4 tyrosine phosphorylation than does 10 nM NRG2α Chg5 in CEM/ErbB4 cells (Figure 4a), stimulates only modest (at best) IL3 independence in the BaF3/EGFR + ErbB4 cell line. This may be because the NRG2α K45F mutant is less potent or has a lower affinity for ErbB4 than the NRG2α Chg5 mutant. The other possibility is that there is an intrinsic difference between these two gain-of-function NRG2α mutants that is independent of their apparent differences in potency or affinity for ErbB4. To distinguish between these two possibilities, we assayed IL3 independence in BaF3/EGFR + ErbB4 cells treated with 73 nM NRG2α K45F, which is the ErbB4 tyrosine phosphorylation EC_{50} in CEM/ErbB4 cells. However, this NRG2α K45F concentration still fails to stimulate
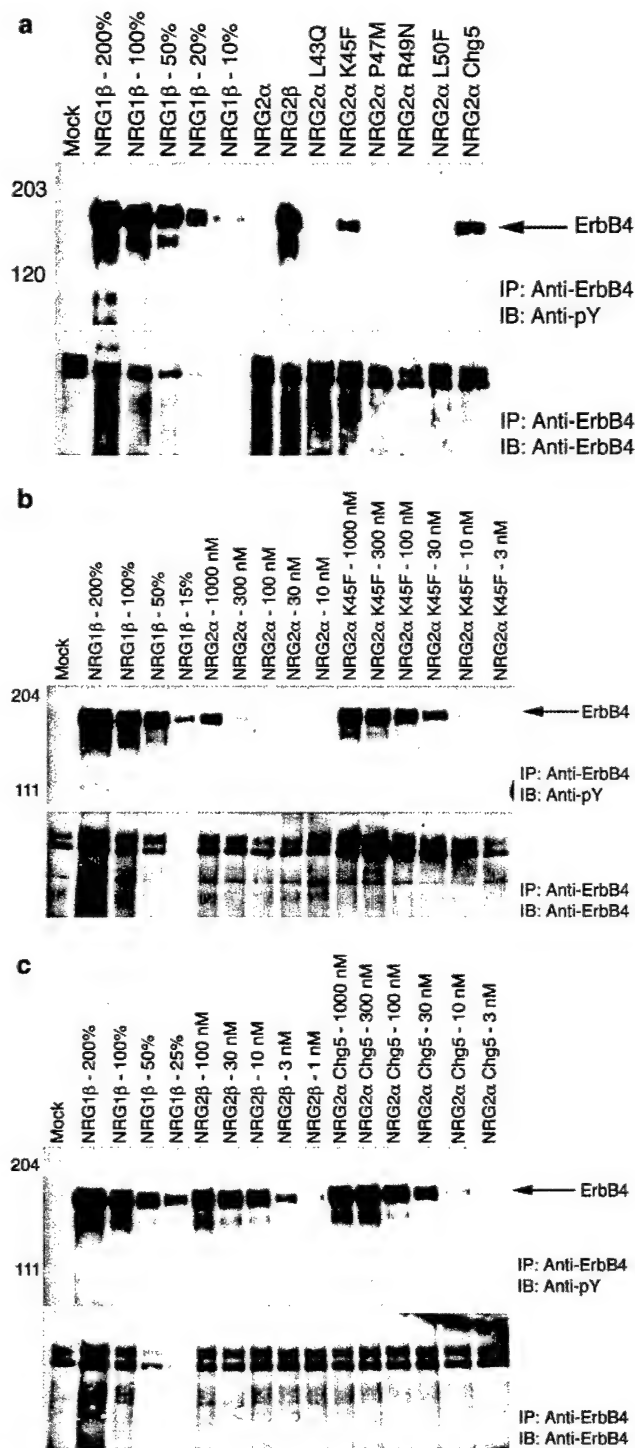
Figure 4 Phenylalanine 45 is sufficient for stimulation of ErbB4 tyrosine phosphorylation by NRG2. CEM/ErbB4 cells were stimulated with the NRGs and NRG mutants as indicated. ErbB4 tyrosine phosphorylation (anti-pY IB) and expression (anti-ErbB4 IB) were analysed by immunoblotting following ErbB4 immunoprecipitation. Tyrosine-phosphorylated ErbB4 is represented by the single band that has slightly greater mobility than the 204 kDa marker. The blot was stripped and reprobed with an anti-ErbB4 antibody (IB: anti-ErbB4). On the ErbB4 blots, ErbB4 is present as a higher molecular weight band that represents the fully processed, mature form of the receptor and a lower molecular weight band that represents the immature form of the receptor. (a) ErbB4 tyrosine phosphorylation and expression following stimulation with 10 nM of the five putative gain-of-function NRG2α mutants. (b) ErbB4 tyrosine phosphorylation and expression following stimulation with increasing concentrations of NRG2α or the NRG2α K45F gain-of-function mutant. (c) ErbB4 tyrosine phosphorylation and expression following stimulation with increasing concentrations of the NRG2α Chg5 gain-of-function mutant
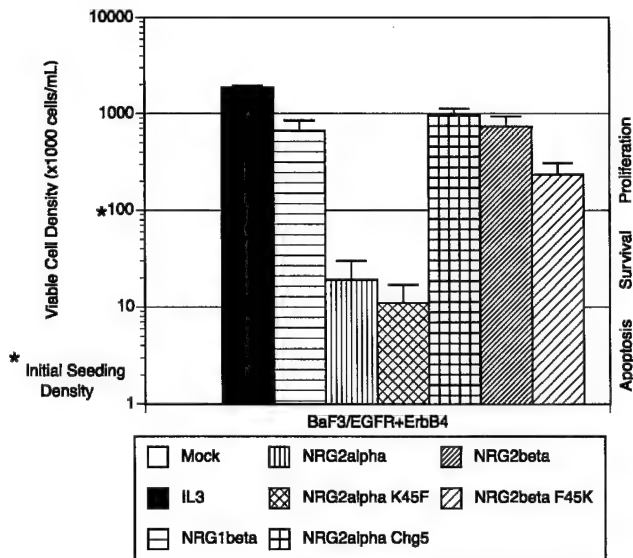
Figure 5 NRG2β F45K and NRG2α Chg5 mutants, but not the NRG2α K45F mutant, stimulate coupling of EGFR and ErbB4 to IL3-independent proliferation in the BaF3/EGFR + ErbB4 cell line. BaF3/EGFR + ErbB4 cells were cultured to saturation density, then seeded in 24-well dishes at a density of 100×10^3 cells/ml in media devoid of IL3 but supplemented with 10 nM of the NRGs or NRG mutants as indicated. Mock stimulated cells (Mock) were seeded in medium devoid of IL3 but supplemented with phosphate-buffered saline (NRG diluent). The positive control (IL3) cells were treated with medium containing IL3. After 4 days, the cells were stained with Trypan blue and the density of viable cells was determined by counting viable cells using a hemacytometer

IL3-independent proliferation in the BaF3/EGFR + ErbB4 cell line (data not shown). In contrast, 10 nM of the NRG2α Chg5 mutant, a concentration that is much less than the ErbB4 tyrosine phosphorylation EC_{50} in CEM/ErbB4 cells, stimulates IL3-independent proliferation (Figure 5). These results are consistent with the differences between the ErbB4 S_{max} values for the NRG2α K45F and Chg5 mutants and provide additional support for our hypothesis that there is an intrinsic difference between the two gain-of-function NRG2α mutants that is independent of their apparent differences in potency or affinity for ErbB4.

At a concentration of 10 nM, the NRG2β F45K mutant stimulates IL3-independent proliferation in the BaF3/EGFR + ErbB4 cells (Figure 5). It must be noted, however, that the NRG2β F45K mutant stimulates a lower level of IL3-independent proliferation than does an equal concentration of wild-type NRG2β. At a concentration of 10 nM, the NRG2β F45K stimulates much less ErbB4 tyrosine phosphorylation in the CEM/ErbB4 cell line than does wild-type NRG2β (Figure 3a). Indeed, the dose–response data shown earlier in this report (Figure 3c) suggest that the NRG2β F45K mutant has a lower affinity for ErbB4 than does wild-type NRG2β. Consistent with such a model, the NRG2β F45K mutant at a final concentration of 90 nM stimulates a level of IL3-independent proliferation in the BaF3/EGFR + ErbB4 cell line comparable to the

level stimulated by 10 nM wild-type NRG2β (data not shown).

NRG2α gain-of-function mutants stimulate modest EGFR and ErbB4 tyrosine phosphorylation in the BaF3/ EGFR + ErbB4 cell line

The failure of the NRG2α K45F mutant to stimulate IL3-independent proliferation in the BaF3/ EGFR + ErbB4 cell line (Figure 5) is not consistent with the ability of the NRG2α K45F mutant to stimulate ErbB4 tyrosine phosphorylation in the CEM/ErbB4 cell line (Figure 4a, b). Indeed, the NRG2α Chg5 mutant stimulates ErbB4 phosphorylation in the CEM/ErbB4 cell line (Figure 4a, c) and also stimulates IL3-independent proliferation in BaF3/EGFR + ErbB4 cells (Figure 5). A simple possible explanation is that the NRG2α K45F mutant stimulates less ErbB receptor tyrosine phosphorylation in the BaF3/EGFR + ErbB4 cell line than does the NRG2α Chg5 mutant. Thus, we examined EGFR and ErbB4 tyrosine phosphorylation in BaF3/EGFR + ErbB4 cells following stimulation with NRG1β, NRG2β, NRG2α K45F, and NRG2α Chg5. We used 10 nM of each ligand except NRG2α K45F, which was used at 73 nM. We used these concentrations of the NRG2α mutants because we had previously shown that 10 nM NRG2α Chg5 stimulates IL3-independent proliferation in the BaF3/EGFR + ErbB4 cell line (Figure 5), whereas 73 nM NRG2α K45F does not (data not shown).

As shown in Figure 6a, NRG1β stimulates abundant EGFR and ErbB4 tyrosine phosphorylation in the BaF3/EGFR + ErbB4 cells. NRG2β stimulates a modest amount of EGFR tyrosine phosphorylation and stimulates abundant ErbB4 phosphorylation in the BaF3/EGFR + ErbB4 cells. NRG2α K45F and NRG2α Chg5 both stimulate modest EGFR and ErbB4 tyrosine phosphorylation in the BaF3/EGFR + ErbB4 cells. Indeed, despite the fact that the NRG2α Chg5 mutant stimulates IL3-independent proliferation of the BaF3/ EGFR + ErbB4 cell line and the NRG2α K45F mutant does not, the two NRG2α mutants stimulate similar levels of ErbB receptor tyrosine phosphorylation in the BaF3/EGFR + ErbB4 cell line. Thus, ligand-induced EGFR and ErbB4 tyrosine phosphorylation does not completely correlate with ligand-induced coupling of EGFR and ErbB4 to IL3-independent proliferation; EGFR and ErbB4 tyrosine phosphorylation is necessary, but does not appear to be sufficient, to couple EGFR and ErbB4 to IL3 independence.

Preliminary results similar to those shown in Figure 6a raised concerns that perhaps our NRG2α K45F stock had degraded and that this accounted for the failure of the NRG2α K45F mutant to stimulate IL3-independent proliferation and abundant ErbB receptor tyrosine phosphorylation in the BaF3/EGFR + ErbB4 cell line. So, in parallel with the stimulations of the BaF3/ EGFR + ErbB4 cells shown in Figure 6a, we also stimulated CEM/ErbB4 cells. The ligand concentrations used were identical to those used to stimulate the BaF3/ ErbB4 cells. At a final concentration of 73 nM, the

a

IB:Anti-pY

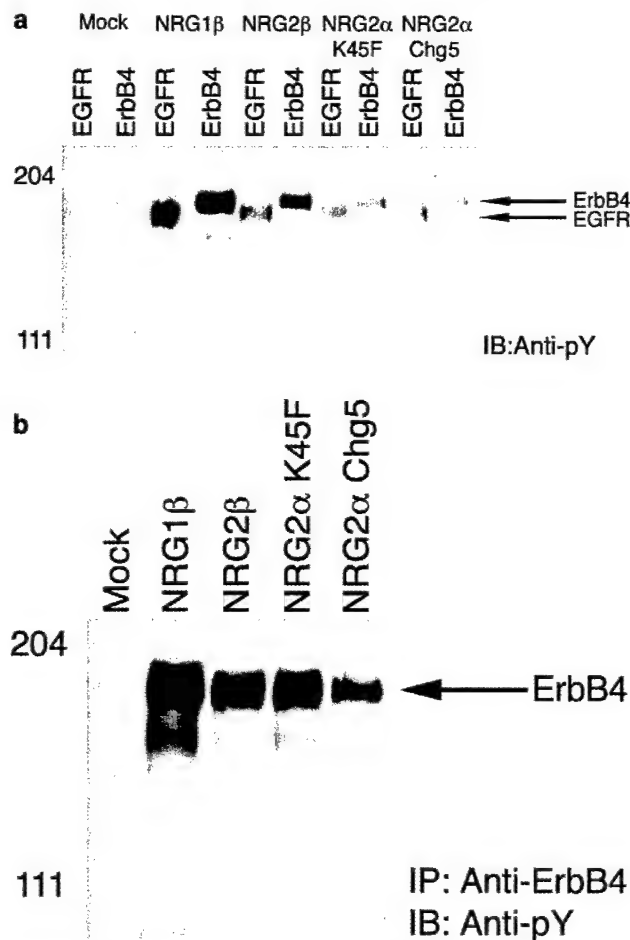**b**

IP: Anti-ErbB4
IB: Anti-pY

Figure 6 NRG2α gain-of-function mutants stimulate modest EGFR and ErbB4 tyrosine phosphorylation in BaF3/EGFR + ErbB4 cells. (a) EGFR and ErbB4 tyrosine phosphorylation in BaF3/EGFR + ErbB4 cells were assayed following stimulation with 10 nM of ligand as indicated except for NRG2α K45F, which was at a concentration of 73 nM. EGFR was immunoprecipitated with an anti-EGFR antibody and ErbB4 was immunoprecipitated with an anti-ErbB4 antibody. EGFR and ErbB4 tyrosine phosphorylation was detected by antiphosphotyrosine immunoblotting. (b) ErbB4 tyrosine phosphorylation in CEM/ErbB4 cells was assayed following stimulation with 10 nM of ligand except for NRG2α K45F, which was a concentration of 73 nM. ErbB4 was immunoprecipitated with an anti-ErbB4 antibody and ErbB tyrosine phosphorylation was detected by antiphosphotyrosine immunoblotting

NRG2α K45F mutant stimulates a greater amount of ErbB4 tyrosine phosphorylation in the CEM/ErbB4 cell line than did 10 nM of the NRG2α Chg5 mutant (Figure 6b). This is despite the fact that the NRG2α K45F mutant at a final concentration of 73 nM and the NRG2α Chg5 mutant at a final concentration of 10 nM stimulate similar levels of ErbB receptor tyrosine phosphorylation in the BaF3/EGFR + ErbB4 cell line. These data indicate that the NRG2α K45F stock was not degraded, and they again suggest that there may be intrinsic differences between the two NRG2α gain-of-function mutants apart from the relatively slight difference in potency (affinity for ErbB4).

Discussion

Phe45 regulates NRG2β potency

The NRG2β F45K mutant fails to stimulate ErbB4 tyrosine phosphorylation (Figure 3a), whereas the NRG2α K45F mutant stimulates abundant ErbB4 tyrosine phosphorylation (Figure 4a). These data suggest that Phe45 is necessary and sufficient for NRG2 stimulation of ErbB4 tyrosine phosphorylation.

One model for the interactions of EGF family hormones with ErbB family receptors features the binding of a single EGF family hormone to a single ErbB family receptor. Two hormone-receptor complexes then associate to form a heterotetrameric complex of two hormone molecules and two receptor molecules (Sherrill and Kyte, 1996; Lemmon et al., 1997; Domagala et al., 2000). The receptor molecules phosphorylate each other (either within or between receptor dimers) and the phosphorylated receptors serve as docking sites for downstream signaling molecules that contain SH2 or PTB domains (Sherrill, 1997; reviewed in Weiss and Schlessinger, 1998; Schlessinger, 2000). Thus, one explanation for the NRG2β F45K loss-of-function mutant and the NRG2α K45F gain-of-function mutant is that Phe45 appears to be part of one of the putative ErbB4 binding sites on NRG2 (Figure 7) and could thereby regulate the affinity of NRG2–ErbB4 interactions. This explanation is consistent with several published observations.

NRG1β Tyr48 (which corresponds to Phe45 of NRG2β) is conserved when a library of randomly generated NRG1β mutants is screened for those that retain high affinity for ErbB3 and for ErbB4 (Ballinger et al., 1998). Substitution of an alanine for Arg45 of EGF (which corresponds to Phe45 of NRG2β) results in a marked increase in the ligand affinity for the chicken EGF receptor (van de Poll et al., 1995). As determined by two-dimensional ¹H NMR, the carboxyl-terminal tails of both EGF and TGFα are flexible in solution (Kline et al., 1990; Kohda and Inagaki, 1992). However,
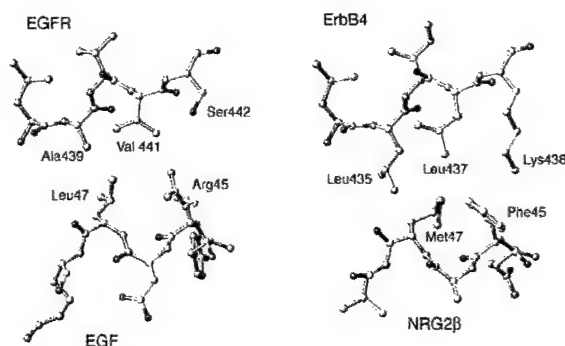

Figure 7 Phe45 of NRG2β may interact with Leu437 and Lys438 of ErbB4. A molecular model of the interaction between Phe45 of NRG2β and ErbB4 was generated using the data from the recently published crystal structure of EGF in complex with EGFR (Ogiso et al., 2002). The gray balls of the ball-and-stick representation indicate carbon atoms. The blue balls indicate nitrogen atoms. The red balls indicate oxygen atoms. The yellow ball indicates a sulfur atom

the carboxyl-terminal TGFα tail (which corresponds to a region of NRG2β that includes Phe45) becomes more ordered upon ligand binding to EGFR, suggesting a direct role of this domain in receptor binding (Hoyt *et al.*, 1994). Finally, scanning alanine mutagenesis of NRG1β reveals that substitution of an alanine for Tyr48 causes a greater than twofold loss of affinity for ErbB4 (Jones *et al.*, 1998). Thus, these published data are consistent with our observation that the NRG2α K45F mutant is a more potent ligand (with respect to stimulation of ErbB4 tyrosine phosphorylation) than is wild-type NRG2α and that the NRG2β F45K mutant is a less potent ligand than is wild-type NRG2β. Of course, direct evaluation of this hypothesis awaits the determination of the affinities of these NRGs and NRG mutants for ErbB4.

Gln43, Met47, Asn49, and Phe50 regulate NRG2β efficacy

The NRG2α and NRG2β mutants in which amino-acid residues 43, 47, 49, and 50 are individually changed are not significantly different from wild-type NRG2α and NRG2β with respect to their ability to stimulate ErbB4 tyrosine phosphorylation (Figures 3a and 4a). However, the NRG2α Chg5 mutant, which has residues 43, 45, 47, 49, and 50 changed, is functionally distinct from the NRG2α K45F mutant, in which only residue 45 is changed. This suggests that Gln43, Met47, Asn49, and Phe50 of NRG2β regulate stimulation of ErbB4 signaling by NRG2β.

The maximal level of ErbB4 tyrosine phosphorylation that is stimulated by the NRG2α Chg5 mutant is similar to, and perhaps greater than, the level stimulated by NRG2β (Figure 4c). In contrast, the maximal level of ErbB4 tyrosine phosphorylation that is stimulated by the NRG2α K45F mutant is approximately 30% less than the level stimulated by NRG2β. Furthermore, the maximal level of tyrosine phosphorylation that is stimulated by the NRG2β F45K mutant is equal to the amount that is stimulated by wild-type NRG2β, despite the fact that the NRG2β F45K mutant is a much less potent stimulus of ErbB4 tyrosine phosphorylation than is wild-type NRG2β. Thus, the potency and perhaps the affinity of NRG2 isoforms and NRG2 mutants are regulated by Phe45. In contrast, the efficacy of NRG2 isoforms and NRG2 mutants appear to be regulated by Gln43, Met47, Asn49, and Phe50 or by some combination of these residues.

Further evidence for the contribution of NRG2β amino acids Gln43, Met47, Asn49, and Phe50 to ligand-induced ErbB4 signaling is revealed in IL3-independence assays using BaF3/EGFR + ErbB4 cells. NRG2β, which stimulates abundant ErbB4 tyrosine phosphorylation, also stimulates IL3-independent proliferation in BaF3/EGFR + ErbB4 cells. In contrast, NRG2α K45F, even at concentrations that stimulate abundant ErbB4 tyrosine phosphorylation in CEM/ErbB4 cells (Figure 6b), does not stimulate IL3-independent proliferation in BaF3/EGFR + ErbB4 cells (Figure 5). This indicates that Phe45 is not sufficient for complete stimulation of ErbB4 signaling by NRG2α. Furthermore, the NRG2α Chg5 and NRG2β F45K mutants stimulate IL3-independent proliferation, indicating Gln43, Met47, Asn49, and Phe50 are critical for complete stimulation of ErbB4 signaling by NRG2. Again, these data indicate that the efficacy of NRG2 isoforms and NRG2 mutants appear to be regulated by Gln43, Met47, Asn49, and Phe50 or by some combination of these residues.

It is tempting to speculate on the mechanism by which Gln43, Met47, Asn49, and Phe50 regulate the efficacy of NRG2 isoforms and mutants. One possibility is suggested by the observation that wild-type NRG2β and the NRG2α Chg5 and NRG2β F45K mutants all stimulate similar levels of maximal ErbB4 tyrosine phosphorylation. In contrast, the NRG2α K45F mutant stimulates a lower level of maximal ErbB4 phosphorylation than these other ligands. This suggests that different numbers of ErbB4 tyrosine residues are being phosphorylated in response to NRG2α K45F stimulation than in response to stimulation with wild-type NRG2β, the NRG2β F45K mutant, and the NRG2α Chg5 mutant.

There are precedents in the literature for this type of differential signaling. We have reported that the ErbB4 ligand NRG4, unlike NRG2β or NRG3, does not stimulate IL3 independence in BaF3/EGFR + ErbB4 cells. This indicates that NRG4, unlike NRG2β and NRG3, fails to stimulate the phosphorylation of ErbB4 tyrosine residues that couple to IL3 independence (Hobbs *et al.*, 2002). These data also suggest that different signaling molecules will be coupled to ErbB4 following stimulation with different ErbB4 ligands. Indeed, stimulation of CEM/ErbB4 cells with BTC, NRG1β, NRG2β, or NRG3 caused differential phosphorylation of downstream signaling molecules such as Akt and Erk1/2. In addition, stimulation of CEM/ErbB4 cells with these ligands caused differential coupling of ErbB4 to Shc and p85. Finally, the different ligands also stimulated phosphorylation of different tyrosine residues on ErbB4. These data indicate that an ErbB4 homodimer can indeed differentially signal depending on the identity of the stimulating ligand (Sweeney *et al.*, 2000).

Of course, we then must speculate on the mechanism by which different ligands can cause ErbB4 to become phosphorylated on different tyrosine residues. We propose the different ligands cause ErbB4 to undergo subtly different conformation changes, resulting in receptor dimers or multimers in which different ErbB4 tyrosine residues are juxtaposed with the ErbB4 kinase domain. Thus, different ligands cause ErbB4 to become phosphorylated on different tyrosine residues.

Several published studies provide support for this model. The structures of liganded and partially liganded EGFR demonstrate that significant structural changes occur in the ectodomain of EGFR when EGFR is bound by either TGFα or EGF. The ectodomain of EGFR is made up of four subdomains, designated as L1, CR1, L2, and CR2. The L1 and L2 domains contain the ligand binding sites on EGFR. The CR1 domain

functions as the 'dimerization arm' that links two EGFR molecules together. The CR2 domain may function as an inhibitor of receptor dimerization in unliganded EGFR by binding the 'dimerization arm' in a manner that prevents the dimerization arm of one EGFR molecule from binding the dimerization arm of another EGFR molecule (Ogiso et al., 2002). In the partially liganded EGFR crystal structure, in which EGF is bound only to the L1 domain, the L1 and L2 domains are separated by a large distance and the ligand-binding sites of the domains are pointed in the opposite direction. In fact, for the L1-bound EGF to bind to the binding sites on the L2 domain, as seen in the liganded EGFR crystal structure, the L1/CR1 domain rigid body has to rotate 130° clockwise and translate 20 Å toward the L2 domain. This large movement disrupts the interaction between domains CR1 and CR2, which frees the CR1 domain to facilitate receptor dimerization (Ferguson et al., 2003).

It has been proposed that the EGFR exists in a dynamic equilibrium between a closed conformation and an open conformation. EGF receptors in the closed conformation, which is characterized by CR1 and CR2 interactions, bind ligands with very low affinity and are incapable of undergoing dimerization. EGF receptors in the open conformation, which is characterized by the absence of CR1/CR2 interactions, bind ligands with high affinity and are capable of undergoing dimerization and signaling. In this model, ligand binds only to those receptors in the open conformation and shifts the dynamic equilibrium in favor of the open conformation, thereby stabilizing these receptors in the conformation suitable for dimerization and signaling (Ferguson et al., 2003).

These data illustrate that in order for ligands to bind ErbBs, large conformational changes in the ErbB structure have to occur. These conformational changes may include conformational changes in the cytoplasmic domains of the ErbBs, which may influence the identity of the tyrosine residues on the cytoplasmic tail that are phosphorylated in response to ligand binding. The crystal structure of TGFα in complex with EGFR indicates that almost 60% of the amino acids in TGFα are in contact with EGFR (Garrett et al., 2002). As a result, it is certainly possible that the conformational changes in ErbB4 that accompany ligand binding may be influenced by the three-dimensional structure of the ligands that bind to the receptor.

The primary sequence of EGF-like ligands and the solved, three-dimensional structures of a couple of ligands indicate a great deal of structural similarity among the EGF-like ligands. A comparison of the crystal structures of EGF (bound to EGFR) and betacellulin (in the absence of EGFR) shows that these ligands share a great deal of similarity in secondary structure; however, there are tertiary differences between the ligands that may influence how they interact with ErbBs (Garrett et al., 2002; Miura et al., 2002). For instance, EGF has a number of residues that fill in the cavity formed by the closing of ligand binding domains of EGFR. Betacellulin, on the hand, is nearly flat on this

face of the ligand that faces toward the dimerization domain of EGFR. This difference may influence the type of conformational changes that EGFR can undergo upon ligand binding.

One explanation for differential phosphorylation of ErbB4 is that each of the ligands somehow causes a conformational change in ErbB4 that causes different tyrosine residues on the cytoplasmic tail of one ErbB4 molecule to be juxtaposed to the kinase domain of another ErbB4 molecule. These proximal tyrosine residues are then tyrosine phosphorylated by the ErbB4 partner.

Of course, such an explanation is dependent upon conformation changes in the ErbB4 extracellular domains being translated to conformation changes in the ErbB4 intracellular domains. A number of experiments indicate that this transfer of structural information across the cell membrane does indeed occur.

Substitution of a single cysteine at several different sites in the juxtamembrane, extracellular region of ErbB2 results in ErbB2 mutants that display elevated, constitutive ErbB2 tyrosine phosphorylation. However, only a subset of these biochemically constitutively active mutants were capable of causing morphologic growth transformation of cultured rodent fibroblast cell lines. Indeed, only cysteine substitutions that occurred on a specific face of the α-helical juxtamembrane domain of ErbB2 resulted in mutants competent for transforming the growth of FR3T3 fibroblasts. This indicates that only those phosphorylated tyrosine residues that align with this face of the α-helical juxtamembrane domain are capable of coupling to growth transformation. Thus, the coupling of ErbB2 tyrosine phosphorylation to downstream biological and biochemical events is specified by the juxtapositioning (conformation) of the ErbB2 monomers within the ErbB2 dimer (Burke and Stern, 1998).

Similar results have been reported for ErbB4. The substitution of a cysteine for Gln646, His647, and Ala648 in the extracellular, juxtamembrane region of ErbB4 results in constitutive, ligand-independent ErbB4 tyrosine phosphorylation. However, the ErbB4 Q646C mutant displays less ErbB4 tyrosine phosphorylation than do the ErbB4 H647C or A648C mutants (Penington et al., 2002). Nonetheless, only the Q646C mutant inhibited drug-resistant colony formation by human DU-145 and PC-3 prostate tumor cell lines. This indicates that the Q646C mutant is phosphorylated on a set of ErbB4 tyrosine residues distinct from those sets of ErbB4 tyrosine residues phosphorylated in the H647C and A648C mutants (Williams et al., 2003). Parenthetically, unpublished data from our laboratory suggest that Tyr1056 is the site of Q646C-specific ErbB4 tyrosine phosphorylation that couples to prostate tumor suppression. In any event, these published and unpublished data indicate that differential conformation changes in the extracellular domains of ErbB family receptors can indeed be translated into differential ErbB receptor tyrosine phosphorylation and support our hypothesis that different EGF family hormones differentially activate ErbB receptor signaling through

differential induction of ErbB receptor conformation changes.

In sum, then, we predict that the major role that Phe45 plays in regulating NRG2β function is to confer high-affinity ErbB4 binding upon NRG2β. Moreover, we predict that when the NRG2α Chg5 mutant, wild-type NRG2β, or the NRG2β F45K mutant binds to ErbB4, the Gln43, Met47, Asn49, and Phe50 residues participate in inducing a conformational change in ErbB4 that is different from the conformational change in ErbB4 induced by the corresponding four residues of wild-type NRG2α or the NRG2α K45F mutant. The differential ErbB4 conformational change induced by NRG2α Chg5, wild-type NRG2β, or the NRG2β F45K mutant causes different tyrosine residues on ErbB4 to be phosphorylated compared to the ErbB4 tyrosine residues whose phosphorylation is stimulated by the binding of wild-type NRG2α or the NRG2α K45F mutant to ErbB4. Naturally, these predictions await ErbB4-binding studies, structural studies of the interactions between ErbB4 and NRGs or NRG mutants, as well as detailed phosphopeptide mapping of ErbB4 following its stimulation with the NRGs and NRG mutants.

Materials and methods

Cell lines and cell culture

The S2 Schneider insect cells were purchased from the American Type Culture Collection. The CEM/ErbB4 cells (Plowman et al., 1993; Riese et al., 1998) are a generous gift of Dr Gregory D Plowman, Exelixis Pharmaceuticals. The BaF3/EGFR + ErbB4 cell lines have been described previously (Riese et al., 1995). All cell lines were maintained according to vendor instructions or published procedures (Plowman et al., 1993; Riese et al., 1995; Feroz et al., 2002; Hobbs et al., 2002).

Construction of NRG2α and NRG2β mutants

The five putative loss-of-function mutants of NRG2β were constructed by 'four-primer' PCR using two flanking primers (used to construct all of the mutants), two mutagenic primers (a different set for each mutant) and the pMT-NRG2β clone (Hobbs et al., 2002) as template. The amplified DNA fragments were cleaved using BglII and SacII and were subcloned into the BglII and SacII sites of pMT/BiP/V5-HisB.

The forward flanking primer used to make all of the mutants is 5'-CTCGAGAGATCTTCGGGGCACGCCCGGAAGTG-3'. The reverse flanking primer used to make all of the mutants is 5'-CTCGAGCCGCGGCTTCTGGTACAGCTCCTC-3'. The forward mutagenic primer used to make the NRG2β Q43L mutant is 5'-GGGGACAGGTGTCTGCAGTTCGCAATG-3'. The reverse mutagenic primer used to make the NRG2β Q43L mutant is the complement. The forward mutagenic primer used to make the NRG2β F45K mutant is 5'-CAGGTGTCAGCAGAAGGCAATGGTCAAC-3'. The reverse mutagenic primer used to make the NRG2β F45K mutant is the complement. The forward mutagenic primer used to make the NRG2β M47P mutant is 5'-CAGCAGTTCG-CACCGGTCAACTTCTCC-3'. The reverse mutagenic primer used to make the NRG2β M47P mutant is the complement. The forward mutagenic primer used to make the NRG2β N49R mutant is 5'-GTTCGCAATGGTCCGCTTCTCCAA-GCAC-3'. The reverse mutagenic primer used to make the

NRG2β N49R mutant is the complement. The forward mutagenic primer used to make the NRG2β F50L mutant is 5'-CGCAATGGTCAACTTGTCCAAGCACCTTG-3'. The reverse mutagenic primer used to make the NRG2β F50L mutant is the complement.

The six putative gain-of-function mutants of NRG2α were generated using the QuikChange site-directed mutagenesis kit (Stratagene). The forward mutagenic primer used to make the NRG2α L43Q mutant is 5'-GTCCAAACGGATTCTTTG-GCCAGAGATGTCAGGA GAAACTGCCTTTGCG-3'. The reverse mutagenic primer used to make the NRG2α L43Q mutant is the complement. The forward mutagenic primer used to make the NRG2α K45F mutant is 5'-CCAAA-CGGATTCTTTGGCCAGAGATGTTTGGAGTTCCTGC-CTTTGCGATTG-3'. The reverse mutagenic primer used to make the NRG2α K45F mutant is the complement. The forward mutagenic primer used to make the NRG2α P47M mutant is 5'-GTTTGGAGAAACTGATGTTGCGATTATA-CATGCCAGATCC-3'. The reverse mutagenic primer used to make the NRG2α P47M mutant is the complement. The forward mutagenic primer used to make the NRG2α R49N mutant is 5'-GGAGAAACTGCCTTTGAACTTATA-CATGCCAGATCC-3'. The reverse mutagenic primer used to make the NRG2α R49N mutant is the complement. The forward mutagenic primer used to make the NRG2α L50F mutant is 5'-GCCTTTGCGATTCTACATGCCAGATC-3'. The reverse mutagenic primer used to make the NRG2α L50F mutant is the complement. The forward mutagenic primer used to make the NRG2α Chg5 mutant is 5'-CGGACAGAGATGTCAGGAGTTCCTGATGTTGAACT-TCTACATGCCAGATC-3'. The reverse mutagenic primer used to make the NRG2α Chg5 mutant is the complement.

Expression, purification, and quantification of recombinant NRGs and NRG mutants

The insect cell expression plasmid pMT/BiP/V5-HisB (Invitrogen) contains a Drosophila metallothionein promoter as well as segments encoding the BiP secretion signal, a V5 epitope tag, and a hexahistidine epitope tag. We have previously described the construction of the recombinant NRG2α and NRG2β insect cell expression vectors based on pMT/BiP/V5-HisB (Hobbs et al., 2002).

We have previously described our strategy for expressing and purifying the recombinant NRGs and NRG mutants (Hobbs et al., 2002). Briefly, S2 cells were co-transfected with 19 μg of the appropriate recombinant pMT-NRG plasmid and 1 μg pCoHygro (Invitrogen), which expresses the hygromycin resistance gene. Cells were transferred to medium containing 300 μg/ml hygromycin B (Calbiochem) to select for stable transformants, which were pooled and expanded into stable cell lines.

The stably transfected S2 cell lines were seeded in serum-free insect cell culture medium supplemented with 1 mM $CuSO_4$ to induce NRG expression. Cells were incubated for 5 days to permit maximal NRG expression and secretion into the culture medium. The cell culture conditioned medium was cleared and was concentrated by ultrafiltration. The retentate was dialysed against phosphate-buffered normal saline (PBS). The NRG was purified from the concentrated crude protein preparation by affinity chromatography using a nickel ion matrix (ProBond. — Invitrogen). The NRG was eluted from the nickel ion matrix using 500 mM imidazole (Sigma). The eluate was concentrated by ultrafiltration and the retentate was dialysed against PBS to remove the imidazole. The purified protein (~4 ml) was divided into aliquots and stored at −80°C.

Anti-V5 immunoblotting was used to quantify the concentrations of the recombinant NRG samples (Hobbs et al., 2002). Briefly, NRG samples were resolved by SDS–PAGE and were electroblotted onto nitrocellulose. The blots were probed using an anti-V5 mouse monoclonal antibody (Invitrogen). The Positope recombinant protein (Invitrogen) was analysed in parallel as a control for V5 immunoblotting and as a standard for quantification. The resulting immunoblots were digitized at 600 dots-per-inch (d.p.i.) using a UMAX Astra 2400S flatbed scanner and the bands were quantified using NIH Image for Macintosh software. We generated dose–response curves of best fit for the Positope control and for each recombinant NRG using Microsoft Excel. These curves were used to calculate the concentration of each recombinant NRG stock.

The concentration of each NRG preparation was determined relative to the concentration of the NRG2β preparation by ELISA using an anti-V5 monoclonal antibody (Invitrogen) (Hobbs et al., 2002). Briefly, the levels of antibody binding were plotted as a function of sample stock volume for NRG2α and the NRG2 mutants. These dose–response curves were compared to a standard dose–response curve generated using NRG2β to determine the relative concentration of the NRG stocks.

Stimulation and analysis of ErbB family receptor tyrosine phosphorylation

We analysed ligand-induced ErbB family receptor tyrosine phosphorylation in CEM/ErbB4 and BaF3/EGFR + ErbB4 cells by antiphosphotyrosine immunoblotting using procedures published previously (Riese et al., 1995, 1996a, b, 1998; Chang et al., 1997; Feroz et al., 2002; Hobbs et al., 2002). Briefly, approximately 10^7 cells were stimulated for 7 min on ice with ligand, after which the cells were lysed in an isotonic lysis buffer supplemented with the nonionic detergent NP40. Nuclei and debris were collected from the lysates by centrifugation and the supernatants were transferred to a fresh tube. The protein content of the lysates was analysed using a modified Bradford assay (Pierce). ErbB family receptors were precipitated from the lysates using an anti-EGFR mouse monoclonal antibody (Santa Cruz Biotechnology) or an anti-ErbB4 rabbit polyclonal antibody (Santa Cruz Biotechnology).

The precipitates were resolved by SDS–PAGE using a 7.5% acrylamide gel. For several of the immunoblots, varying amounts of tyrosine phosphorylated ErbB4 immunoprecipitates were used as controls. We generated these controls by stimulating four aliquots of 10^7 CEM/ErbB4 cells with 10 nM NRG1β. We immunoprecipitated ErbB4 from each aliquot, eluted the ErbB4 from the immunocomplexes, and pooled the eluates. Typically, eluate volumes corresponding to 200, 100, 50, and 25% of a standard stimulation (10^7 CEM/ErbB4 cells) were loaded onto the gels to serve as controls.

The resolved samples were electroblotted onto nitrocellulose. The blots were probed using an antiphosphotyrosine mouse monoclonal antibody (Upstate Biotechnology). Primary antibody binding was detected using a goat anti-mouse antibody conjugated to horseradish peroxidase (Pierce). Secondary antibody binding was visualized by chemiluminescence (Amersham).

The chemilumigrams were digitized at 600 d.p.i. using a UMAX Astra 2400S flatbed scanner and the volumes of the bands were quantified using NIH Image software for Macintosh. From the CEM/ErbB4 immunoblots, ErbB4 phosphotyrosine standard curves were constructed from the NRG1β load–response data using Microsoft Excel. The maximal level of ErbB4 tyrosine phosphorylation (ErbB4

S_{max}) that is stimulated by each ligand was calculated using the ErbB4 tyrosine phosphorylation load–response standard curve generated in Microsoft Excel. The resulting values are expressed as a percentage of ErbB4 tyrosine phosphorylation stimulated by NRG1β. In Figures 3 and 4, the load–response standard curves were used to calculate relative levels of maximal ErbB4 tyrosine phosphorylation that are stimulated by NRG2α, NRG2β, and the NRG2 mutants. The resulting data are expressed as a percentage of ErbB4 tyrosine phosphorylation stimulated by NRG1β. We also analysed ErbB4 tyrosine phosphorylation following stimulation of CEM/ErbB4 cells with increasing concentrations of NRG2α, NRG2β, and the NRG2 mutants. These dose–response data were analysed with the GraphPad Prism 3.0 software for Macintosh to determine the concentration of each ligand that yields half-maximal ErbB4 tyrosine phosphorylation (EC_{50}).

Stimulation and analysis of ErbB family receptor coupling to IL3 independence

We have previously demonstrated that certain combinations of tyrosine phosphorylated ErbB family receptors couple to IL3-independent survival and/or proliferation in the IL3-dependent BaF3 lymphoid cell line (Riese et al., 1995, 1996a, b). Thus, we analysed the NRG2 mutants for ligand-induced ErbB family receptor coupling to IL3 independence in BaF3/EGFR + ErbB4 cells using procedures published previously (Riese et al., 1995, 1996a, b, 1998; Chang et al., 1997; Hobbs et al., 2002). Briefly, cells were seeded in 24-well dishes at a density of 10^5 cells/ml in medium lacking IL3, in medium supplemented with IL3, or in media lacking IL3 but supplemented with 10 nM of a recombinant NRG. Cells were incubated for 96 h, after which viable cells were counted using a hemacytometer. If the viable cell density was greater than 10^5 cells/ml, the cells were judged to be proliferating. If the viable cell density was between 10^4 and 10^5 cells/ml, the cells were judged to be surviving. If the viable cells density was below 10^4 cells/ml, the cells were judged to be dying.

Generation of a molecular model for the interaction between NRG2β and ErbB4

The X-ray crystal structure coordinates of EGF in complex with EGFR were obtained from the Protein Data Bank (Accession Number 1IVO). These data were manipulated using the Sybyl 6.9 software (Tripos) on a Silicon Graphics O2 workstation. Amino acids Tyr44 through Glu51 of EGF were mutated to the corresponding amino acids (Gln44 through Ser51) of NRG2β. In addition, amino acids Ala439 through Gly446 of EGFR were mutated to the corresponding amino acids (Leu435 through Gln442) of ErbB4. Finally, a subset energy minimization was performed using the MMFF94s force field equation on a 'hot' region defined as being within 6 Å or less away from the mutated region and on an 'interesting' region defined as being between 6 and 12 Å away from the mutated region. In the energy minimizations, the atomic coordinates are changed over a number of iterations to minimize the free energy of the region. Atoms within the 'hot' region are fully minimized, whereas atoms within the 'interesting' region are only partially minimized (Halgren, 1999).

References

Ballinger MD, Jones JT, Lofgren JA, Fairbrother WJ, Akita RW, Sliwkowski MX and Wells JA. (1998). *J. Biol. Chem.*, **273**, 11675–11684.

Buonanno A and Fischbach GD. (2001). *Curr. Opin. Neurobiol.*, **11**, 287–296.

Burke CL and Stern DF. (1998). *Mol. Cell. Biol.*, **18**, 5371–5379.

Carraway III KL, Weber JL, Unger MJ, Ledesma J, Yu N, Gassmann M and Lai C. (1997). *Nature*, **387**, 512–516.

Chang H, Riese II DJ, Gilbert W, Stern DF and McMahan UJ. (1997). *Nature*, **387**, 509–512.

Culouscou JM, Plowman GD, Carlton GW, Green JM and Shoyab M. (1993). *J. Biol. Chem.*, **268**, 18407–18410.

Domagala T, Konstantopoulos N, Smyth F, Jorissen RN, Fabri L, Geleick D, Lax I, Schlessinger J, Wawyer W, Howlett GJ, Burgess AW and Nice EC. (2000). *Growth Factors*, **18**, 11–29.

Feroz K, Williams E and Riese II DJ. (2002). *Cell. Signal.*, **14**, 793–798.

Ferguson KM, Berger MB, Mendrola JM, Cho S, Leahy DJ and Lemmon M. (2003). *Mol. Cell*, **11**, 507–517.

Garrett TPJ, McKern NM, Lou M, Elleman TC, Adams TE, Lovrecz GO, Zhu HJ, Walker F, Frenkel MJ, Hoyne PA, Jorissen RN, Nice EC, Burgess AW and Ward CW. (2002). *Cell*, **110**, 763–773.

Gullick WJ. (2001). *Endocrine-Related Cancer*, **8**, 75–82.

Halgren TA. (1999). *J. Comput. Chem.*, **20**, 720–729.

Harari D, Tzahar E, Romano J, Shelly M, Pierce JH, Andrews GC and Yarden Y. (1999). *Oncogene*, **18**, 2681–2689.

Hobbs SS, Coffing SL, Le ATD, Cameron EM, Williams EE, Andrew M, Blommel EN, Hammer RP, Chang H and Riese II DJ. (2002). *Oncogene*, **21**, 8442–8452.

Hoyt DW, Harkins RN, Debanne MT, O'Connor MC, Court M and Sykes BD. (1994). *Biochemistry*, **33**, 11928–11939.

Jones JT, Ballinger MD, Pisacane PI, Lofgren JA, Fitzpatrick VD, Fairbrother WJ, Wells JA and Sliwkowski MX. (1998). *J. Biol. Chem.*, **273**, 11667–11674.

Kline TP, Brown FK, Brown SC, Jeffs B, Koppel K and Mueller L. (1990). *Biochemistry*, **29**, 7805–7813.

Kohda D and Inagaki F. (1992). *Biochemistry*, **31**, 11928–11939.

Lemmon MA, Bu Z, Ladbury JE, Zhou M, Pinchasi D, Lax I, Engelman DM and Schlessinger J. (1997). *EMBO J.*, **16**, 281–294.

Miura K, Doura H, Aizawa T, Tada H, Seno M, Yamada H and Kawano K. (2002). *Biochem. Biophys. Res. Commun.*, **294**, 1040–1046.

Ogiso H, Ishitani R, Nureki O, Fukai S, Yamanaka M, Kim JH, Saito K, Sakamoto A, Inoue M, Shirouzu M and Yokoyama S. (2002). *Cell*, **110**, 775–787.

Penington DJ, Bryant I and Riese II DJ. (2002). *Cell Growth Differ.*, **13**, 247–256.

Plowman GD, Green JM, Culouscou J-M, Carlton GW, Rothwell VM and Buckley S. (1993). *Nature*, **366**, 473–475.

Riese II DJ, Bermingham Y, van Raaij TM, Buckley S, Plowman GD and Stern DF. (1996a). *Oncogene*, **12**, 345–353.

Riese II DJ, Kim ED, Elenius K, Buckley S, Klagsbrun M, Plowman GD and Stern DF. (1996b). *J. Biol. Chem.*, **271**, 20047–20052.

Riese II DJ, Komurasaki T, Plowman GD and Stern DF. (1998). *J. Biol. Chem.*, **273**, 11288–11294.

Riese II DJ, van Raaij TM, Plowman GD, Andrews GC and Stern DF. (1995). *Mol. Cell. Biol.*, **15**, 5770–5776.

Schlessinger J. (2000). *Cell*, **103**, 211–225.

Sherrill JM. (1997). *Biochemistry*, **36**, 12890–12896.

Sherrill JM and Kyte J. (1996). *Biochemistry*, **35**, 5705–5718.

Sweeney C, Lai C, Riese II DJ, Diamonti AJ, Cantley LC and Carraway III KL. (2000). *J. Biol. Chem.*, **275**, 19803–19807.

Tzahar E, Levkowitz D, Karunagaran D, Yi L, Peles E, Lavi S, Chang D, Liu N, Yayon A, Wen D and Yarden Y. (1994). *J. Biol. Chem.*, **269**, 25226–25233.

van de Poll MLM, Lenferink AEG, van Vugt MJH, Jacobs JJL, Janssen JWH, Joldersma M and van Zoelen EJJ. (1995). *J. Biol. Chem.*, **270**, 22337–22343.

Weiss A and Schlessinger J. (1998). *Cell*, **94**, 277–280.

Williams EE, Trout LJ, Gallo RM, Pitfield SE, Bryant I, Penington DJ and Riese II DJ. (2003). *Cancer Lett.*, **192**, 67–74.

Zhang D, Sliwkowski MX, Mark M, Frantz G, Akita R, Sun Y, Hillan K, Crowley C, Brush J and Godowski PJ. (1997). *Proc. Natl. Acad. Sci. USA*, **94**, 9562–9667.